https://doi.org/10.5194/egusphere-2023-3069
Preprint. Discussion started: 29 January 2024

Influence of plant traits on water cycle processes in the Amazon Basin

Kien Nguyen [1] and Maria J. Santos [1]

[1]Department of Geography, University of Zurich, Switzerland

Correspondence: Kien Nguyen (kien.nguyen@geo.uzh.ch)

Abstract. Plants play a key role in the soil-plant-atmosphere-climate hydrological continuum. Plants depend on the water cycle and, in return, several hydrological processes could be impacted via vegetation-induced mechanisms. Changes in plant composition are known to affect this relationship, however, detailed understanding on how plant characteristics, i.e., their traits, are seldom included in observational and modeling studies. Here we examine the effect of plant traits on water cycle processes in the Amazon Basin. We used remotely-sensed estimates of four plant traits, namely Specific Leaf Area (SLA), Leaf Dry Matter Content (LDMC), Leaf Phosphorus Content (LPC), Leaf Nitrogen Content (LNC), and two vegetation indices, the Normalised Difference Vegetation Index (NDVI), and Leaf Area Index (LAI), for 10 years between 2001 and 2010. We examined the relationship between plant traits and six parameters relevant for water cycle processes, namely Evapotranspiration (ET), Potential Evapotranspiration (PET), Vapour Pressure Deficit (VPD), Land Surface Temperature (LST) Day/Night and Soil Moisture (SM). We used multivariate and quantile regressions to analyse how plant traits explain the average and standard deviation in water cycle process parameters. We find that SLA, NDVI, and LAI exert the strongest effects across the whole of Amazon basin and the sub-basins, most important for the regulation of atmospheric water content and of land surface temperature, but little effect on the regulation of soil moisture content. These effects are exacerbated at extreme values of water process parameters, where plant traits exert an even stronger effect at low values of ET and PET and high values of VPD and LST. Leaf gas exchange traits are most important in comparison to the other traits, and these results also highlight that if water cycle process parameters achieve extreme values, plant traits are key to the persistence of hydrological processes fundamental to the resilience of the Amazon.

1 Introduction

Water distribution and cycling is a fundamental earth system process that may be strongly modified by the plant properties that regulate water transport and storage within plants (Matthews, 2006). Plants are fundamental in the transport of water from the soil into the atmosphere (Jackson et al., 2000; Caldwell et al., 1998) driving soil-plant-atmosphere-climate interactions (Katul et al., 2012). These processes maintain the hydrological flows that regulate climate, and are fundamental to understand the response of ecosystems to droughts, floods and other water redistribution processes such as moisture recycling (Salati et al., 1979; Keys et al., 2017; O'Connor et al., 2021; Van Der Ent et al., 2014), which contributes on average to 40% of the terrestrial precipitation, up to around 60-70% in locations like West Africa, western North America, China, Siberia and Mongolia (Van

https://doi.org/10.5194/egusphere-2023-3069
Preprint. Discussion started: 29 January 2024

Der Ent et al., 2010). Alterations in soil-plant-atmosphere-climate interactions lead to changes in the hydrological regime, biosphere distribution, and the provision of precipitable water with potential loss of resilience to hydrological shocks (Keys et al., 2019; Zemp et al., 2014; O'Connor et al., 2021; Zemp et al., 2017; Satyamurty et al., 2012). Plants, through their traits, mediate water exchange processes, yet their effects have been seldom examined (Funk et al., 2017). Currently, we know that water availability determines plant trait distribution and adaptation (Sanchez-Martinez et al., 2020; Blasini et al., 2022; Hultine et al., 2020), yet these same plant traits may feedback into how plants regulate and interact with hydrological processes (Gentine et al., 2019).

Vegetation cover, composition and function affects several hydrological processes, over space (te Wierik et al., 2021) and time (Caballero et al., 2022). Plant traits are characteristics of plants that describe morphological, anatomical, physiological, biochemical and phenological features at individual, community or ecosystem levels (Kattge et al., 2011). Trait-based approaches (Garnier and Navas, 2012) have been well established in ecology and are very useful to understand the relationship between plants (and other organisms) and environmental conditions (Green et al., 2022), and therefore could be useful as an approach to understand the function of plants in hydrological processes (Anderegg et al., 2018, 2014). Recent studies have shown, for example, how hydraulic traits mediate ecosystem responses to drought and thus provide resilience (Anderegg et al., 2018), how variation in bark thickness provides resistance to fire (Staver et al., 2020), and how plant trait diversity increases ecosystem resilience (Sakschewski et al., 2016) and improves ecosystem function (Yan et al., 2023). Some plant traits might influence multiple hydrological processes (Matheny et al., 2017), or some specific processes, as reflected in the growing literature on hydraulic traits (Anderegg, 2015; Anderegg et al., 2019). For example, leaf water exchange, stomata density, specific leaf area, and xylem pressure at 50% conductivity have a role on the tolerance of plants to droughts (Powell et al., 2017). Some plant hydraulic traits, such as specific leaf area, hydraulic safety margin, and the water potential at 50% loss of stem hydraulic conductivity mediate drought intensification and land–atmosphere feedbacks (Anderegg et al., 2019). Root depth controls soil water uptake, and such process is mediated by soil water holding capacity and affects other processes in the soil-plant-atmosphere-climate continuum (O'connor et al., 2019). Therefore plants traits may exert many, yet underexplored, controls on hydrological processes.

Plant functional trait values and distribution may act as mediators of processes along the soil-plant-atmosphere-climate continuum that drive fluxes of water, such as regulation of atmospheric water content, regulation of land surface temperature, and regulation of soil water content. Plants are fundamental to these fluxes through their role in transpiration (Kool et al., 2014; Christoffersen et al., 2014), photosynthesis (Gu et al., 2003), rainfall interception (Magliano et al., 2022; Van Dijk and Bruijnzeel, 2001), and root water uptake (Aroca et al., 2012; O'connor et al., 2019; Ehleringer and Dawson, 1992). Transpiration accounts for 61% of evapotranspiration (ET) globally, and in tropical regions it can contribute as much as 70% (Schlesinger and Jasechko, 2014). Changes in vegetation cover may result in changes in the fractional contribution of transpiration to ET. For example, (Wang et al., 2010) reported a 22% increase in ET when woody plant cover increased from 25% to 100%, and these increases may vary during the growing season (Ashktorab et al., 1994). Stomatal regulation alone accounts for 80-90% water exchange to the atmosphere (Verma and Verma, 2007), and this process is controlled by factors like temperature, humidity, wind and solar radiance, the number of stomata in a leaf surface, the percentage of stomata opening and the structure

https://doi.org/10.5194/egusphere-2023-3069
Preprint. Discussion started: 29 January 2024

of the canopy (Zhao et al., 2013; Ward, 1971; Feng et al., 2020). In general, the more abundant and larger the leaves are, the higher rate of transpiration (Kool et al., 2014; Christoffersen et al., 2014). Interception also greatly impacts the water cycle (Miralles et al., 2010; Savenije, 2004), as it may account for 10%-40% of the total precipitation (Crockford and Richardson, 2000; Gash et al., 1980). Larger leaves likely intercept more water, making this water available for latent heat exchanges and contributing moisture to the atmosphere (Magliano et al., 2022; Van Dijk and Bruijnzeel, 2001). Photosynthesis affects the fluxes of water into the atmosphere as it requires water drawn-up from the soil, decreasing the evaporative flux of soil water while increasing water exchange through evapotranspiration at the leaf and canopy levels (Gu et al., 2003). Root depth and soil hydraulic redistribution regulate how water is drawn-up from the soil at different depths (O'connor et al., 2019). These mechanisms highlight the potential roles of plant traits on water exchanges, however, the direction and the magnitude of these effects and how they vary spatially is still sparsely known.

Direct links between plant traits and hydrological processes may be hard to assess because of the direct and indirect relationships between single or multiple traits at several stages of the hydrological cycle (Van Bodegom et al., 2012) and across the variety of scales at which plant-water exchange may occur from stomata to whole ecosystems (Aleixo et al., 2019); further, the relationship may differ across regions with varying environmental conditions (Aleixo et al., 2019). First, plant traits do not operate in isolation, i.e. occur as a set of co-functioning traits often named trait syndromes (Pan et al., 2021). Some traits are activated upon the enactment of a previous trait, e.g., root characteristics and depth determine water available to plants, which only upon transport to the canopy may activate stomatal conductivity and determine leaf water exchange (Mencuccini et al., 2019). In a trait syndrome, some traits may exert a positive effect on plant-water relations, while others might have a negative effect, and the net effect may vary upon a gradient of environmental conditions. For example, the soil–plant continuum breaks if forced to transport water beyond its capacity (Hultine et al., 2020). Leaf cooling and hydraulic properties exhibit strong trade-offs along a gradient of aridity (Blasini et al., 2022). While synergies and trade-offs in trait functioning led to coordinated co-evolution of hydraulic traits (Sanchez-Martinez et al.), in some cases there are mismatched or no responses to water stress, especially in regions that have not yet experienced this type of stress (Signori-Müller et al., 2021). Net effects of plant traits on hydrological processes may also be determined by intra- and interspecific variation in trait values. Plant traits may take values across a range, varying by species, plant communities and ecosystems (Kattge et al., 2020, 2011), with unknown effects on the outcome of soil-plant-atmosphere-climate interactions. Second, there is a variety of scales at which plant-water exchange may occur from leaf stomata to canopy and ecosystems, and these scales are hard to capture in models. A variety of models have been devised to predict the relationship between trait and water processes at the stomata level (e.g. (Lu et al., 2020)), leaf level (e.g. (Collatz et al., 1992)), canopy level (e.g. (Mirfenderesgi et al., 2016)), and global level (e.g. moisture recycling tracking model (Tuinenburg and Staal, 2020)). The integration of such models is often difficult, and sometimes generally comes at the expense of exclusion of processes from models (Baudena et al., 2015). Observational studies and statistical models complement the range of processed-based models used to study plant-water interactions across scales, and there also observations vary with scale (e.g. remote sensing and field measurements (Liu et al., 2021)). Experiments seldom occur at larger scales, restricted to plot level and certain geographies, and extrapolated to large scale models. Some plant-water processes are not conducive for experimental work given the scale at which they operate (e.g. moisture recycling), therefore limiting the ability

https://doi.org/10.5194/egusphere-2023-3069
Preprint. Discussion started: 29 January 2024

to connect models and processes where desirable. Third, the relationship may differ across regions with varying environmental conditions. Plant hydraulic traits are known to vary upon gradients of water stress (Hultine et al., 2020; Anderegg, 2015) and water logging (Blasini et al., 2022). These environmental gradients lead to variability in the trait values themselves, and may also be effected by the role of plant traits in mediating hydraulic processes.

Here we examine the effect of plant traits on soil-plant-atmosphere-climate interactions. We hypothesize an effect of plant traits on three water exchange processes, namely regulation of atmospheric water content, regulation of land surface temperature, and regulation of soil water content. More specifically, we ask the following questions: (i) is there a relation between plant traits and water cycle parameters in the Amazon Basin?, (ii) if so, is this relationship sensitive to the extreme values of water cycle parameters?, and (iii) do the relationships hold for the sub-basins within the Amazon? The persistence of the Amazon forest hugely relies on its water cycle because 25% of its precipitation is contributed by regional ET (Eltahir and Bras, 1994). Vegetation cover in the Amazon has an active role in the soil-plant-atmosphere continuum, through their effects regulating ET, interception and formation of condensation (Hasler and Avissar, 2007; Xu et al., 2019; Casagrande et al., 2021; Zheng and Jia, 2020), the maintenance of soil moisture dynamics (Laio et al., 2001), reducing soil erosion and floods (Durán Zuazo and Rodríguez Pleguezuelo, 2008), modulating water run-off to streams and oceans (Nagase and Dunnett, 2012; Blanusa and Hadley, 2019), and hydraulic regulation on water flux and water status (Deng et al., 2017). We expect that by going beyond vegetation cover to examine specific plant traits, we can provide fundamental understanding of hydrological and ecological feedbacks, and also useful information to guide conservation strategies that ensure the Amazon's hydrological and ecological processes fundamental to ensure a sustainable rate of precipitation for the forest, croplands (O'connor et al., 2019) and livelihoods given the impacts of deforestation, land use changes and climate change (Marengo, 2006).

2 Methods

2.1 Study area

The Amazon Basin is a vast region of 6.3 million km^2, established along the Amazon river and its distributary channels ($(-80.5°, -48.5°)$, $(6°, -20.5°)$, Figure 2). The basin includes seven sub-basins, the Amazonas, Madeira, Negro, Solimões, Tapajós, Trombetas and Xingu sub-basins. The majority of the basin is covered by rainforest (5.5 million km^2), of which 60% occurs within Brazil, 13% in Peru, 10% in Colombia and the rest to countries including Venezuela, Ecuador, Bolivia, Guyana, Suriname and French Guiana. Being the largest rainforest on Earth, the Amazon holds a great importance as it is one of the regions with highest biodiversity globally, being home to about 40,000 plants, 427 mammals, 1300 birds, 378 reptiles, 400 amphibians and 3000 fish species (Da Silva et al., 2005). The Amazon forest is also fundamental to regulating the Earth's climate.

https://doi.org/10.5194/egusphere-2023-3069
Preprint. Discussion started: 29 January 2024

2.2 Datasets

2.2.1 Choices of plant traits/indices and water cycle parameters

We chose a set of water cycle parameters that are important to the three environmental processes we are examining, as show in Figure 1. Several hypotheses can be advanced for the role of plant traits on these processes. Larger and heavier leaves (e.g. measured with Specific Leaf Area (SLA) and Leaf Dry Matter Content (LDMC)) might have higher number of stomata (Wang et al., 2019a), leading to higher transpiration and more interception (Magliano et al., 2022; Van Dijk and Bruijnzeel, 2001), hence, leading to higher evapotranspiration (ET) and potential evapotranspiration (PET). These higher exchanges of water at the leaf level would therefore directly reduce evaporative water demand (e.g. measured with Vapour Pressure Deficit (VPD)) at the canopy level (Massmann et al., 2019), leading to evaporative cooling thus reducing canopy temperature (e.g. measured as Land Surface Temperature (LST)) (Chakraborty et al., 2021), and exert a need for water in the soil therefore lowering soil moisture (SM) (Wang et al., 2021). Plant and leaf biochemistry and physiology (as measured, e.g. through Leaf Phosphorous Content (LPC) and Leaf Nitrogen Content (LNC)), in particular in tropical areas which tend to be phosphorus limited (Turner et al., 2018), could mediate evaporative fluxes with subsequent effects on evaporative cooling and demands for soil water. On the other hand, higher LDMC would likely exert a negative effect on water fluxes as more dry matter would result in less photosynthetic capacity, and therefore the expected relationship with LDMC would be the reverse of that expected for vegetation indices such as Leaf Area Index (LAI) and Normalized Difference Vegetation Index (NDVI) and that for the other three traits.

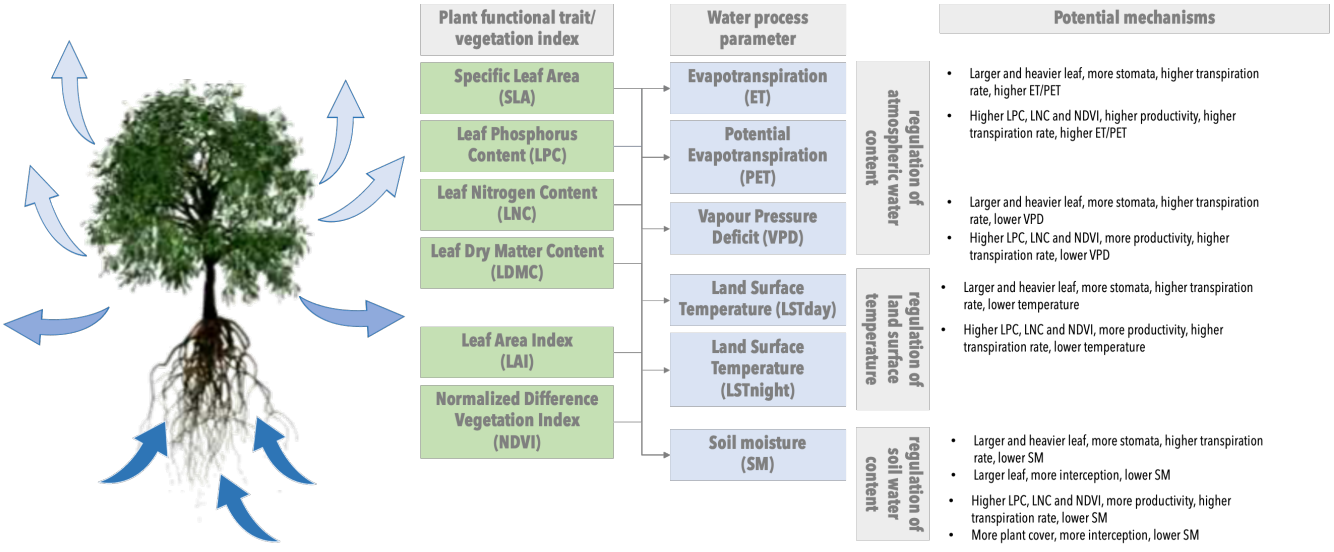

Figure 1. Conceptual diagram of expected relationships between plant traits and water process parameters

https://doi.org/10.5194/egusphere-2023-3069
Preprint. Discussion started: 29 January 2024

Trait/environment parameters	Unit	Spatial Resolution	Temporal Resolution	Source
LDMC	g/g	3km	10-year average	Moreno-Martínez et al. (2018a)
SLA	mm2/mg	3km	10-year average	Moreno-Martínez et al. (2018a)
LPC	mg/g	3km	10-year average	Moreno-Martínez et al. (2018a)
LNC	mg/g	3km	10-year average	Moreno-Martínez et al. (2018a)
NDVI	No unit	0.05°	Monthly	Didan (2021)
LAI	No unit	500m	Monthly	Myneni et al. (2015)
ET	mm/year	1km	Yearly	Mu et al. (2013)
PET	mm/year	1km	Yearly	Mu et al. (2013)
VPD	kPa	4km	Monthly	Abatzoglou et al. (2018)
LST (Day/Night)	Kelvin	0.05°	Monthly	Wan et al. (2015)
SM	m3/m3	0.25°	Monthly	Guevara et al. (2021)

Table 1. Data sources

2.2.2 Plant traits and vegetation indices

Several global trait maps have been produced by modeling the relationship between in-situ trait measurements (e.g. TRY database (Kattge et al., 2020), or citizen science data (Wolf et al., 2022)), and satellite remote sensing and other auxiliary data to generate spatially explicit trait distributions (Dechant et al., 2023). The review of these multiple approaches (Dechant et al., 2023), showed that the best predictions of plant functional traits at global scale includes that of (Moreno-Martínez et al., 2018b). These authors computed these traits over a time period from 2000–2010 and at 1km and 3km spatial resolution, of which we used the 3km version in our analyses (Table 1, Figure 1).

For NDVI and LAI, we used analysis-ready products from the Moderate Resolution Imaging Spectroradiometer (MODIS) for NDVI (MOD13 (Didan, 2021)) and LAI (MOD15 (Myneni et al., 2015)), at monthly intervals and at 500m for LAI and 0.05° for NDVI (Table 1, Figure 1). The spatial resolution of all datasets used in the analyses was harmonized as described in section 2.3.1.

2.2.3 Water cycle parameters

For regulation of atmospheric water content, we chose to analyze Evapotranspiration (ET), Potential Evapotranspiration (PET) and Vapour Pressure Deficit (VPD). For regulation of land surface temperature, we use Land Surface Temperature (LST) at day and night (LSTday and LSTnight). Finally, for regulation of soil water content, we use Soil Moisture (SM). For ET and PET we used the MOD16A3 dataset (Mu et al., 2013), at 500m resolution and yearly between 2001 and 2010 to match the timeframe of the trait data (Table 1). For VPD we used the TerraClimate dataset (Abatzoglou et al., 2018), at 4km, monthly, and again between 2001 and 2010. For LST, we used the MODIS MOD11C3 dataset (Wan et al., 2015) at 0.05° spatial resolution

https://doi.org/10.5194/egusphere-2023-3069
Preprint. Discussion started: 29 January 2024

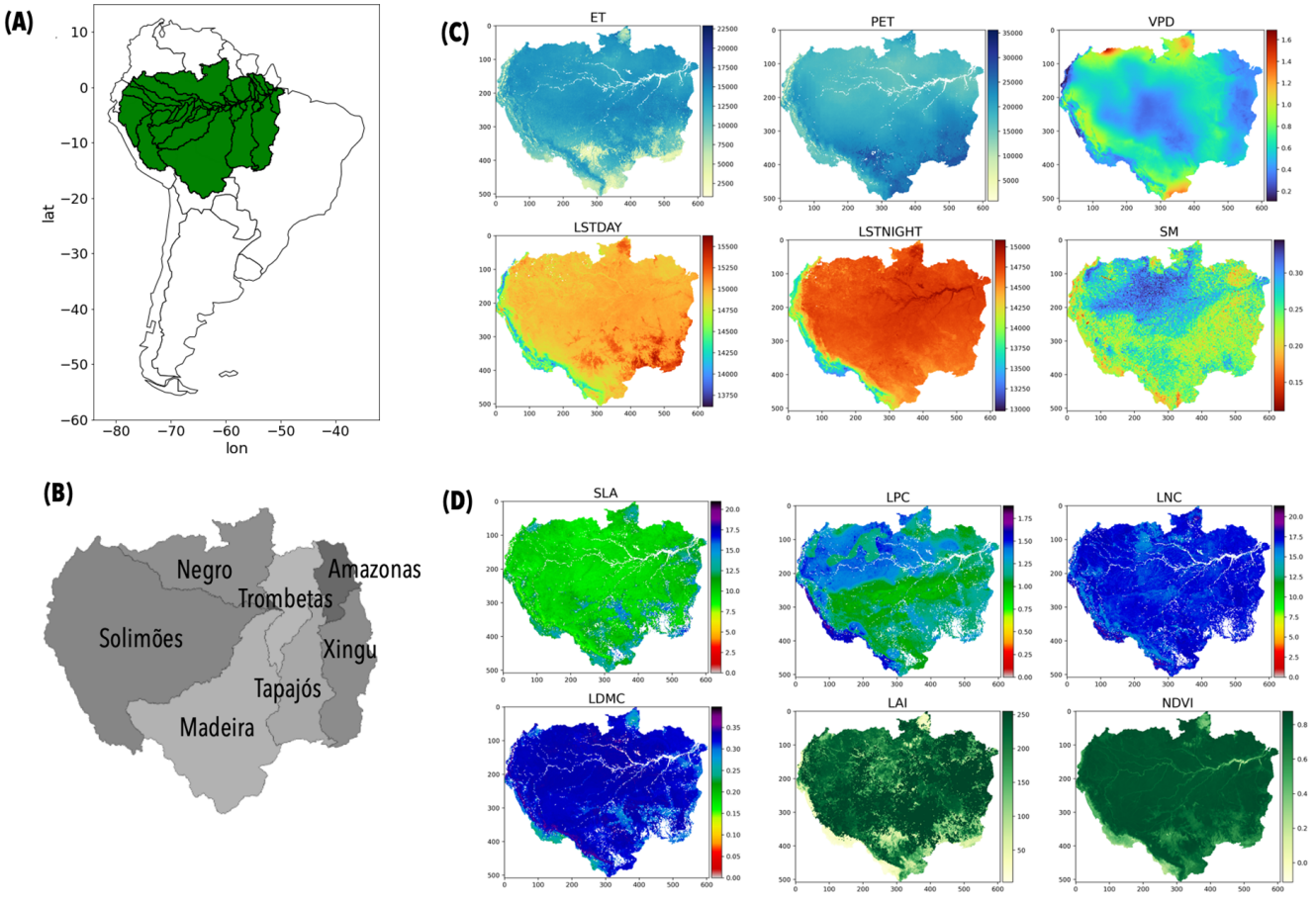

Figure 2. (A) Study area location, (B) Sub-basins of the Amazon, (C) water process parameters between 2001 and 2010: average ET and average PET based on MOD16A3 data (Running et al., 2021), average VPD based on the TerraClimate dataset (Abatzoglou et al., 2018), LST based on MOD11C3 dataset (Wan et al., 2015) and SM based on a global soil moisture dataset (Guevara et al., 2021) and (D) four plant traits average over 10 years (2001-2010) calculated by (Moreno-Martínez et al., 2018b) used in this study, NDVI based on MOD13 dataset (Didan, 2021) and LAI based on MOD15 dataset (Myneni et al., 2015))

160 and with monthly temporal resolution also between 2001 and 2010. For SM we used a global soil moisture dataset (Guevara et al., 2021), at monthly frequency for the same time period, at $0.25°$ resolution.

https://doi.org/10.5194/egusphere-2023-3069
Preprint. Discussion started: 29 January 2024

2.3 Data Analysis

2.3.1 Data pre-processing

We chose as base spatial resolution $0.05°$ because it is the resolution of the plant trait data (Moreno-Martínez et al., 2018b). Hence, we obtained NDVI with resolution of $0.05°$ and datasets with different spatial resolution were either downsampled or upsampled using a cubic resampling method to match the base resolution. Gaps present in the resampled datasets were filled by linear interpolation. We calculated the 10-year mean and standard deviation for the water process parameters and for LAI and NDVI, while the four plant trait datasets were already available as aggregated products between 2001-2010.

2.3.2 Statistical analysis

First, we selected only vegetated pixels for the analysis by defining a NDVI threshold greater or equal to 0.3, as this corresponds this has been demonstrated to separate vegetation and non-vegetation areas in the Amazon Basin (Hashimoto et al., 2021; Fragal et al., 2016) and other regions in the world (Frappart et al., 2006; Yu et al., 2016; Bhandari et al., 2012). This resulted in 191,932 pixels for analysis.

Second, we developed 12 multivariate linear regression models, where each model examined whether there was an association between the each of the four plant traits and the two vegetation indices as predictor variables and each of the water process parameters average and standard deviation as responses. To avoid model overfitting, we assessed multicollinearity by calculating the Variance Inflation Factor (VIF) for each variable contributing to the models. The VIF indicates how much of model variance is inflated due to non-orthogonal relationships between variables. We found that all variables had low VIF, therefore could be included in the analyses (highest VIF = 2.15 for SLA; figure A1 in the appendix). We calculated the adjusted coefficient of determination, i.e. pseudo r-square, which measures the fit of the model to the data penalized by the number of parameters in the model. For each of the traits and vegetation indices, we used the standardized coefficients as a measure of their effect sizes and assessed whether the confidence interval of the estimates of standardized coefficients crossed zero, as this would indicate a non-reliable estimate.

Third, we investigated the sensitivity of the relationships between plant traits and vegetation indices and water process parameters to extreme values. Quantile regression has been frequently used to understand ecological processes (Brennan et al., 2015; Good and Caylor, 2011; Liu et al., 2013; Cade et al., 2005), since it examines how responses vary across the range of the dependent variable (Cade and Noon, 2003); in our case it indicates the stability or volatility of the effect of plant traits on the range of values of water process parameters. In other words, quantile regression allows detecting whether the strength of the relationship becomes higher (steeper slope) or lower (shallower slope) when analysing just the extreme values of dependent variables. We conducted quantile regressions for each of the trait/index-water cycle parameter pair (72 pairs in total) (Koenker and Hallock, 2001). For each relationship, we evaluated the relationship at the 5th quantile (extreme low values), the median, and the 95th quantile (extreme high values). The quantile regression was performed using the *statsmodel* package (v0.13.2: www.statsmodels.org) in Python 3.6.13. We calculated a pseudo R-square (Koenker and Machado, 1999), to represent the goodness-of-fit of the models.

https://doi.org/10.5194/egusphere-2023-3069
Preprint. Discussion started: 29 January 2024

195 Lastly, we repeated the analysis for the seven sub-basins of the Amazon to examine whether the Amazon-wide response would be similar or dissimilar within its basins. The boundaries of the sub-basins were taken from the HydroBASINS database (Lehner and Grill, 2013), in which a basin is divided into sub-basins where a river splits into its tributaries, each of which have upstream areas of at least $100km^2$.

ENV_PARAM	STAT	LAI	LDMC	LNC	LPC	NDVI	SLA
ET_mean	β^*	0.115	-0.144	0.134	0.098	0.600	-0.306
(r^2: 0.542)	t-value	67.606	-66.709	66.136	59.073	285.292	-134.874
	p-value	0.000	0.000	0.000	0.000	0.000	0.000
ET_std	β^*	0.003	0.135	-0.136	-0.205	-0.069	0.388
(r^2: 0.125)	t-value	1.165	45.413	-48.445	-89.359	-23.752	123.717
	p-value	0.244	0.000	0.000	0.000	0.000	0.000
PET_mean	β^*	-0.291	0.067	-0.016	-0.388	0.112	0.469
(r^2: 0.364)	t-value	-144.934	26.306	-6.699	-198.106	45.341	175.543
	p-value	0.000	0.000	0.000	0.000	0.000	0.000
PET_std	β^*	0.140	0.139	-0.117	-0.148	-0.052	0.220
(r^2: 0.055)	t-value	57.324	44.950	-40.122	-61.951	-17.079	67.494
	p-value	0.000	0.000	0.000	0.000	0.000	0.000
VPD_mean	β^*	-0.383	0.082	-0.034	-0.340	0.102	0.367
(r^2: 0.324)	t-value	-184.861	31.449	-13.763	-168.270	39.788	133.132
	p-value	0.000	0.000	0.000	0.000	0.000	0.000
VPD_std	β^*	-0.197	0.028	0.014	-0.463	0.039	0.454
(r^2: 0.386)	t-value	-99.818	11.147	5.848	-240.973	15.980	173.059
	p-value	0.000	0.000	0.000	0.000	0.000	0.000
LSTday_mean	β^*	-0.542	-0.131	0.069	-0.151	0.426	0.305
(r^2: 0.404)	t-value	-278.614	-53.378	29.719	-79.922	177.709	118.156
	p-value	0.000	0.000	0.000	0.000	0.000	0.000
LSTday_std	β^*	-0.009	-0.034	0.002	-0.044	-0.733	0.182
(r^2: 0.715)	t-value	-6.845	-20.256	1.517	-33.594	-441.665	101.648
	p-value	0.000	0.000	0.129	0.000	0.000	0.000
LSTnight_mean	β^*	-0.340	0.049	-0.036	-0.156	0.694	0.161
(r^2: 0.436)	t-value	-179.404	20.291	-15.859	-84.494	297.600	64.093
	p-value	0.000	0.000	0.000	0.000	0.000	0.000
LSTnight_std	β^*	0.119	0.049	-0.110	-0.015	-0.165	0.237
(r^2: 0.076)	t-value	49.049	15.973	-38.420	-6.420	-55.252	73.603
	p-value	0.000	0.000	0.000	0.000	0.000	0.000
SM_mean	β^*	-0.282	0.080	-0.092	0.205	0.306	-0.103
(r^2: 0.175)	t-value	-123.127	27.734	-33.684	92.073	108.514	-33.806
	p-value	0.000	0.000	0.000	0.000	0.000	0.000
SM_std	β^*	0.032	-0.008	-0.010	-0.233	0.034	0.221
(r^2: 0.083)	t-value	13.163	-2.643	-3.445	-99.109	11.286	68.880
	p-value	0.000	0.008	0.001	0.000	0.000	0.000

Table 2. Multivariate regression results for the Amazon Basin

https://doi.org/10.5194/egusphere-2023-3069
Preprint. Discussion started: 29 January 2024

3 Results

3.1 Amazon Basin

Plant traits across the Amazon basin had significant effects on both regulation of atmospheric water and regulation of land surface temperature, while they exerted no significant effect on the regulation of soil water content (Figures 3, 4 and 6, Table 2). In the next subsections we will detail the results for each of the processes.

3.1.1 Regulation of atmospheric water content

We find strong associations between SLA and NDVI with ET, yet these are negative for SLA and positive for NDVI (ET_mean: $r^2 = 0.542, p < 0.0001$, SLA $\beta^* = -0.306, p < 0.001$, NDVI $\beta^* = 0.6, p < 0.001$). We also find strong associations of SLA, LPC and LAI with PET (PET_mean: $r^2 = 0.364, p < 0.0001$, SLA $\beta^* = 0.469, p < 0.001$, LPC $\beta^* = -0.388, p < 0.001$, and LAI $\beta^* = -0.291, p < 0.001$) and with VPD (VPD_mean: $r^2 = 0.324, p < 0.0001$, SLA $\beta^* = 0.367, p < 0.001$, LPC $\beta^* = -0.340, p < 0.001$, and LAI $\beta^* = -0.383, p < 0.001$), in both cases positive for SLA and negative for LPC and LAI. The associations were stronger for the mean of these parameters than for their standard deviation, except for VPD (Table 2).

Generally, we find that the direction of the associations between traits and atmospheric water parameters changes at the extreme values of the response environmental parameters. First, we find that the explained variance of the quantile regression models tends to be higher at extreme high values and lower at extreme low values of the atmospheric water parameter, except for ET_mean (Figure 3). Second, we find that the relationships between SLA with ET become decoupled (i.e. no relationship) at extreme high values while stronger at extreme low values (Figure 4). Yet, the relationships of SLA with PET and VPD show the opposite patterns, stronger at extreme high values and decoupled at extreme low values. LPC and LNC show generally weak associations at both extreme low and extreme high values of all the atmospheric water parameters. Associations of LDMC with PET and VPD are decoupled at extreme low values and strongly negative at extreme high values. LDMC with ET associate with a stronger positive effect at extreme low values while decoupling at extreme high values (Figure 4). Finally, the vegetation indices somewhat mimick this pattern, but only with NDVI showing strong associations with ET at extreme low values but not at extreme high values (Tables B9 and B25 in the appendix with quantile regression results).

3.1.2 Regulation of land surface temperature

Like for the regulation of atmospheric water content, both traits and vegetation indices regulate day and night LST (Table 2). We find that SLA and NDVI are positively associated with LSTday_mean, while the other traits and LAI are negatively associated with LSTday_mean ($r^2 = 0.404, p < 0.0001$, SLA $\beta^* = 0.305, p < 0.001$, LPC $\beta^* = -0.151, p < 0.001$, LDMC $\beta^* = -0.131, p < 0.001$, NDVI $\beta^* = 0.426, p < 0.001$, LAI $\beta^* = -0.542, p < 0.001$). Models for LSTnight_mean perform better, however, effect sizes are weaker for SLA and LAI, stronger for NDVI and not significant for LDMC ($r^2 = 0.436, p < 0.0001$, SLA $\beta^* = 0.161, p < 0.001$, LPC $\beta^* = -0.156, p < 0.001$, NDVI $\beta^* = 0.694, p < 0.001$, LAI $\beta^* = -0.340, p < 0.001$; Fig-

https://doi.org/10.5194/egusphere-2023-3069
Preprint. Discussion started: 29 January 2024

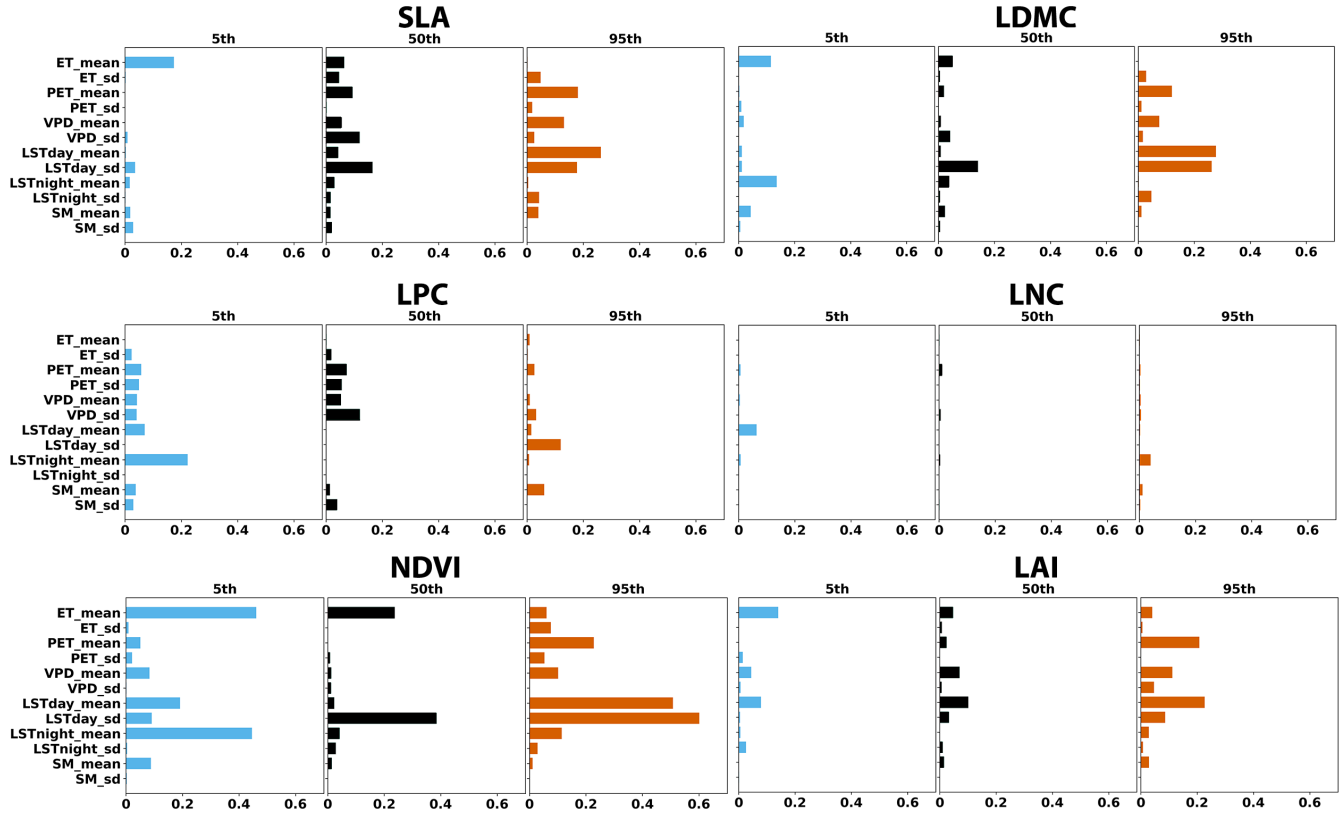

Figure 3. The percentage of explained variance at the 5th, 50th and 95th quantiles of water cycle parameters in response to plant traits and vegetation indices. All regressions are significant with $p < 0.0001$.

ure 3). In contrast, only few associations emerge between traits and the standard deviation of land surface temperature, between LSTday_stdev and NDVI ($\beta^* = -0.733, p < 0.001$) and SLA ($\beta^* = 0.182, p < 0.001$).

The direction and magnitude of the relationships between traits and land surface temperature also changes at extreme values, and we generally obtain stronger models at extreme high values (Figure 3). We find stronger and generally positive relationships of SLA, LDMC, NDVI and LAI with extreme high and low values of LSTday, but no relationship with LPC (Figure 3). Fewer traits, SLA, LDMC and NDVI, show stronger relationships at extreme values of LSTnight mostly for the extreme low values of LSTnight, yet the relationship decouples for LPC and LAI (Figure 3). Yet the explanatory power of these relationships is low (Figures 3 and 6, Table B9 in the appendix).

https://doi.org/10.5194/egusphere-2023-3069
Preprint. Discussion started: 29 January 2024

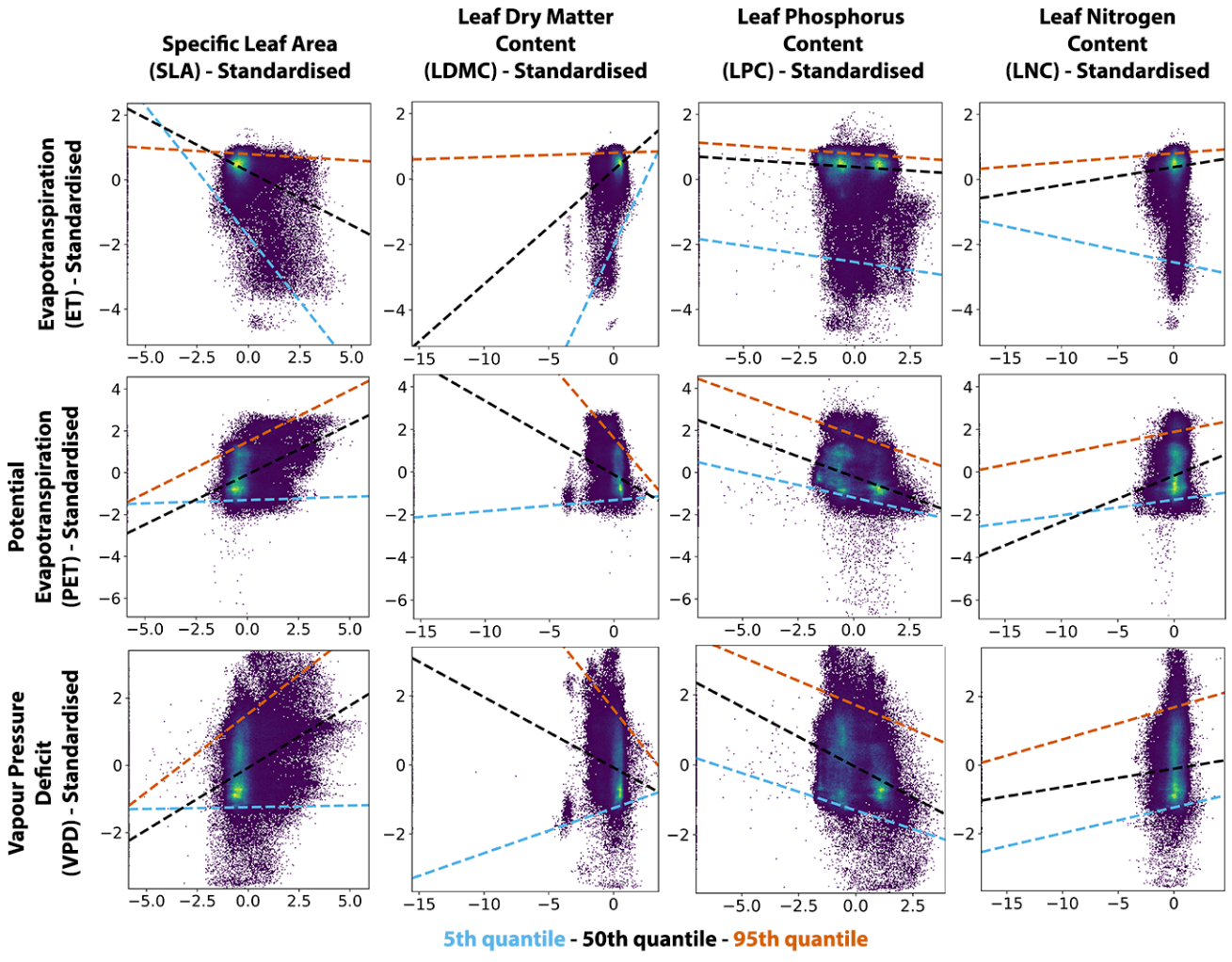

Figure 4. Quantile regressions for the relation between plant traits and environmental parameters related to the regulation of atmospheric water content for the Amazon Basin.

3.1.3 Regulation of soil moisture content

We find very little influence of traits and vegetation indices on SM, with just a small contribution of SLA and LPC (Figure 3). Further, the direction of the relationships does not change at extreme values, with the exception of LPC at extreme low values of SM (Figure 6).

https://doi.org/10.5194/egusphere-2023-3069
Preprint. Discussion started: 29 January 2024

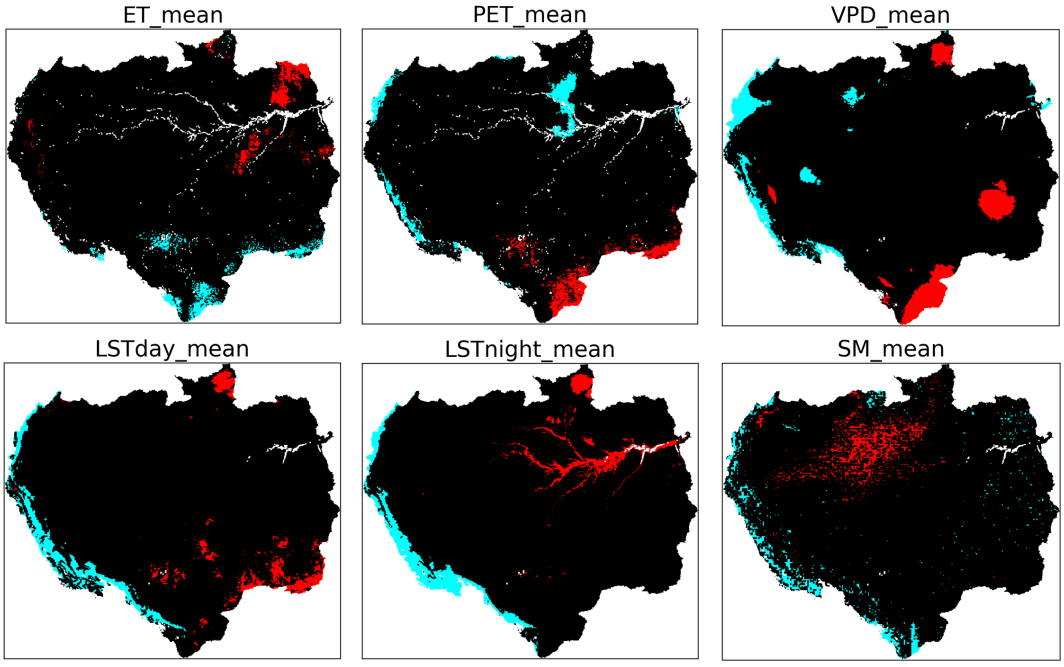

Figure 5. Location of extreme values of water cycle parameters (extreme low - 5th quantile: blue, extreme high - 95th quantile: red)

3.2 Sub-basins:

Our analysis at the sub-basin level reveals that also at this local scale both traits and vegetation indices display generally a stronger control over atmospheric water content and land surface temperature than over soil moisture content. In general, we find the same traits and vegetation indices controlling these processes at the sub-basin level, yet with stronger effects, as detailed in the next sections and in appendix B.

3.2.1 Regulation of atmospheric water content

At the sub-basin level, the models tend to be stronger than those for the whole of the Amazon basin, in particular for the Xingu and Madeira sub-basins. For ET, model performance almost doubled for five sub-basins (Xingu: $r^2 = 0.741$, Tapajós: $r^2 = 0.702$, Negro: $r^2 = 0.632$, Madeira: $r^2 = 0.627$, Solimões: $r^2 = 0.62$) and was lower for the Amazonas and Trombetas sub-basins (Amazonas: $r^2 = 0.474$, Trombetas: $r^2 = 0.352$). Model performance for PET also improved for four sub-basins (Xingu: $r^2 = 0.799$, Tapajós: $r^2 = 0.667$, Amazonas: $r^2 = 0.48$, Madeira: $r^2 = 0.422$), and for VPD model performance was higher in 3 sub-basins (Xingu: $r^2 = 0.614$, Negro: $r^2 = 0.549$, Madeira: $r^2 = 0.437$).

The most influential traits and vegetation indices were similar to those we observed for the whole basin analysis, yet some changed the direction of their effect. Specifically, LAI switched effect direction for all sub-basins, LPC and SLA switched effect for four sub-basins, and NDVI for two. Further, in two sub-basins, LNC and LDMC effect became significant (LNC:

https://doi.org/10.5194/egusphere-2023-3069
Preprint. Discussion started: 29 January 2024

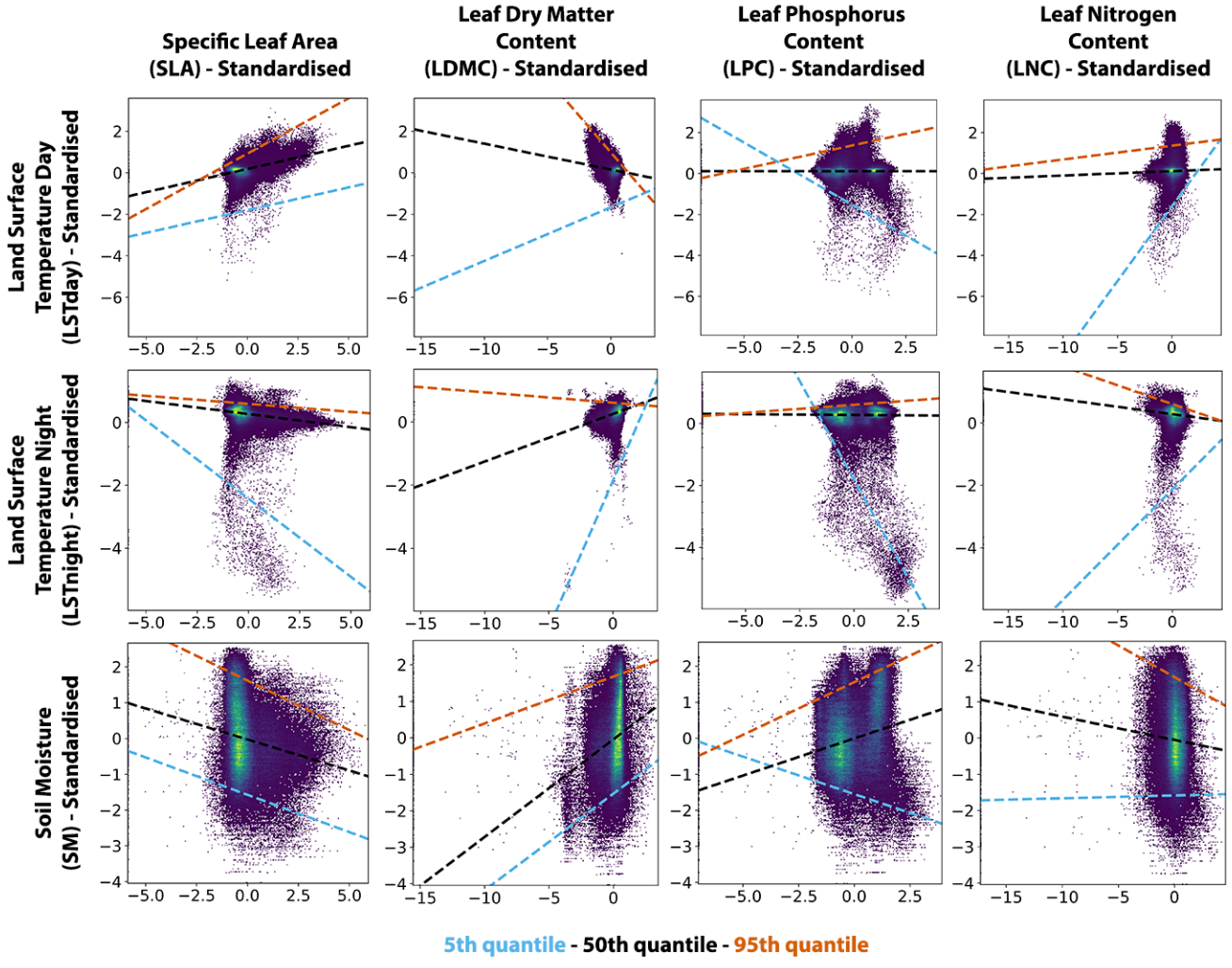

Figure 6. Quantile regressions for the relation between plant traits and environmental parameters related to regulation of surface temperature and soil moisture for the Amazon Basin.

Xingu and Amazonas; LDMC: Negro and Solimões). Most of these changes were due to significant relationships between traits and vegetation indices with VPD, which had not emerged at the whole basin analysis.

We also find that for the sub-basins, the effect of traits and vegetation indices changed at extreme values mostly for ET and only twice for PET and VPD. We find that at extreme low values of ET, SLA increases model explanatory power for the Negro ($r^2 = 0.303, p < 0.0001$, SLA $\beta^* = -1.068, p < 0.001$) and Xingu sub-basins ($r^2 = 0.179, p < 0.0001$, SLA $\beta^* = -0.748, p < 0.001$). In addition, also for extreme low values of ET, LDMC effect becomes significant in four sub-basins, namely at Negro (ET: $r^2 = 0.301$), Solimões (ET: $r^2 = 0.177$), Tapajós (ET: $r^2 = 0.174$) and Xingu (ET: $r^2 = 0.197$). Further,

https://doi.org/10.5194/egusphere-2023-3069
Preprint. Discussion started: 29 January 2024

at low values of ET, LPC is important in Tapajós (ET: $r^2 = 0.157$). Models with NDVI have more explanatory power for six out of the seven sub-basins, only not different for Trombetas. Further, LAI becomes important for Tapajós and Xingu both for ET and PET, and even VPD in Xingu (Tapajós: ET: $r^2 = 0.368$, PET: $r^2 = 0.263$; Xingu: ET: $r^2 = 0.395$, PET: $r^2 = 0.5$, VPD: $r^2 = 0.232$). At extreme high values of ET, we found no strong associations. Meanwhile, for extreme high values of PET we found a higher explanatory power of models for Madeira (LAI: $r^2 = 0.271$), Negro (NDVI: $r^2 = 0.305$, SLA: $r^2 = 0.3$, LDMC: $r^2 = 0.339$), Tapajós (LAI: $r^2 = 0.402$, NDVI: $r^2 = 0.471$, LDMC: $r^2 = 0.183$, LPC: $r^2 = 0.149$), and Xingu (LAI: $r^2 = 0.584$, NDVI: $r^2 = 0.408$). For VPD, we find additional significant models for Madeira (NDVI and LAI) and Negro (NDVI, SLA and LDMC) at extreme high and low values.

3.2.2 Regulation of land surface temperature

At the sub-basin level, also for LST, the models were stronger than those for the whole of the Amazon basin for six of the sub-basins. For LSTday, model performance doubled for three sub-basins (Xingu: $r^2 = 0.862$, Tapajós: $r^2 = 0.838$, Negro: $r^2 = 0.774$), while was also higher than the model for the whole basin for three other sub-basins (Solimões: $r^2 = 0.695$, Amazonas: $r^2 = 0.598$, Madeira: $r^2 = 0.437$). Trombetas was the only sub-basin with lower model performance than the whole basin (Trombetas $r^2 = 0.398$). At the whole basin, all traits and vegetation indices regulated LSTday, except for LNC which becomes significant for Madeira. The other traits and vegetation indices switched their importance at the sub-basin level; LPC and NDVI switched for five sub-basins (both not switching for Madeira, LPC not switching for Trombetas, and NDVI not switching for Solimões), SLA, LDMC and LAI switched for two sub-basins.

For LSTnight, model performance doubled for one sub-basin (Solimões: $r^2 = 0.803$), while also much higher than the model for the whole basin for five other sub-basins (Amazonas: $r^2 = 0.605$, Tapajós: $r^2 = 0.564$, Xingu: $r^2 = 0.561$, Trombetas: $r^2 = 0.559$, Negro $r^2 = 0.46$, Madeira: $r^2 = 0.439$). At the whole basin all traits and vegetation indices regulated LSTnight, except for LNC which becomes significant for Amazonas and Madeira. The other traits and vegetation indices switched their importance at the sub-basin level; SLA switched its importance for five sub-basins (not switching for Amazonas and Tapajós), LPC for four sub-basins, LAI and NDVI for three, and LDMC for only one sub-basin (Negro).

We also find that the effect of traits and vegetation indices changes at extreme values of LST for the sub-basins. At extreme low values of LSTday_mean, only the vegetation indices become significant, mostly through the addition of LAI to the models for three sub-basins (Negro ($r^2 = 0.286$), Trombetas ($r^2 = 0.272$) and Xingu ($r^2 = 0.234$)). Finally, for Solimões, model explanatory power increased at extreme low values of LSTday_mean for NDVI ($r^2 = 0.264$). At extreme high values of LSTday_mean, model explanatory power increased for both vegetation indices in Negro, Tapajós and Xingu, and also LAI for Amazonas. In general, higher LSTday values became less important, except for the Negro sub-basin where SLA and LDMC increased model performance, and in Xingu where we find a new effect of LPC ($r^2 = 0.164$). For LSTnight, we find new significant models for four of the six sub-basins, namely Amazonas (LNC, NDVI and LAI), Negro (NDVI, LAI), Trombetas (LNC, NDVI, LAI), and Xingu (LAI).

https://doi.org/10.5194/egusphere-2023-3069
Preprint. Discussion started: 29 January 2024

3.2.3 Regulation of soil moisture content

Unlike the two other processes, trait effects on the regulation of soil moisture content were also mostly not significant at the sub-basin level. Yet, we find that this process becomes locally important at Solimões ($r^2 = 0.349, p < 0.0001$, LPC $\beta^* = 0.200, p < 0.001$, LAI $\beta^* = -0.381, p < 0.001$, NDVI $\beta^* = 0.495, p < 0.001$), Tapajós ($r^2 = 0.225, p < 0.0001$, LAI $\beta^* = -0.210, p < 0.001$, NDVI $\beta^* = -0.342, p < 0.001$) and Trombetas ($r^2 = 0.118, p < 0.0001$, LPC $\beta^* = 0.232, p < 0.001$, NDVI $\beta^* = -0.238, p < 0.001$). We find no differences in model performance at either extreme of soil moisture values at the sub-basin level, with the exception of Tapajós where both vegetation indices become significant at extreme high values of SM_mean (NDVI: $r^2 = 0.221$, $\beta^* = -0.691, p < 0.001$, LAI: $r^2 = 0.15$, $\beta^* = -0.584, p < 0.001$).

4 Discussion

In our study we examined whether plant traits affect water related processes for the whole Amazon basin and its sub-basins. We find that at the Amazon basin scale, both traits and vegetation indices have strong effects on the regulation of atmospheric water content and land surface temperature parameters but not on the regulation of soil moisture content, and these relationships generally became stronger at extreme values of water process parameters. More specifically, SLA and both NDVI and LAI exerted the greatest influences on all water processes, with some contribution of LPC to atmospheric water regulation. We find generally consistent results for both the entire Amazon basin and its sub-basins, yet the effect of traits on water-related processes became stronger at sub-basin level.

4.1 Plant traits and regulation of atmospheric water content

Plants with larger leaves likely intercept more water, making this water available to the atmosphere (Liu et al., 2019), yet surprisingly we find a negative effect of SLA on ET_mean while positive with PET_mean, VPD_mean and VPD_std. First, these results could be a function of the method and data we used. It could be that the estimates of SLA we used (Moreno-Martínez et al., 2018b) are not sufficiently accurate; yet, the authors report a mean error of 0.01 and a root mean square error (RMSE) of 3.13 for the values of SLA, and a mean error of -0.031 and RMSE of 3.18 for the overall model, which suggests that the modeled SLA values are reasonable. Further, (Moreno-Martínez et al., 2018b) report that SLA has lower values and the lowest RMSE for broad-leaf evergreen vegetation in comparison to other traits in tropical areas. The approach by (Moreno-Martínez et al., 2018b) was deemed one of the best approaches to estimate traits in comparison with other global approaches (Dechant et al., 2023). Previous studies showed that SLA is generally well estimated using remote sensing spectral information, and tends to be more stable than the estimates of, for example, LNC and LPC (Asner and Martin, 2008). In addition, the predicted SLA values from (Moreno-Martínez et al., 2018b) achieve higher correlation with those predicted based on theoretical optimality of plant function than other traits (Dong et al., 2023). Yet the vertical stratification of SLA in the Amazon forest, lower at the top of the canopy and almost double at the bottom of the canopy (McWilliam et al., 1993), could have an effect in what is measurable from remote sensing. Second, in our multivariate model other traits could potentially

https://doi.org/10.5194/egusphere-2023-3069
Preprint. Discussion started: 29 January 2024

uptake the variance space of SLA. SLA is expected to be correlated with LNC and LPC (Moreno-Martínez et al., 2018b), so the inclusion of the later two variables in the model could have had an effect on the magnitude and direction of the effect SLA has on water process parameters. Yet, the correlation between SLA and LNC and LNP is still under debate (Ordoñez et al., 2009; García-Palacios et al., 2018; Chu and Farrell, 2022; Reich et al., 1999). Further, we tested for variance inflation by multicollinear variables and found weak pair-wise correlations, therefore we can assume that the variance attributable to SLA is not being affected by LNC and LPC. Third, since we are using averages over a ten year period when there was substantial deforestation over the Amazon, this could have affected the values of SLA in specific areas. We do find that the strong negative relationship between SLA and ET_mean is most exclusively restricted to the Amazonas and Madeira sub-basins, where the majority of deforestation occurred (Acre - 3.2%, Rondônia - 12%, Beni - 3% (Potapov et al., 2022)). As primary forest was lost, degraded or replaced by secondary forest or other vegetation types, SLA could have decreased. Deforestation has been reported to significantly decrease ET (Davin and Noblet-Ducoudré, 2010; Devaraju et al., 2015) in particular in the Amazon (Baker and Spracklen, 2019; Heerspink et al., 2020). Mechanistically, we know that old trees tend to have higher dry matter content and smaller leaf area compared to young trees (Lohbeck et al., 2013, 2015), and old leaves could have lower gas exchange capacity, which would result in lower SLA values and therefore explain the negative relationships. Further, the leaves of Amazonian trees show a trade-off between tissue toughness and organ size with leaf display (Poorter et al., 2018), which could constrain SLA values and how they relate with ET. A meta-analysis conducted by (Niinemets et al., 1999) suggests that SLA may not have a consistent effect of photosynthesis as leaf thickness and leaf density showed opposing effects, and therefore could explain our results for gas exchange. Finally, much local variation exists in traits that could result in the overall negative effect we found for the whole Amazon. We found that for four other sub-basins the relationship between SLA and ET switched from negative to positive. Models were stronger at the sub-basin level, almost doubling their explanatory power thus suggesting that further analysis is needed to understand what drives the relationships between SLA and water processes at different scales.

We find a negative relationship between LPC and PET_mean, VPD_mean and VPD_std. The negative relationship with PET_mean could be attributed to the characteristic phosphorous limitation on photosynthesis of tropical forests (Mercado et al., 2011), not meeting the potential ET that could have been achieved. The negative relationships of LPC with VPD were well-aligned with previous results by (Grossiord et al., 2020), which showed declines in stomatal conductance with increases in VPD. High VPD tends to occur in more arid environments (Fang et al., 2022) and therefore we would not expect that to be the case in the Amazon. Yet, within the typical range of VPD for tropical forests, we would expect some response mediated by LPC given that phosphorous limits photosynthetic activity in these ecosystems. Photosynthesis rates in tropical areas are more sensitive to LPC than LNC (Walker et al., 2014), and this sensitivity is very important in models of carbon fluxes over the Amazon (Mercado et al., 2011). Yet, (Grossiord et al., 2020) also showed that transpiration increased with VPD until a VPD threshold, with potential subsequent effects up to hydraulic failure. Thus, this suggests that it is important to address the effect of multiple traits simultaneously to better understand plant trait effects on water processes, to obtain more detailed information under which conditions one trait effect may or not supersede that of another trait, as we see in our results and suggest as avenue for future research.

https://doi.org/10.5194/egusphere-2023-3069
Preprint. Discussion started: 29 January 2024

Traits and vegetation indices show different effects, with only a positive strong relationship between NDVI and ET_mean. Previous studies using data from eddy covariance sites in tropical areas, showed that NDVI was the second most influencing factor in determining ET, after solar radiation (Fisher et al., 2009). NDVI is an integrative measure of plant performance and therefore could be indicating the overall net trait effects, yet because it is very general and its values tend to asymptote in high canopy density (i.e. higher NDVI does not linearly relate with higher vegetation cover), these relationships need to be addressed with more detailed information such as that provided by individual plant traits or with plant trait syndromes. We suggest that more detailed studies need to be conducted to further our understanding of the net effect of multiple traits and under which conditions do they result in different NDVI values, so that this metric, very valuable for its applicability, can be better interpreted. We found that LAI was strongly negatively associated with PET_mean, VPD_mean and VPD_std, suggesting a strong control in the water exchange capacity by plants and aligned with our previous results, yet ET potential was not fully achieved. Several factors may contribute to these results. The negative relationships of LAI with VPD align with reported controls of plant water status and phenology on LAI, which may constrain tree and stand transpiration as obtained from eddy-covariance measurements on tropical semi-deciduous trees in the southern Amazon Basin (Vourlitis et al., 2008) and in central Brazil (Giambelluca et al., 2009). Further, if considering that an increase in LAI could lead to increase in rainfall interception as shown by (Gómez et al., 2001) and rise in canopy conductance (Van Heerwaarden and Teuling, 2014), which in turn would result in decreases in VPD. Finally, the decrease in the rate of water loss with increasing leaf size (Wang et al., 2019b) could be because plants with small leaves may more quickly loose water and therefore exert a stronger control on VPD and result in lower than expected PET. These results align with the results we obtained for SLA, which suggest that maybe through an effect of deforestation, drought or volatility in hydrological conditions over space or time, or the effects of different traits superseding the effects of other traits under varying conditions, would have resulted in this lower than expected PET.

4.2 Plant traits and regulation of land surface temperature

We found strong relationships between SLA, NDVI, LPC and LAI and LSTday_mean and LSTnight_mean, with the first two having overall warming effects and the later two showing cooling effects in the Amazon Basin. We find strong positive associations of SLA with LST at both basin and sub-basin scales, and aligns with the negative relationship that we observe between SLA and ET. With high SLA yet low ET there is less potential for evaporative cooling, hence higher LST as a result. Similarly, at the sub-basin scale we also find significant positive associations between SLA and extreme high values of LSTday_mean, while only one sub-basin maintains the relationship at extreme low values of LSTday_mean. As mentioned above, the relationship and effects of SLA on water cycle processes are still under debate, yet our finding that SLA may induce higher land surface temperature deserves more attention, as this is potentially problematic as it might exacerbate local effects of climate change that might emerge from land use and deforestation in some regions of the basin.

Like for the regulation of atmospheric water content, LPC also exerts controls over LST, with an observed negative effect. Therefore increasing LPC and its effect on photosynthesis, increases the potential for evaporative cooling and therefore decreases in land surface temperature. Limitation in phosphorus has been reported to affect plant adaptation strategies, and particularly for the Amazon Basin, total amount of phosphorus in the soil was found to be a strong predictor of wood produc-

https://doi.org/10.5194/egusphere-2023-3069
Preprint. Discussion started: 29 January 2024

tion (Quesada et al., 2012). Yet, at the sub-basin level, LPC switches the direction of the effect for a large fraction of the basin, only not switching for Madeira and Trombetas for LSTday_mean and Tapajós for LSTnight_mean. These local effects could be linked to the differences in soil phosphorus distribution across the Amazon Basin. Soil in western regions of the Amazon contain significantly larger phosphorus concentrations than the northern, southern, eastern and central regions (Reichert et al., 2022), and this distribution aligns well with the sub-basins where we found a shift in effect.

We also find that LAI and NDVI exert controls over land surface temperature. We found negative controls of LAI over both LSTday and LSTnight, which agrees on the reported cooling effect induced by vegetation. Dense and highly productive tropical forests have strong cooling effects on local climatology (Li et al., 2015), reported to result in a difference in temperature between vegetation-covered and open areas of $-2.41°C$ on average. In the Amazon, vegetation in protected areas has been shown to have net cooling effects between $0.51 - 0.98°C$ (Huang et al., 2022). The vegetation cooling effect may be driven by the enactment of two mechanisms. Canopy shading may reduce canopy temperature by blocking direct sun light. The other mechanism, evaporative cooling, reduces latent heat as it uses this energy to transfer water from liquid to vapour states (Tan et al., 2018; Ghafarian et al., 2022). On both basin-wide and sub-basin scales of the Amazon, vegetation cooling effects have been shown to be much stronger during daytime than nighttime (Huang et al., 2022). This is consistent with what we found, with a steeper slope of the relationship between LAI and LSTday_mean than LSTnight_mean (-0.54 versus -0.34). This difference could be explained by the lack of incident radiation during the nighttime, yet still with a strong effect of the emission of shortwave radiation during the night time from radiation that was absorbed during daytime (Michiles and Gielow, 2008). Though, since daytime evaporative cooling largely compensates nighttime warming, there is a net cooling effect at night (Li et al., 2015).

In contrast with LAI, we found positive relationships between NDVI and LST at the whole basin level and mixed relationships at the sub-basin level (6 significant negative and 4 significant positive relationships). These mixed responses are misaligned with the result that NDVI has significant positive relationships with ET_mean across all sub-basins, which would imply higher evaporative cooling potential. It could be that evaporative cooling is not the sole mechanism that links NDVI and LST, and that there are differences in irradiation across the sub-basins which would not be compensated by evaporative cooling. Further, as already mentioned above, it could also be because of the assymptotic behavior of NDVI, and therefore the effect of NDVI through evaporative cooling can only be detected for intermediate NDVI values. Further it could be that under higher temperature at local scales, photosynthesis rate increases until the optimum temperature is reached, after which the rate sharply decreases (Crous et al., 2022).

4.3 Plant traits and regulation of soil moisture content

We found no regulation of plant traits on soil moisture content, except for a few weak relationships for at Solimões, Tapajós and Trombetas sub-basins. Previous studies report that higher canopy cover could reduce soil moisture content, via increases in both evaporation and interception of precipitation (Zhang et al., 2020; Dai et al., 2022) and root uptake (Chen et al., 2008; Fan et al., 2017; Gavrilescu, 2021), which could ultimately lead to a positive feedback between soil moisture and plant performance (D'Odorico et al., 2007). However, these studies were conducted in arid and semi-arid ecosystems (Cheng et al.,

https://doi.org/10.5194/egusphere-2023-3069
Preprint. Discussion started: 29 January 2024

2021; Yang et al., 2012; Gou and Zhu, 2021) where water is the limiting factor with average annual rainfall below 600mm. In our study area annual rainfall ranges between 1400mm and 3000mm (Mu and Jones, 2022) and with large floodplains over which approximately 30% of Amazon discharge passes through (Miguez-Macho and Fan, 2012). In addition, soil moisture in shallow soil layers across the Amazon Basin could be restored by water fluxes from the deeper level via capillary tension (Miguez-Macho and Fan, 2012; Romero-Saltos et al., 2005) and hydraulic redistribution, especially during the dry seasons. Yet, we know that for the Amazon basin in particular, water table depth exerts a strong control on water processes (O'connor et al., 2019), yet it could be that because we do not have measurements of root traits such as root architecture and root depth, we are unable to capture these effects using mostly gas exchange and photosynthesis related traits.

Overall, and importantly, we the quantile regression results show a very strong and potential feedback mediated by plant traits. Plant traits exert a stronger control at extreme low values of ET and PET at the same time the same traits exert a stronger control at extreme high values of VPD and LST, which are internally consistent. These results suggest that plant traits may have a yet underexplored capacity to control water fluxes especially as current and future conditions for the Amazon basin are predicted to be higher temperature and VPD, which could in turn result in a feedback reducing ET and PET. In Figure 5, we show the potentially problematic areas in the Amazon basin for the timeperiod we examined, where there are extreme low values of ET and PET and extreme high values of values of VPD and LST. We find that while these values are distributed across the basin suggesting that this potential effect mediated by plant traits may not be yet taking place, in Xingu and Tapajós there is already some spatial overlap between low ET and PET and high LST and VPD where plant traits may already have this double mediating effect.

4.4 Limitations of the study

In this study, we analyzed the relationship between plant traits and water cycle parameters using a selected set of 4 plant traits and 2 vegetation indices and 6 water process parameters. While the relationships between plant traits and water regulation have been previously hypothesized, these indicators were selected as a combination of known effects and available data. Firstly, the plant characteristics we examined in this study were limited to those describing phenology (SLA, LDMC, NDVI), biochemistry (LPC, LNC), and vegetation cover (NDVI and LAI). Other plant traits have been shown to play significant roles in regulating evapotranspiration, such as stomatal conductance per leaf area or leaf dry mass (Wehr et al., 2017; Ding et al.) and root traits (fine root dry mass, rooting depth) (Fort et al., 2017; Delfin et al., 2021; Shao et al., 2022). Yet data for the later set of traits is currently not available in a spatially continuous way over the entire basin nor with a large sampling at point locations within the basin as reflected in the low number of values in the TRY database (Kattge et al., 2020). It would be interesting to follow up our study by examining other traits, even if in a non spatially-explicit manner. Second, plant trait values were generated using machine learning (Moreno-Martínez et al., 2018b). The generated trait distribution prediction had a reasonable agreement with in-situ measurements and other studies with similar goals. Third, our analysis was conducted on averages over ten years which may not capture finer temporal dynamics between plants and water cycle parameters, but rather broad associations. For example, the Amazon exhibits a strong seasonal variation in ET with annual minima between April-June and maxima between August-October and with peaks during the dry season and lower ET during the wet season (Baker et al., 2021), which may not

https://doi.org/10.5194/egusphere-2023-3069
Preprint. Discussion started: 29 January 2024

be captured with averages over a decade. Decreasing precipitation and intensifying solar radiation accelerates photosynthesis activities, and the trend has been reported to be more significant especially in wet parts of the Amazon Basin (Green et al., 2020; Guan et al., 2015; Kim et al., 2012). As such these limitations in the data and methods used could be further explored as additional trait data becomes available, for example from new remote sensing products (Ustin and Middleton, 2021) and we better understand the role of biodiversity on ecosystem functioning (Yan et al., 2023).

5 Conclusion

We found that plant traits have significant effects on the regulation of atmospheric water and the regulation of land surface temperature but not on the regulation of soil moisture content. The most important effects were driven by SLA and LPC, as well as the two vegetation indices, LAI and NDVI, and these relationships tended to be stronger at the sub-basin level. This knowledge would have major implications on our understanding of the stability of the Amazon forest but more fundamentally on how traits affect earth system processes. Further, we find regulating effects on atmospheric water exchange and land surface temperature but not on soil moisture content, likely because the later is driven by root depth, a trait that is not (yet) measurable with remote sensing. Most importantly, we might have unveiled an emerging effect of plant traits on water processes through the coupled effect of plant traits on high VPD and LST and low ET and PET (Figure 5). These results can already unveil some hypotheses on how water cycle processes might unveil into the future, which could be potentially problematic for the persistence of the Amazon as it might suggest less capacity to respond to ongoing and non-linear climate changes. Our results suggest this to be the case for ET and PET which would correspond to a potential drying out of the system and reduced capacity for processes like moisture recycling to maintain the forest (O'connor et al., 2019). On the other hand, with such reduction in ET and PET we would expect a move towards higher VPD and LST values, which we also found to be more sensitive to the effects of plant trait composition. As such the potential of trait-based approaches is not yet fully explored and dimensions of effects like the ones examined herein as well as overall functional diversity. Also, the stronger local effects are interesting and potentially resulting from localized impacts of land use change and deforestation, which might scale up to water fluxes potential to regulate climate at local and global scales. Together, these results suggest that plant traits can in fact be an important component to the regulation of the processes that maintain the Amazon forest, potentially amplifying or mediating feedbacks, yet to date seldom analyzed despite their potential effects in regulating the Amazon responses to ongoing and future global changes.

Competing interests. The contact author has declared that none of the authors has any competing interests.

Author contributions. KN and MJS designed the study; KN performed the data analysis; KN and MJS wrote the manuscript.

https://doi.org/10.5194/egusphere-2023-3069
Preprint. Discussion started: 29 January 2024

EGUsphere
Preprint repository

490 *Code and data availability.* All raw data and code can be provided by the corresponding authors upon request.

https://doi.org/10.5194/egusphere-2023-3069
Preprint. Discussion started: 29 January 2024

References

Abatzoglou, J. T., Dobrowski, S. Z., Parks, S. A., and Hegewisch, K. C.: TerraClimate, a high-resolution global dataset of monthly climate and climatic water balance from 1958–2015, Scientific Data 2018 5:1, 5, 1–12, https://doi.org/10.1038/sdata.2017.191, 2018.

Aleixo, I., Norris, D., Hemerik, L., Barbosa, A., Prata, E., Costa, F., and Poorter, L.: Amazonian rainforest tree mortality driven by climate and functional traits, Nature Climate Change, 9, 384–388, https://doi.org/10.1038/s41558-019-0458-0, number: 5 Publisher: Nature Publishing Group, 2019.

Anderegg, W. R., Anderegg, L. D., Berry, J. A., and Field, C. B.: Loss of whole-tree hydraulic conductance during severe drought and multi-year forest die-off, Oecologia, 175, 11–23, https://doi.org/10.1007/s00442-013-2875-5, publisher: Springer Verlag, 2014.

Anderegg, W. R., Trugman, A. T., Bowling, D. R., Salvucci, G., and Tuttle, S. E.: Plant functional traits and climate influence drought intensification and land–atmosphere feedbacks, Proceedings of the National Academy of Sciences of the United States of America, 116, 14 071–14 076, https://doi.org/10.1073/pnas.1904747116, 2019.

Anderegg, W. R. L.: Spatial and temporal variation in plant hydraulic traits and their relevance for climate change impacts on vegetation, New Phytologist, 205, 1008–1014, https://doi.org/10.1111/nph.12907, _eprint: https://onlinelibrary.wiley.com/doi/pdf/10.1111/nph.12907, 2015.

Anderegg, W. R. L., Konings, A. G., Trugman, A. T., Yu, K., Bowling, D. R., Gabbitas, R., Karp, D. S., Pacala, S., Sperry, J. S., Sulman, B. N., and Zenes, N.: Hydraulic diversity of forests regulates ecosystem resilience during drought, Nature, 561, 538–541, https://doi.org/10.1038/s41586-018-0539-7, 2018.

Aroca, R., Porcel, R., and Ruiz-Lozano, J. M.: Regulation of root water uptake under abiotic stress conditions, Journal of Experimental Botany, 63, 43–57, https://doi.org/10.1093/JXB/ERR266, 2012.

Ashktorab, H., Pruitt, W. O., and Paw U, K. T.: Partitioning of Evapotranspiration Using Lysimeter and Micro-Bowen-Ratio System, Journal of Irrigation and Drainage Engineering, 120, 450–464, https://doi.org/10.1061/(ASCE)0733-9437(1994)120:2(450), publisher: American Society of Civil Engineers, 1994.

Asner, G. P. and Martin, R. E.: Spectral and chemical analysis of tropical forests: Scaling from leaf to canopy levels, Remote Sensing of Environment, 112, 3958–3970, https://doi.org/10.1016/j.rse.2008.07.003, 2008.

Baker, J. C. A. and Spracklen, D. V.: Climate Benefits of Intact Amazon Forests and the Biophysical Consequences of Disturbance, Frontiers in Forests and Global Change, 2, https://www.frontiersin.org/articles/10.3389/ffgc.2019.00047, 2019.

Baker, J. C. A., Garcia-Carreras, L., Gloor, M., Marsham, J. H., Buermann, W., da Rocha, H. R., Nobre, A. D., de Araujo, A. C., and Spracklen, D. V.: Evapotranspiration in the Amazon: spatial patterns, seasonality, and recent trends in observations, reanalysis, and climate models, Hydrology and Earth System Sciences, 25, 2279–2300, https://doi.org/10.5194/hess-25-2279-2021, publisher: Copernicus GmbH, 2021.

Baudena, M., Dekker, S. C., van Bodegom, P. M., Cuesta, B., Higgins, S. I., Lehsten, V., Reick, C. H., Rietkerk, M., Scheiter, S., Yin, Z., Zavala, M. A., and Brovkin, V.: Forests, savannas, and grasslands: bridging the knowledge gap between ecology and Dynamic Global Vegetation Models, Biogeosciences, 12, 1833–1848, https://doi.org/10.5194/bg-12-1833-2015, publisher: Copernicus GmbH, 2015.

Bhandari, A. K., Kumar, A., and Singh, G. K.: Feature Extraction using Normalized Difference Vegetation Index (NDVI): A Case Study of Jabalpur City, Procedia Technology, 6, 612–621, https://doi.org/10.1016/j.protcy.2012.10.074, 2012.

Blanusa, T. and Hadley, J.: Impact of plant choice on rainfall runoff delay and reduction by hedge species, Landscape and Ecological Engineering, 15, 401–411, https://doi.org/10.1007/s11355-019-00390-x, 2019.

https://doi.org/10.5194/egusphere-2023-3069
Preprint. Discussion started: 29 January 2024

Blasini, D. E., Koepke, D. F., Bush, S. E., Allan, G. J., Gehring, C. A., Whitham, T. G., Day, T. A., and Hultine, K. R.: Tradeoffs between leaf cooling and hydraulic safety in a dominant arid land riparian tree species, Plant, Cell & Environment, 45, 1664–1681, https://doi.org/10.1111/pce.14292, _eprint: https://onlinelibrary.wiley.com/doi/pdf/10.1111/pce.14292, 2022.

Brennan, A., Cross, P. C., and Creel, S.: Managing more than the mean: using quantile regression to identify factors related to large elk groups, The Journal of Applied Ecology, 52, 1656, https://doi.org/10.1111/1365-2664.12514, 2015.

Caballero, C. B., Ruhoff, A., and Biggs, T.: Land use and land cover changes and their impacts on surface-atmosphere interactions in Brazil: A systematic review, Science of The Total Environment, 808, 152 134, https://doi.org/10.1016/j.scitotenv.2021.152134, 2022.

Cade, B. S. and Noon, B. R.: A gentle introduction to quantile regression for ecologists, www.frontiersinecology.org Front Ecol Environ, 1, 412–420, https://doi.org/10.1890/1540-9295, 2003.

Cade, B. S., Noon, B. R., and Flather, C. H.: QUANTILE REGRESSION REVEALS HIDDEN BIAS AND UNCERTAINTY IN HABITAT MODELS, Ecology, 86, 786–800, https://doi.org/10.1890/04-0785, 2005.

Caldwell, M. M., Dawson, T. E., and Richards, J. H.: Hydraulic Lift: Consequences of Water Efflux from the Roots of Plants, Oecologia, 113, 151–161, https://www.jstor.org/stable/4221835, publisher: Springer, 1998.

Casagrande, E., Recanati, F., Rulli, M. C., Bevacqua, D., and Melià, P.: Water balance partitioning for ecosystem service assessment. A case study in the Amazon, Ecological Indicators, 121, 107 155, https://doi.org/10.1016/j.ecolind.2020.107155, 2021.

Chakraborty, T., Lee, X., and Lawrence, D. M.: Strong Local Evaporative Cooling Over Land Due to Atmospheric Aerosols, Journal of Advances in Modeling Earth Systems, 13, e2021MS002 491, https://doi.org/10.1029/2021MS002491, _eprint: https://onlinelibrary.wiley.com/doi/pdf/10.1029/2021MS002491, 2021.

Chen, H., Shao, M., and Li, Y.: The characteristics of soil water cycle and water balance on steep grassland under natural and simulated rainfall conditions in the Loess Plateau of China, Journal of Hydrology, 360, 242–251, https://doi.org/10.1016/j.jhydrol.2008.07.037, 2008.

Cheng, Y., Yang, W., Zhan, H., Jiang, Q., Shi, M., Wang, Y., Li, X., and Xin, Z.: On Change of Soil Moisture Distribution With Vegetation Reconstruction in Mu Us Sandy Land of China, With Newly Designed Lysimeter, Frontiers in Plant Science, 12, https://www.frontiersin.org/articles/10.3389/fpls.2021.609529, 2021.

Christoffersen, B. O., Restrepo-Coupe, N., Arain, M. A., Baker, I. T., Cestaro, B. P., Ciais, P., Fisher, J. B., Galbraith, D., Guan, X., Gulden, L., van den Hurk, B., Ichii, K., Imbuzeiro, H., Jain, A., Levine, N., Miguez-Macho, G., Poulter, B., Roberti, D. R., Sakaguchi, K., Sahoo, A., Schaefer, K., Shi, M., Verbeeck, H., Yang, Z. L., Araújo, A. C., Kruijt, B., Manzi, A. O., da Rocha, H. R., von Randow, C., Muza, M. N., Borak, J., Costa, M. H., Gonçalves de Gonçalves, L. G., Zeng, X., and Saleska, S. R.: Mechanisms of water supply and vegetation demand govern the seasonality and magnitude of evapotranspiration in Amazonia and Cerrado, Agricultural and Forest Meteorology, 191, 33–50, https://doi.org/10.1016/J.AGRFORMET.2014.02.008, 2014.

Chu, H.-H. and Farrell, C.: Fast plants have water-use and drought strategies that balance rainfall retention and drought survival on green roofs, Ecological Applications, 32, e02 486, https://doi.org/10.1002/eap.2486, _eprint: https://onlinelibrary.wiley.com/doi/pdf/10.1002/eap.2486, 2022.

Collatz, G. J., Ribas-Carbo, M., and Berry, J. A.: Coupled Photosynthesis-Stomatal Conductance Model for Leaves of C4 Plants, Functional Plant Biology, 19, 519–538, https://doi.org/10.1071/pp9920519, publisher: CSIRO PUBLISHING, 1992.

Crockford, R. H. and Richardson, D. P.: Partitioning of rainfall into throughfall, stemslow∠d interception effect of forest type, ground cover and climate, Hydrological Processes, 14, 2903–2920, https://doi.org/10.1002/1099-1085(200011/12)14:16/17<2903::AID-HYP126>3.0.CO;2-6, publisher: John Wiley & Sons Ltd, 2000.

https://doi.org/10.5194/egusphere-2023-3069
Preprint. Discussion started: 29 January 2024

Crous, K. Y., Uddling, J., and De Kauwe, M. G.: Temperature responses of photosynthesis and respiration in evergreen trees from boreal to tropical latitudes, 234, 353–374, https://doi.org/10.1111/nph.17951, number: 2 _eprint: https://onlinelibrary.wiley.com/doi/pdf/10.1111/nph.17951, 2022.

Da Silva, J. M. C., Rylands, A. B., and Da Fonseca, G. A.: The fate of the Amazonian areas of endemism, Conservation Biology, 19, 689–694, https://doi.org/10.1111/j.1523-1739.2005.00705.x, 2005.

Dai, L., Fu, R., Guo, X., Du, Y., Zhang, F., and Cao, G.: Soil Moisture Variations in Response to Precipitation Across Different Vegetation Types on the Northeastern Qinghai-Tibet Plateau, Frontiers in Plant Science, 13, https://www.frontiersin.org/articles/10.3389/fpls.2022.854152, 2022.

Davin, E. L. and Noblet-Ducoudré, N. d.: Climatic Impact of Global-Scale Deforestation: Radiative versus Nonradiative Processes, Journal of Climate, 23, 97–112, https://doi.org/10.1175/2009JCLI3102.1, publisher: American Meteorological Society Section: Journal of Climate, 2010.

Dechant, B., Kattge, J., Pavlick, R., Schneider, F., Sabatini, F., Moreno-Martinez, A., Butler, E., Bodegom, P. v., Vallicrosa, H., Kattenborn, T., Boonman, C., Madani, N., Wright, I., Dong, N., Feilhauer, H., Penuelas, J., Sardans, J., Aguirre-Gutierrez, J., Reich, P., Leitao, P., Cavender-Bares, J., Myers-Smith, I. H., Duran, S., Croft, H., Prentice, I. C., Huth, A., Rebel, K., Zaehle, S., Simova, I., Diaz, S., Reichstein, M., Schiller, C., Bruehlheide, H., Mahecha, M., Wirth, C., Malhi, Y., and Townsend, P.: Intercomparison of global foliar trait maps reveals fundamental differences and limitations of upscaling approaches, https://eartharxiv.org/repository/view/5266/, publisher: EarthArXiv, 2023.

Delfin, E. F., Drobnitch, S. T., and Comas, L. H.: Plant strategies for maximizing growth during water stress and subsequent recovery in Solanum melongena L. (eggplant), 16, e0256 342, https://doi.org/10.1371/journal.pone.0256342, number: 9 Publisher: Public Library of Science, 2021.

Deng, Z., Guan, H., Hutson, J., Forster, M. A., Wang, Y., and Simmons, C. T.: A vegetation-focused soil-plant-atmospheric continuum model to study hydrodynamic soil-plant water relations, Water Resources Research, 53, 4965–4983, https://doi.org/10.1002/2017WR020467, _eprint: https://onlinelibrary.wiley.com/doi/pdf/10.1002/2017WR020467, 2017.

Devaraju, N., Bala, G., and Modak, A.: Effects of large-scale deforestation on precipitation in the monsoon regions: Remote versus local effects, Proceedings of the National Academy of Sciences, 112, 3257–3262, https://doi.org/10.1073/pnas.1423439112, publisher: Proceedings of the National Academy of Sciences, 2015.

Didan, K.: MODIS/Terra Vegetation Indices Monthly L3 Global 0.05Deg CMG V061, https://doi.org/10.5067/MODIS/MOD13C2.061, 2021.

Ding, R., Kang, S., Du, T., Hao, X., and Zhang, Y.: Scaling Up Stomatal Conductance from Leaf to Canopy Using a Dual-Leaf Model for Estimating Crop Evapotranspiration, 9, e95 584, https://doi.org/10.1371/journal.pone.0095584, number: 4 Publisher: Public Library of Science.

D'Odorico, P., Caylor, K., Okin, G. S., and Scanlon, T. M.: On soil moisture–vegetation feedbacks and their possible effects on the dynamics of dryland ecosystems, Journal of Geophysical Research: Biogeosciences, 112, https://doi.org/10.1029/2006JG000379, _eprint: https://onlinelibrary.wiley.com/doi/pdf/10.1029/2006JG000379, 2007.

Dong, N., Dechant, B., Wang, H., Wright, I. J., and Prentice, I. C.: Global leaf-trait mapping based on optimality theory, Global Ecology and Biogeography, 32, 1152–1162, https://doi.org/10.1111/geb.13680, _eprint: https://onlinelibrary.wiley.com/doi/pdf/10.1111/geb.13680, 2023.

https://doi.org/10.5194/egusphere-2023-3069
Preprint. Discussion started: 29 January 2024

Durán Zuazo, V. H. and Rodríguez Pleguezuelo, C. R.: Soil-erosion and runoff prevention by plant covers. A review, Agronomy for Sustainable Development, 28, 65–86, https://doi.org/10.1051/agro:2007062, 2008.

Ehleringer, J. R. and Dawson, T. E.: Water uptake by plants: perspectives from stable isotope composition, Plant, Cell & Environment, 15, 1073–1082, https://doi.org/10.1111/j.1365-3040.1992.tb01657.x, _eprint: https://onlinelibrary.wiley.com/doi/pdf/10.1111/j.1365-3040.1992.tb01657.x, 1992.

Eltahir, E. a. B. and Bras, R. L.: Precipitation recycling in the Amazon basin, Quarterly Journal of the Royal Meteorological Society, 120, 861–880, https://doi.org/10.1002/qj.49712051806, _eprint: https://onlinelibrary.wiley.com/doi/pdf/10.1002/qj.49712051806, 1994.

Fan, Y., Miguez-Macho, G., Jobbágy, E. G., Jackson, R. B., and Otero-Casal, C.: Hydrologic regulation of plant rooting depth, Proceedings of the National Academy of Sciences, 114, 10 572–10 577, https://doi.org/10.1073/pnas.1712381114, publisher: Proceedings of the National Academy of Sciences, 2017.

Fang, Z., Zhang, W., Brandt, M., Abdi, A. M., and Fensholt, R.: Globally Increasing Atmospheric Aridity Over the 21st Century, 10, e2022EF003 019, https://doi.org/10.1029/2022EF003019, _eprint: https://onlinelibrary.wiley.com/doi/pdf/10.1029/2022EF003019, 2022.

Feng, S., Liu, J., Zhang, Q., Zhang, Y., Singh, V. P., Gu, X., and Sun, P.: A global quantitation of factors affecting evapotranspiration variability, Journal of Hydrology, 584, 124 688, https://doi.org/10.1016/J.JHYDROL.2020.124688, 2020.

Fisher, J. B., Malhi, Y., Bonal, D., Da Rocha, H. R., De Araújo, A. C., Gamo, M., Goulden, M. L., Hirano, T., Huete, A. R., Kondo, H., Kumagai, T., Loescher, H. W., Miller, S., Nobre, A. D., Nouvellon, Y., Oberbauer, S. F., Panuthai, S., Roupsard, O., Saleska, S., Tanaka, K., Tanaka, N., Tu, K. P., and Von Randow, C.: The land–atmosphere water flux in the tropics, Global Change Biology, 15, 2694–2714, https://doi.org/10.1111/j.1365-2486.2008.01813.x, _eprint: https://onlinelibrary.wiley.com/doi/pdf/10.1111/j.1365-2486.2008.01813.x, 2009.

Fort, F., Volaire, F., Guilioni, L., Barkaoui, K., Navas, M.-L., and Roumet, C.: Root traits are related to plant water-use among rangeland Mediterranean species, 31, 1700–1709, https://doi.org/10.1111/1365-2435.12888, number: 9 _eprint: https://onlinelibrary.wiley.com/doi/pdf/10.1111/1365-2435.12888, 2017.

Fragal, E. H., Silva, T. S. F., and Novo, E. M. L. d. M.: Reconstructing historical forest cover change in the Lower Amazon floodplains using the LandTrendr algorithm, Acta Amazonica, 46, 13–24, https://doi.org/10.1590/1809-4392201500835, publisher: Instituto Nacional de Pesquisas da Amazônia, 2016.

Frappart, F., Minh, K. D., L'Hermitte, J., Cazenave, A., Ramillien, G., Le Toan, T., and Mognard-Campbell, N.: Water volume change in the lower Mekong from satellite altimetry and imagery data, Geophysical Journal International, 167, 570–584, https://doi.org/10.1111/j.1365-246X.2006.03184.x, 2006.

Funk, J. L., Larson, J. E., Ames, G. M., Butterfield, B. J., Cavender-Bares, J., Firn, J., Laughlin, D. C., Sutton-Grier, A. E., Williams, L., and Wright, J.: Revisiting the Holy Grail: using plant functional traits to understand ecological processes, Biological Reviews, 92, 1156–1173, https://doi.org/10.1111/brv.12275, _eprint: https://onlinelibrary.wiley.com/doi/pdf/10.1111/brv.12275, 2017.

García-Palacios, P., Gross, N., Gaitán, J., and Maestre, F. T.: Climate mediates the biodiversity–ecosystem stability relationship globally, Proceedings of the National Academy of Sciences, 115, 8400–8405, https://doi.org/10.1073/pnas.1800425115, publisher: Proceedings of the National Academy of Sciences, 2018.

Garnier, E. and Navas, M. L.: A trait-based approach to comparative functional plant ecology: Concepts, methods and applications for agroecology. A review, Agronomy for Sustainable Development, 32, 365–399, https://doi.org/10.1007/s13593-011-0036-y, 2012.

Gash, J. H., Wright, I. R., and Lloyd, C. R.: Comparative estimates of interception loss from three coniferous forests in Great Britain, Journal of Hydrology, 48, 89–105, https://doi.org/10.1016/0022-1694(80)90068-2, publisher: Elsevier, 1980.

https://doi.org/10.5194/egusphere-2023-3069
Preprint. Discussion started: 29 January 2024

Gavrilescu, M.: Water, Soil, and Plants Interactions in a Threatened Environment, Water, 13, 2746, https://doi.org/10.3390/w13192746, number: 19 Publisher: Multidisciplinary Digital Publishing Institute, 2021.

Gentine, P., Massmann, A., Lintner, B. R., Hamed Alemohammad, S., Fu, R., Green, J. K., Kennedy, D., and Vilà-Guerau de Arellano, J.: Land–atmosphere interactions in the tropics – a review, Hydrology and Earth System Sciences, 23, 4171–4197, https://doi.org/10.5194/hess-23-4171-2019, publisher: Copernicus GmbH, 2019.

Ghafarian, F., Wieland, R., and Nendel, C.: Estimating the Evaporative Cooling Effect of Irrigation within and above Soybean Canopy, Water, 14, 319, https://doi.org/10.3390/w14030319, number: 3 Publisher: Multidisciplinary Digital Publishing Institute, 2022.

Giambelluca, T. W., Scholz, F. G., Bucci, S. J., Meinzer, F. C., Goldstein, G., Hoffmann, W. A., Franco, A. C., and Buchert, M. P.: Evapotranspiration and energy balance of Brazilian savannas with contrasting tree density, 149, 1365–1376, https://doi.org/10.1016/j.agrformet.2009.03.006, 2009.

Good, S. P. and Caylor, K. K.: Climatological determinants of woody cover in Africa, 108, 4902–4907, https://doi.org/10.1073/pnas.1013100108, 2011.

Gou, Q. and Zhu, Q.: Response of deep soil moisture to different vegetation types in the Loess Plateau of northern Shannxi, China, Scientific Reports, 11, 15 098, https://doi.org/10.1038/s41598-021-94758-5, number: 1 Publisher: Nature Publishing Group, 2021.

Green, J. K., Berry, J., Ciais, P., Zhang, Y., and Gentine, P.: Amazon rainforest photosynthesis increases in response to atmospheric dryness, Science Advances, 6, eabb7232, https://doi.org/10.1126/sciadv.abb7232, publisher: American Association for the Advancement of Science, 2020.

Green, S. J., Brookson, C. B., Hardy, N. A., and Crowder, L. B.: Trait-based approaches to global change ecology: moving from description to prediction, Proceedings of the Royal Society B: Biological Sciences, 289, 20220 071, https://doi.org/10.1098/rspb.2022.0071, publisher: Royal Society, 2022.

Grossiord, C., Buckley, T. N., Cernusak, L. A., Novick, K. A., Poulter, B., Siegwolf, R. T., Sperry, J. S., and McDowell, N. G.: Plant responses to rising vapor pressure deficit, New Phytologist, 226, 1550–1566, https://doi.org/10.1111/NPH.16485, publisher: John Wiley & Sons, Ltd, 2020.

Gu, L., Post, W. M., Baldocchi, D., Andy Black, T., Verma, S. B., Vesala, T., and Wofsy, S. C.: Phenology of Vegetation Photosynthesis, pp. 467–485, https://doi.org/10.1007/978-94-007-0632-3_29, 2003.

Guan, K., Pan, M., Li, H., Wolf, A., Wu, J., Medvigy, D., Caylor, K. K., Sheffield, J., Wood, E. F., Malhi, Y., Liang, M., Kimball, J. S., Saleska, S. R., Berry, J., Joiner, J., and Lyapustin, A. I.: Photosynthetic seasonality of global tropical forests constrained by hydroclimate, Nature Geoscience, 8, 284–289, https://doi.org/10.1038/ngeo2382, number: 4 Publisher: Nature Publishing Group, 2015.

Guevara, M., Taufer, M., and Vargas, R.: Gap-free global annual soil moisture: 15 km grids for 1991–2018, Earth System Science Data, 13, 1711–1735, https://doi.org/10.5194/essd-13-1711-2021, 2021.

Gómez, J. A., Giráldez, J. V., and Fereres, E.: Rainfall interception by olive trees in relation to leaf area, 49, 65–76, https://doi.org/10.1016/S0378-3774(00)00116-5, 2001.

Hashimoto, H., Wang, W., Dungan, J. L., Li, S., Michaelis, A. R., Takenaka, H., Higuchi, A., Myneni, R. B., and Nemani, R. R.: New generation geostationary satellite observations support seasonality in greenness of the Amazon evergreen forests, Nature Communications, 12, 684, https://doi.org/10.1038/s41467-021-20994-y, publisher: Nature Publishing Group, 2021.

Hasler, N. and Avissar, R.: What Controls Evapotranspiration in the Amazon Basin?, Journal of Hydrometeorology, 8, 380–395, https://doi.org/10.1175/JHM587.1, 2007.

https://doi.org/10.5194/egusphere-2023-3069
Preprint. Discussion started: 29 January 2024

Heerspink, B. P., Kendall, A. D., Coe, M. T., and Hyndman, D. W.: Trends in streamflow, evapotranspiration, and groundwater storage across the Amazon Basin linked to changing precipitation and land cover, Journal of Hydrology: Regional Studies, 32, 100 755, https://doi.org/10.1016/j.ejrh.2020.100755, 2020.

Huang, A., Xu, X., Jia, G., and Shen, R.: Asymmetrical cooling effects of Amazonian protected areas across spatiotemporal scales, 17, 054 038, https://doi.org/10.1088/1748-9326/ac6a6d, publisher: IOP Publishing, 2022.

Hultine, K. R., Froend, R., Blasini, D., Bush, S. E., Karlinski, M., and Koepke, D. F.: Hydraulic traits that buffer deep-rooted plants from changes in hydrology and climate, Hydrological Processes, 34, 209–222, https://doi.org/10.1002/hyp.13587, _eprint: https://onlinelibrary.wiley.com/doi/pdf/10.1002/hyp.13587, 2020.

Jackson, R. B., Sperry, J. S., and Dawson, T. E.: Root water uptake and transport: using physiological processes in global predictions, Trends in Plant Science, 5, 482–488, https://doi.org/10.1016/S1360-1385(00)01766-0, 2000.

Kattge, J., Díaz, S., Lavorel, S., Prentice, I. C., Leadley, P., Bönisch, G., Garnier, E., Westoby, M., Reich, P. B., Wright, I. J., Cornelissen, J. H., Violle, C., Harrison, S. P., Van Bodegom, P. M., Reichstein, M., Enquist, B. J., Soudzilovskaia, N. A., Ackerly, D. D., Anand, M., Atkin, O., Bahn, M., Baker, T. R., Baldocchi, D., Bekker, R., Blanco, C. C., Blonder, B., Bond, W. J., Bradstock, R., Bunker, D. E., Casanoves, F., Cavender-Bares, J., Chambers, J. Q., Chapin, F. S., Chave, J., Coomes, D., Cornwell, W. K., Craine, J. M., Dobrin, B. H., Duarte, L., Durka, W., Elser, J., Esser, G., Estiarte, M., Fagan, W. F., Fang, J., Fernández-Méndez, F., Fidelis, A., Finegan, B., Flores, O., Ford, H., Frank, D., Freschet, G. T., Fyllas, N. M., Gallagher, R. V., Green, W. A., Gutierrez, A. G., Hickler, T., Higgins, S. I., Hodgson, J. G., Jalili, A., Jansen, S., Joly, C. A., Kerkhoff, A. J., Kirkup, D., Kitajima, K., Kleyer, M., Klotz, S., Knops, J. M., Kramer, K., Kühn, I., Kurokawa, H., Laughlin, D., Lee, T. D., Leishman, M., Lens, F., Lenz, T., Lewis, S. L., Lloyd, J., Llusià, J., Louault, F., Ma, S., Mahecha, M. D., Manning, P., Massad, T., Medlyn, B. E., Messier, J., Moles, A. T., Müller, S. C., Nadrowski, K., Naeem, S., Niinemets, , Nöllert, S., Nüske, A., Ogaya, R., Oleksyn, J., Onipchenko, V. G., Onoda, Y., Ordoñez, J., Overbeck, G., Ozinga, W. A., Patiño, S., Paula, S., Pausas, J. G., Peñuelas, J., Phillips, O. L., Pillar, V., Poorter, H., Poorter, L., Poschlod, P., Prinzing, A., Proulx, R., Rammig, A., Reinsch, S., Reu, B., Sack, L., Salgado-Negret, B., Sardans, J., Shiodera, S., Shipley, B., Siefert, A., Sosinski, E., Soussana, J. F., Swaine, E., Swenson, N., Thompson, K., Thornton, P., Waldram, M., Weiher, E., White, M., White, S., Wright, S. J., Yguel, B., Zaehle, S., Zanne, A. E., and Wirth, C.: TRY - a global database of plant traits, Global Change Biology, 17, 2905–2935, https://doi.org/10.1111/j.1365-2486.2011.02451.x, publisher: Blackwell Publishing Ltd, 2011.

Kattge, J., Bönisch, G., Díaz, S., Lavorel, S., Prentice, I. C., Leadley, P., Tautenhahn, S., Werner, G. D., Aakala, T., Abedi, M., Acosta, A. T., Adamidis, G. C., Adamson, K., Aiba, M., Albert, C. H., Alcántara, J. M., Alcázar C, C., Aleixo, I., Ali, H., Amiaud, B., Ammer, C., Amoroso, M. M., Anand, M., Anderson, C., Anten, N., Antos, J., Apgaua, D. M. G., Ashman, T. L., Asmara, D. H., Asner, G. P., Aspinwall, M., Atkin, O., Aubin, I., Baastrup-Spohr, L., Bahalkeh, K., Bahn, M., Baker, T., Baker, W. J., Bakker, J. P., Baldocchi, D., Baltzer, J., Banerjee, A., Baranger, A., Barlow, J., Barneche, D. R., Baruch, Z., Bastianelli, D., Battles, J., Bauerle, W., Bauters, M., Bazzato, E., Beckmann, M., Beeckman, H., Beierkuhnlein, C., Bekker, R., Belfry, G., Belluau, M., Beloiu, M., Benavides, R., Benomar, L., Berdugo-Lattke, M. L., Berenguer, E., Bergamin, R., Bergmann, J., Bergmann Carlucci, M., Berner, L., Bernhardt-Römermann, M., Bigler, C., Bjorkman, A. D., Blackman, C., Blanco, C., Blonder, B., Blumenthal, D., Bocanegra-González, K. T., Boeckx, P., Bohlman, S., Böhning-Gaese, K., Boisvert-Marsh, L., Bond, W., Bond-Lamberty, B., Boom, A., Boonman, C. C., Bordin, K., Boughton, E. H., Boukili, V., Bowman, D. M., Bravo, S., Brendel, M. R., Broadley, M. R., Brown, K. A., Bruelheide, H., Brumnich, F., Bruun, H. H., Bruy, D., Buchanan, S. W., Bucher, S. F., Buchmann, N., Buitenwerf, R., Bunker, D. E., Bürger, J., Burrascano, S., Burslem, D. F., Butterfield, B. J., Byun, C., Marques, M., Scalon, M. C., Caccianiga, M., Cadotte, M., Cailleret, M., Camac, J., Camarero, J. J., Campany, C., Campetella, G., Campos, J. A., Cano-Arboleda, L., Canullo, R., Carbognani, M., Carvalho, F., Casanoves, F., Castagneyrol, B., Catford,

https://doi.org/10.5194/egusphere-2023-3069
Preprint. Discussion started: 29 January 2024

J. A., Cavender-Bares, J., Cerabolini, B. E., Cervellini, M., Chacón-Madrigal, E., Chapin, K., Chapin, F. S., Chelli, S., Chen, S. C., Chen, A., Cherubini, P., Chianucci, F., Choat, B., Chung, K. S., Chytrý, M., Ciccarelli, D., Coll, L., Collins, C. G., Conti, L., Coomes, D., Cornelissen, J. H., Cornwell, W. K., Corona, P., Coyea, M., Craine, J., Craven, D., Cromsigt, J. P., Csecserits, A., Cufar, K., Cuntz, M., da Silva, A. C., Dahlin, K. M., Dainese, M., Dalke, I., Dalle Fratte, M., Dang-Le, A. T., Danihelka, J., Dannoura, M., Dawson, S., de Beer, A. J., De Frutos, A., De Long, J. R., Dechant, B., Delagrange, S., Delpierre, N., Derroire, G., Dias, A. S., Diaz-Toribio, M. H., Dimitrakopoulos, P. G., Dobrowolski, M., Doktor, D., Dřevojan, P., Dong, N., Dransfield, J., Dressler, S., Duarte, L., Ducouret, E., Dullinger, S., Durka, W., Duursma, R., Dymova, O., E-Vojtkó, A., Eckstein, R. L., Ejtehadi, H., Elser, J., Emilio, T., Engemann, K., Erfanian, M. B., Erfmeier, A., Esquivel-Muelbert, A., Esser, G., Estiarte, M., Domingues, T. F., Fagan, W. F., Fagúndez, J., Falster, D. S., Fan, Y., Fang, J., Farris, E., Fazlioglu, F., Feng, Y., Fernandez-Mendez, F., Ferrara, C., Ferreira, J., Fidelis, A., Finegan, B., Firn, J., Flowers, T. J., Flynn, D. F., Fontana, V., Forey, E., Forgiarini, C., François, L., Frangipani, M., Frank, D., Frenette-Dussault, C., Freschet, G. T., Fry, E. L., Fyllas, N. M., Mazzochini, G. G., Gachet, S., Gallagher, R., Ganade, G., Ganga, F., García-Palacios, P., Gargaglione, V., Garnier, E., Garrido, J. L., de Gasper, A. L., Gea-Izquierdo, G., Gibson, D., Gillison, A. N., Giroldo, A., Glasenhardt, M. C., Gleason, S., Gliesch, M., Goldberg, E., Göldel, B., Gonzalez-Akre, E., Gonzalez-Andujar, J. L., González-Melo, A., González-Robles, A., Graae, B. J., Granda, E., Graves, S., Green, W. A., Gregor, T., Gross, N., Guerin, G. R., Günther, A., Gutiérrez, A. G., Haddock, L., Haines, A., Hall, J., Hambuckers, A., Han, W., Harrison, S. P., Hattingh, W., Hawes, J. E., He, T., He, P., Heberling, J. M., Helm, A., Hempel, S., Hentschel, J., Hérault, B., Hereş, A. M., Herz, K., Heuertz, M., Hickler, T., Hietz, P., Higuchi, P., Hipp, A. L., Hirons, A., Hock, M., Hogan, J. A., Holl, K., Honnay, O., Hornstein, D., Hou, E., Hough-Snee, N., Hovstad, K. A., Ichie, T., Igić, B., Illa, E., Isaac, M., Ishihara, M., Ivanov, L., Ivanova, L., Iversen, C. M., Izquierdo, J., Jackson, R. B., Jackson, B., Jactel, H., Jagodzinski, A. M., Jandt, U., Jansen, S., Jenkins, T., Jentsch, A., Jespersen, J. R. P., Jiang, G. F., Johansen, J. L., Johnson, D., Jokela, E. J., Joly, C. A., Jordan, G. J., Joseph, G. S., Junaedi, D., Junker, R. R., Justes, E., Kabzems, R., Kane, J., Kaplan, Z., Kattenborn, T., Kavelenova, L., Kearsley, E., Kempel, A., Kenzo, T., Kerkhoff, A., Khalil, M. I., Kinlock, N. L., Kissling, W. D., Kitajima, K., Kitzberger, T., Kjøller, R., Klein, T., Kleyer, M., Klimešová, J., Klipel, J., Kloeppel, B., Klotz, S., Knops, J. M., Kohyama, T., Koike, F., Kollmann, J., Komac, B., Komatsu, K., König, C., Kraft, N. J., Kramer, K., Kreft, H., Kühn, I., Kumarathunge, D., Kuppler, J., Kurokawa, H., Kurosawa, Y., Kuyah, S., Laclau, J. P., Lafleur, B., Lallai, E., Lamb, E., Lamprecht, A., Larkin, D. J., Laughlin, D., Le Bagousse-Pinguet, Y., le Maire, G., le Roux, P. C., le Roux, E., Lee, T., Lens, F., Lewis, S. L., Lhotsky, B., Li, Y., Li, X., Lichstein, J. W., Liebergesell, M., Lim, J. Y., Lin, Y. S., Linares, J. C., Liu, C., Liu, D., Liu, U., Livingstone, S., Llusià, J., Lohbeck, M., López-García, , Lopez-Gonzalez, G., Lososová, Z., Louault, F., Lukács, B. A., Lukeš, P., Luo, Y., Lussu, M., Ma, S., Maciel Rabelo Pereira, C., Mack, M., Maire, V., Mäkelä, A., Mäkinen, H., Malhado, A. C. M., Mallik, A., Manning, P., Manzoni, S., Marchetti, Z., Marchino, L., Marcilio-Silva, V., Marcon, E., Marignani, M., Markesteijn, L., Martin, A., Martínez-Garza, C., Martínez-Vilalta, J., Mašková, T., Mason, K., Mason, N., Massad, T. J., Masse, J., Mayrose, I., McCarthy, J., McCormack, M. L., McCulloh, K., McFadden, I. R., McGill, B. J., McPartland, M. Y., Medeiros, J. S., Medlyn, B., Meerts, P., Mehrabi, Z., Meir, P., Melo, F. P., Mencuccini, M., Meredieu, C., Messier, J., Mészáros, I., Metsaranta, J., Michaletz, S. T., Michelaki, C., Migalina, S., Milla, R., Miller, J. E., Minden, V., Ming, R., Mokany, K., Moles, A. T., Molnár, A., Molofsky, J., Molz, M., Montgomery, R. A., Monty, A., Moravcová, L., Moreno-Martínez, A., Moretti, M., Mori, A. S., Mori, S., Morris, D., Morrison, J., Mucina, L., Mueller, S., Muir, C. D., Müller, S. C., Munoz, F., Myers-Smith, I. H., Myster, R. W., Nagano, M., Naidu, S., Narayanan, A., Natesan, B., Negoita, L., Nelson, A. S., Neuschulz, E. L., Ni, J., Niedrist, G., Nieto, J., Niinemets, , Nolan, R., Nottebrock, H., Nouvellon, Y., Novakovskiy, A., Nystuen, K. O., O'Grady, A., O'Hara, K., O'Reilly-Nugent, A., Oakley, S., Oberhuber, W., Ohtsuka, T., Oliveira, R., Öllerer, K., Olson, M. E., Onipchenko, V., Onoda, Y., Onstein, R. E., Ordonez, J. C., Osada, N., Ostonen, I., Ottaviani, G., Otto, S., Overbeck, G. E., Ozinga, W. A., Pahl, A. T., Paine, C. E., Pakeman, R. J., Papageorgiou, A. C., Parfionova, E., Pärtel, M., Patacca, M., Paula, S., Paule,

https://doi.org/10.5194/egusphere-2023-3069
Preprint. Discussion started: 29 January 2024

J., Pauli, H., Pausas, J. G., Peco, B., Penuelas, J., Perea, A., Peri, P. L., Petisco-Souza, A. C., Petraglia, A., Petritan, A. M., Phillips, O. L., Pierce, S., Pillar, V. D., Pisek, J., Pomogaybin, A., Poorter, H., Portsmuth, A., Poschlod, P., Potvin, C., Pounds, D., Powell, A. S., Power, S. A., Prinzing, A., Puglielli, G., Pyšek, P., Raevel, V., Rammig, A., Ransijn, J., Ray, C. A., Reich, P. B., Reichstein, M., Reid, D. E., Réjou-Méchain, M., de Dios, V. R., Ribeiro, S., Richardson, S., Riibak, K., Rillig, M. C., Riviera, F., Robert, E. M., Roberts, S., Robroek, B., Roddy, A., Rodrigues, A. V., Rogers, A., Rollinson, E., Rolo, V., Römermann, C., Ronzhina, D., Roscher, C., Rosell, J. A., Rosenfield, M. F., Rossi, C., Roy, D. B., Royer-Tardif, S., Rüger, N., Ruiz-Peinado, R., Rumpf, S. B., Rusch, G. M., Ryo, M., Sack, L., Saldaña, A., Salgado-Negret, B., Salguero-Gomez, R., Santa-Regina, I., Santacruz-García, A. C., Santos, J., Sardans, J., Schamp, B., Scherer-Lorenzen, M., Schleuning, M., Schmid, B., Schmidt, M., Schmitt, S., Schneider, J. V., Schowanek, S. D., Schrader, J., Schrodt, F., Schuldt, B., Schurr, F., Selaya Garvizu, G., Semchenko, M., Seymour, C., Sfair, J. C., Sharpe, J. M., Sheppard, C. S., Sheremetiev, S., Shiodera, S., Shipley, B., Shovon, T. A., Siebenkäs, A., Sierra, C., Silva, V., Silva, M., Sitzia, T., Sjöman, H., Slot, M., Smith, N. G., Sodhi, D., Soltis, P., Soltis, D., Somers, B., Sonnier, G., Sørensen, M. V., Sosinski, E. E., Soudzilovskaia, N. A., Souza, A. F., Spasojevic, M., Sperandii, M. G., Stan, A. B., Stegen, J., Steinbauer, K., Stephan, J. G., Sterck, F., Stojanovic, D. B., Strydom, T., Suarez, M. L., Svenning, J. C., Svitková, I., Svitok, M., Svoboda, M., Swaine, E., Swenson, N., Tabarelli, M., Takagi, K., Tappeiner, U., Tarifa, R., Tauugourdeau, S., Tavsanoglu, C., te Beest, M., Tedersoo, L., Thiffault, N., Thom, D., Thomas, E., Thompson, K., Thornton, P. E., Thuiller, W., Tichý, L., Tissue, D., Tjoelker, M. G., Tng, D. Y. P., Tobias, J., Török, P., Tarin, T., Torres-Ruiz, J. M., Tóthmérész, B., Treurnicht, M., Trivellone, V., Trolliet, F., Trotsiuk, V., Tsakalos, J. L., Tsiripidis, I., Tysklind, N., Umehara, T., Usoltsev, V., Vadeboncoeur, M., Vaezi, J., Valladares, F., Vamosi, J., van Bodegom, P. M., van Breugel, M., Van Cleemput, E., van de Weg, M., van der Merwe, S., van der Plas, F., van der Sande, M. T., van Kleunen, M., Van Meerbeek, K., Vanderwel, M., Vanselow, K. A., Vårhammar, A., Varone, L., Vasquez Valderrama, M. Y., Vassilev, K., Vellend, M., Veneklaas, E. J., Verbeeck, H., Verheyen, K., Vibrans, A., Vieira, I., Villacís, J., Violle, C., Vivek, P., Wagner, K., Waldram, M., Waldron, A., Walker, A. P., Waller, M., Walther, G., Wang, H., Wang, F., Wang, W., Watkins, H., Watkins, J., Weber, U., Weedon, J. T., Wei, L., Weigelt, P., Weiher, E., Wells, A. W., Wellstein, C., Wenk, E., Westoby, M., Westwood, A., White, P. J., Whitten, M., Williams, M., Winkler, D. E., Winter, K., Womack, C., Wright, I. J., Wright, S. J., Wright, J., Pinho, B. X., Ximenes, F., Yamada, T., Yamaji, K., Yanai, R., Yankov, N., Yguel, B., Zanini, K. J., Zanne, A. E., Zelený, D., Zhao, Y. P., Zheng, J., Zheng, J., Ziemińska, K., Zirbel, C. R., Zizka, G., Zo-Bi, I. C., Zotz, G., and Wirth, C.: TRY plant trait database – enhanced coverage and open access, Global Change Biology, 26, 119–188, https://doi.org/10.1111/gcb.14904, publisher: Blackwell Publishing Ltd, 2020.

Katul, G. G., Oren, R., Manzoni, S., Higgins, C., and Parlange, M. B.: Evapotranspiration: A process driving mass transport and energy exchange in the soil-plant-atmosphere-climate system, Reviews of Geophysics, 50, https://doi.org/10.1029/2011RG000366, _eprint: https://onlinelibrary.wiley.com/doi/pdf/10.1029/2011RG000366, 2012.

Keys, P. W., Wang-Erlandsson, L., Gordon, L. J., Galaz, V., and Ebbesson, J.: Approaching moisture recycling governance, Global Environmental Change, 45, 15–23, https://doi.org/10.1016/j.gloenvcha.2017.04.007, publisher: Elsevier Ltd, 2017.

Keys, P. W., Porkka, M., Wang-Erlandsson, L., Fetzer, I., Gleeson, T., and Gordon, L. J.: Invisible water security: Moisture recycling and water resilience, Water Security, 8, 100 046, https://doi.org/10.1016/J.WASEC.2019.100046, publisher: Elsevier, 2019.

Kim, Y., Knox, R. G., Longo, M., Medvigy, D., Hutyra, L. R., Pyle, E. H., Wofsy, S. C., Bras, R. L., and Moorcroft, P. R.: Seasonal carbon dynamics and water fluxes in an Amazon rainforest, Global Change Biology, 18, 1322–1334, https://doi.org/10.1111/j.1365-2486.2011.02629.x, _eprint: https://onlinelibrary.wiley.com/doi/pdf/10.1111/j.1365-2486.2011.02629.x, 2012.

Koenker, R. and Hallock, K. F.: Quantile Regression, Journal of Economic Perspectives, 15, 143–156, https://doi.org/10.1257/JEP.15.4.143, 2001.

https://doi.org/10.5194/egusphere-2023-3069
Preprint. Discussion started: 29 January 2024

Koenker, R. and Machado, J. A. F.: Goodness of Fit and Related Inference Processes for Quantile Regression, Journal of the American Statistical Association, 94, 1296–1310, https://doi.org/10.1080/01621459.1999.10473882, publisher: Taylor & Francis _eprint: https://www.tandfonline.com/doi/pdf/10.1080/01621459.1999.10473882, 1999.

Kool, D., Agam, N., Lazarovitch, N., Heitman, J. L., Sauer, T. J., and Ben-Gal, A.: A review of approaches for evapotranspiration partitioning, Agricultural and Forest Meteorology, 184, 56–70, https://doi.org/10.1016/J.AGRFORMET.2013.09.003, 2014.

Laio, F., Porporato, A., Ridolfi, L., and Rodriguez-Iturbe, I.: Plants in water-controlled ecosystems: active role in hydrologic processes and response to water stress: II. Probabilistic soil moisture dynamics, Advances in Water Resources, 24, 707–723, https://doi.org/10.1016/S0309-1708(01)00005-7, 2001.

Lehner, B. and Grill, G.: Global river hydrography and network routing: baseline data and new approaches to study the world's large river systems, Hydrological Processes, 27, 2171–2186, https://doi.org/10.1002/hyp.9740, _eprint: https://onlinelibrary.wiley.com/doi/pdf/10.1002/hyp.9740, 2013.

Li, Y., Zhao, M., Motesharrei, S., Mu, Q., Kalnay, E., and Li, S.: Local cooling and warming effects of forests based on satellite observations, 6, 6603, https://doi.org/10.1038/ncomms7603, number: 1 Publisher: Nature Publishing Group, 2015.

Liu, C., Li, Y., Xu, L., Chen, Z., and He, N.: Variation in leaf morphological, stomatal, and anatomical traits and their relationships in temperate and subtropical forests, Scientific Reports, 9, 5803, https://doi.org/10.1038/s41598-019-42335-2, number: 1 Publisher: Nature Publishing Group, 2019.

Liu, G., Liu, H., and Yin, Y.: Global patterns of NDVI-indicated vegetation extremes and their sensitivity to climate extremes, Environmental Research Letters, 8, 025 009, https://doi.org/10.1088/1748-9326/8/2/025009, 2013.

Liu, Y., Holtzman, N. M., and Konings, A. G.: Global ecosystem-scale plant hydraulic traits retrieved using model–data fusion, Hydrology and Earth System Sciences, 25, 2399–2417, https://doi.org/10.5194/hess-25-2399-2021, publisher: Copernicus GmbH, 2021.

Lohbeck, M., Poorter, L., Lebrija-Trejos, E., Martínez-Ramos, M., Meave, J. A., Paz, H., Pérez-García, E. A., Romero-Pérez, I. E., Tauro, A., and Bongers, F.: Successional changes in functional composition contrast for dry and wet tropical forest, Ecology, 94, 1211–1216, https://doi.org/10.1890/12-1850.1, _eprint: https://onlinelibrary.wiley.com/doi/pdf/10.1890/12-1850.1, 2013.

Lohbeck, M., Lebrija-Trejos, E., Martínez-Ramos, M., Meave, J. A., Poorter, L., and Bongers, F.: Functional Trait Strategies of Trees in Dry and Wet Tropical Forests Are Similar but Differ in Their Consequences for Succession, PLOS ONE, 10, e0123 741, https://doi.org/10.1371/journal.pone.0123741, publisher: Public Library of Science, 2015.

Lu, Y., Duursma, R. A., Farrior, C. E., Medlyn, B. E., and Feng, X.: Optimal stomatal drought response shaped by competition for water and hydraulic risk can explain plant trait covariation, New Phytologist, 225, 1206–1217, https://doi.org/10.1111/nph.16207, _eprint: https://onlinelibrary.wiley.com/doi/pdf/10.1111/nph.16207, 2020.

Magliano, P. N., Whitworth-Hulse, J. I., Cid, F. D., Leporati, J. L., Van Stan, J. T., and Jobbágy, E. G.: Global rainfall partitioning by dryland vegetation: Developing general empirical models, Journal of Hydrology, 607, 127 540, https://doi.org/10.1016/J.JHYDROL.2022.127540, 2022.

Marengo, J.: On the hydrological cycle of the Amazon basin: a historical review and current state-of-the-art, Revista Brasileira de Meteorologica, 21, 2006.

Massmann, A., Gentine, P., and Lin, C.: When Does Vapor Pressure Deficit Drive or Reduce Evapotranspiration?, Journal of Advances in Modeling Earth Systems, 11, 3305–3320, https://doi.org/10.1029/2019MS001790, _eprint: https://onlinelibrary.wiley.com/doi/pdf/10.1029/2019MS001790, 2019.

https://doi.org/10.5194/egusphere-2023-3069
Preprint. Discussion started: 29 January 2024

Matheny, A. M., Mirfenderesgi, G., and Bohrer, G.: Trait-based representation of hydrological functional properties of plants in weather and ecosystem models, Plant Diversity, 39, 1–12, https://doi.org/10.1016/j.pld.2016.10.001, publisher: KeAi Publishing Communications Ltd., 2017.

Matthews, D.: The water cycle freshens up, Nature, 439, 793–794, https://doi.org/10.1038/439793a, number: 7078 Publisher: Nature Publishing Group, 2006.

McWilliam, A.-L. C., Roberts, J. M., Cabral, O. M. R., Leitao, M. V. B. R., de Costa, A. C. L., Maitelli, G. T., and Zamparoni, C. A. G. P.: Leaf Area Index and Above-Ground Biomass of terra firme Rain Forest and Adjacent Clearings in Amazonia, Functional Ecology, 7, 310–317, https://doi.org/10.2307/2390210, publisher: [British Ecological Society, Wiley], 1993.

Mencuccini, M., Rosas, T., Rowland, L., Choat, B., Cornelissen, H., Jansen, S., Kramer, K., Lapenis, A., Manzoni, S., Niinemets, , Reich, P. B., Schrodt, F., Soudzilovskaia, N., Wright, I. J., and Martínez-Vilalta, J.: Leaf economics and plant hydraulics drive leaf : wood area ratios, New Phytologist, 224, 1544–1556, https://doi.org/10.1111/nph.15998, _eprint: https://onlinelibrary.wiley.com/doi/pdf/10.1111/nph.15998, 2019.

Mercado, L. M., Patiño, S., Domingues, T. F., Fyllas, N. M., Weedon, G. P., Sitch, S., Quesada, C. A., Phillips, O. L., Aragão, L. E. O. C., Malhi, Y., Dolman, A. J., Restrepo-Coupe, N., Saleska, S. R., Baker, T. R., Almeida, S., Higuchi, N., and Lloyd, J.: Variations in Amazon forest productivity correlated with foliar nutrients and modelled rates of photosynthetic carbon supply, Philosophical Transactions: Biological Sciences, 366, 3316–3329, https://www.jstor.org/stable/23076296, publisher: The Royal Society, 2011.

Michiles, A. A. d. S. and Gielow, R.: Above-ground thermal energy storage rates, trunk heat fluxes and surface energy balance in a central Amazonian rainforest, Agricultural and Forest Meteorology, 148, 917–930, https://doi.org/10.1016/j.agrformet.2008.01.001, 2008.

Miguez-Macho, G. and Fan, Y.: The role of groundwater in the Amazon water cycle: 1. Influence on seasonal streamflow, flooding and wetlands, Journal of Geophysical Research: Atmospheres, 117, https://doi.org/10.1029/2012JD017539, _eprint: https://onlinelibrary.wiley.com/doi/pdf/10.1029/2012JD017539, 2012.

Miralles, D. G., Gash, J. H., Holmes, T. R., De Jeu, R. A., and Dolman, A. J.: Global canopy interception from satellite observations, Journal of Geophysical Research Atmospheres, 115, https://doi.org/10.1029/2009JD013530, publisher: Blackwell Publishing Ltd, 2010.

Mirfenderesgi, G., Bohrer, G., Matheny, A. M., Fatichi, S., de Moraes Frasson, R. P., and Schäfer, K. V. R.: Tree level hydrodynamic approach for resolving aboveground water storage and stomatal conductance and modeling the effects of tree hydraulic strategy, Journal of Geophysical Research: Biogeosciences, 121, 1792–1813, https://doi.org/10.1002/2016JG003467, _eprint: https://onlinelibrary.wiley.com/doi/pdf/10.1002/2016JG003467, 2016.

Moreno-Martínez, , Camps-Valls, G., Kattge, J., Robinson, N., Reichstein, M., van Bodegom, P., Kramer, K., Cornelissen, J. H. C., Reich, P., Bahn, M., Niinemets, , Peñuelas, J., Craine, J. M., Cerabolini, B. E., Minden, V., Laughlin, D. C., Sack, L., Allred, B., Baraloto, C., Byun, C., Soudzilovskaia, N. A., and Running, S. W.: A methodology to derive global maps of leaf traits using remote sensing and climate data, Remote Sensing of Environment, 218, 69–88, https://doi.org/10.1016/j.rse.2018.09.006, publisher: Elsevier Inc., 2018a.

Moreno-Martínez, , Camps-Valls, G., Kattge, J., Robinson, N., Reichstein, M., van Bodegom, P., Kramer, K., Cornelissen, J. H. C., Reich, P., Bahn, M., Niinemets, , Peñuelas, J., Craine, J. M., Cerabolini, B. E. L., Minden, V., Laughlin, D. C., Sack, L., Allred, B., Baraloto, C., Byun, C., Soudzilovskaia, N. A., and Running, S. W.: A methodology to derive global maps of leaf traits using remote sensing and climate data, Remote Sensing of Environment, 218, 69–88, https://doi.org/10.1016/j.rse.2018.09.006, 2018b.

Mu, Q., Zhao, M., and Running, S. W.: MODIS Global Terrestrial Evapotranspiration (ET) Product (NASA MOD16A2/A3) Collection 5, https://lpdaac.usgs.gov/products/mod16a2v006/, 2013.

https://doi.org/10.5194/egusphere-2023-3069
Preprint. Discussion started: 29 January 2024

Mu, Y. and Jones, C.: An observational analysis of precipitation and deforestation age in the Brazilian Legal Amazon, Atmospheric Research, 271, 106 122, https://doi.org/10.1016/j.atmosres.2022.106122, 2022.

Myneni, R., Knyazikhin, Y., and Park, T.: MOD15A2H MODIS/Terra Leaf Area Index/FPAR 8-Day L4 Global 500m SIN Grid V006, https://doi.org/10.5067/MODIS/MOD15A2H.006, 2015.

Nagase, A. and Dunnett, N.: Amount of water runoff from different vegetation types on extensive green roofs: Effects of plant species, diversity and plant structure, Landscape and Urban Planning, 104, 356–363, https://doi.org/10.1016/j.landurbplan.2011.11.001, 2012.

Niinemets, , Tenhunen, J. D., Harley, P. C., and Steinbrecher, R.: A model of isoprene emission based on energetic requirements for isoprene synthesis and leaf photosynthetic properties for Liquidambar and Quercus, Plant, Cell & Environment, 22, 1319–1335, https://doi.org/10.1046/j.1365-3040.1999.00505.x, _eprint: https://onlinelibrary.wiley.com/doi/pdf/10.1046/j.1365-3040.1999.00505.x, 1999.

O'connor, J., Santos, M. J., Rebel, K. T., and Dekker, S. C.: The influence of water table depth on evapotranspiration in the Amazon arc of deforestation, Hydrology and Earth System Sciences, 23, 3917–3931, https://doi.org/10.5194/HESS-23-3917-2019, 2019.

O'Connor, J. C., Dekker, S. C., Staal, A., Tuinenburg, O. A., Rebel, K. T., and Santos, M. J.: Forests buffer against variations in precipitation, Global Change Biology, 27, 4686–4696, https://doi.org/10.1111/GCB.15763, 2021.

Ordoñez, J. C., Van Bodegom, P. M., Witte, J.-P. M., Wright, I. J., Reich, P. B., and Aerts, R.: A global study of relationships between leaf traits, climate and soil measures of nutrient fertility, Global Ecology and Biogeography, 18, 137–149, https://doi.org/10.1111/j.1466-8238.2008.00441.x, _eprint: https://onlinelibrary.wiley.com/doi/pdf/10.1111/j.1466-8238.2008.00441.x, 2009.

Pan, Y., Yuan, D., Wu, Q., Jin, L., Xie, M., Gu, Y., and Duan, C.: Effect of water exchange rate on interspecies competition between submerged macrophytes: functional trait hierarchy drives competition, Plant and Soil, 466, 631–647, https://doi.org/10.1007/s11104-021-05081-x, 2021.

Poorter, L., Castilho, C. V., Schietti, J., Oliveira, R. S., and Costa, F. R. C.: Can traits predict individual growth performance? A test in a hyperdiverse tropical forest, New Phytologist, 219, 109–121, https://doi.org/10.1111/nph.15206, _eprint: https://onlinelibrary.wiley.com/doi/pdf/10.1111/nph.15206, 2018.

Potapov, P., Hansen, M. C., Pickens, A., Hernandez-Serna, A., Tyukavina, A., Turubanova, S., Zalles, V., Li, X., Khan, A., Stolle, F., Harris, N., Song, X.-P., Baggett, A., Kommareddy, I., and Kommareddy, A.: The Global 2000-2020 Land Cover and Land Use Change Dataset Derived From the Landsat Archive: First Results, Frontiers in Remote Sensing, 3, https://www.frontiersin.org/articles/10.3389/frsen.2022.856903, 2022.

Powell, T. L., Wheeler, J. K., de Oliveira, A. A., da Costa, A. C. L., Saleska, S. R., Meir, P., and Moorcroft, P. R.: Differences in xylem and leaf hydraulic traits explain differences in drought tolerance among mature Amazon rainforest trees, Global Change Biology, 23, 4280–4293, https://doi.org/10.1111/gcb.13731, publisher: Blackwell Publishing Ltd, 2017.

Quesada, C. A., Phillips, O. L., Schwarz, M., Czimczik, C. I., Baker, T. R., Patiño, S., Fyllas, N. M., Hodnett, M. G., Herrera, R., Almeida, S., Alvarez Dávila, E., Arneth, A., Arroyo, L., Chao, K. J., Dezzeo, N., Erwin, T., di Fiore, A., Higuchi, N., Honorio Coronado, E., Jimenez, E. M., Killeen, T., Lezama, A. T., Lloyd, G., López-González, G., Luizão, F. J., Malhi, Y., Monteagudo, A., Neill, D. A., Núñez Vargas, P., Paiva, R., Peacock, J., Peñuela, M. C., Peña Cruz, A., Pitman, N., Priante Filho, N., Prieto, A., Ramírez, H., Rudas, A., Salomão, R., Santos, A. J. B., Schmerler, J., Silva, N., Silveira, M., Vásquez, R., Vieira, I., Terborgh, J., and Lloyd, J.: Basin-wide variations in Amazon forest structure and function are mediated by both soils and climate, 9, 2203–2246, https://doi.org/10.5194/bg-9-2203-2012, number: 6 Publisher: Copernicus GmbH, 2012.

https://doi.org/10.5194/egusphere-2023-3069
Preprint. Discussion started: 29 January 2024

Reich, P. B., Ellsworth, D. S., Walters, M. B., Vose, J. M., Gresham, C., Volin, J. C., and Bowman, W. D.: Generality of Leaf Trait Relationships: A Test Across Six Biomes, Ecology, 80, 1955–1969, https://doi.org/10.1890/0012-9658(1999)080[1955:GOLTRA]2.0.CO;2, _eprint: https://onlinelibrary.wiley.com/doi/pdf/10.1890/0012-9658%281999%29080%5B1955%3AGOLTRA%5D2.0.CO%3B2, 1999.

Reichert, T., Rammig, A., Fuchslueger, L., Lugli, L. F., Quesada, C. A., and Fleischer, K.: Plant phosphorus-use and -acquisition strategies in Amazonia, 234, 1126–1143, https://doi.org/10.1111/nph.17985, number: 4 _eprint: https://onlinelibrary.wiley.com/doi/pdf/10.1111/nph.17985, 2022.

Romero-Saltos, H., Sternberg, L. d. S. L., Moreira, M. Z., and Nepstad, D. C.: Rainfall exclusion in an eastern Amazonian forest alters soil water movement and depth of water uptake, American Journal of Botany, 92, 443–455, https://doi.org/10.3732/ajb.92.3.443, _eprint: https://onlinelibrary.wiley.com/doi/pdf/10.3732/ajb.92.3.443, 2005.

Running, S., Mu, Q., Zhao, M., and Moreno, A.: MODIS/Terra Net Evapotranspiration Gap-Filled Yearly L4 Global 500m SIN Grid V061 [Data set], https://doi.org/10.5067/MODIS/MOD16A3GF.061, 2021.

Sakschewski, B., Von Bloh, W., Boit, A., Poorter, L., Peña-Claros, M., Heinke, J., Joshi, J., and Thonicke, K.: Resilience of Amazon forests emerges from plant trait diversity, Nature Climate Change, 6, 1032–1036, https://doi.org/10.1038/nclimate3109, 2016.

Salati, E., Dall'Olio, A., Matsui, E., and Gat, J. R.: Recycling of water in the Amazon Basin: An isotopic study, Water Resources Research, 15, 1250–1258, https://doi.org/10.1029/WR015i005p01250, 1979.

Sanchez-Martinez, P., Martínez-Vilalta, J., Dexter, K. G., Segovia, R. A., and Mencuccini, M.: Adaptation and coordinated evolution of plant hydraulic traits, 23, 1599–1610, https://doi.org/10.1111/ele.13584, number: 11 _eprint: https://onlinelibrary.wiley.com/doi/pdf/10.1111/ele.13584.

Sanchez-Martinez, P., Martínez-Vilalta, J., Dexter, K. G., Segovia, R. A., and Mencuccini, M.: Adaptation and coordinated evolution of plant hydraulic traits, Ecology Letters, 23, 1599–1610, https://doi.org/10.1111/ele.13584, _eprint: https://onlinelibrary.wiley.com/doi/pdf/10.1111/ele.13584, 2020.

Satyamurty, P., da Costa, C. P. W., and Manzi, A. O.: Moisture source for the Amazon Basin: a study of contrasting years, Theoretical and Applied Climatology 2012 111:1, 111, 195–209, https://doi.org/10.1007/S00704-012-0637-7, 2012.

Savenije, H. H. G.: The importance of interception and why we should delete the term evapotranspiration from our vocabulary, Hydrological Processes, 18, 1507–1511, https://doi.org/10.1002/hyp.5563, 2004.

Schlesinger, W. H. and Jasechko, S.: Transpiration in the global water cycle, Agricultural and Forest Meteorology, 189-190, 115–117, https://doi.org/10.1016/j.agrformet.2014.01.011, publisher: Elsevier, 2014.

Shao, R., Zhang, B., and He, X.: Implementation of Dynamic Effective Rooting Depth in Evapotranspiration Model Deepens Understanding of Evapotranspiration Partitioning Under Soil Moisture Gradients in China, 58, e2022WR032962, https://doi.org/10.1029/2022WR032962, number: 11 _eprint: https://onlinelibrary.wiley.com/doi/pdf/10.1029/2022WR032962, 2022.

Signori-Müller, C., Oliveira, R. S., Barros, F. d. V., Tavares, J. V., Gilpin, M., Diniz, F. C., Zevallos, M. J. M., Yupayccana, C. A. S., Acosta, M., Bacca, J., Chino, R. S. C., Cuellar, G. M. A., Cumapa, E. R. M., Martinez, F., Mullisaca, F. M. P., Nina, A., Sanchez, J. M. B., da Silva, L. F., Tello, L., Tintaya, J. S., Ugarteche, M. T. M., Baker, T. R., Bittencourt, P. R. L., Borma, L. S., Brum, M., Castro, W., Coronado, E. N. H., Cosio, E. G., Feldpausch, T. R., Fonseca, L. d. M., Gloor, E., Llampazo, G. F., Malhi, Y., Mendoza, A. M., Moscoso, V. C., Araujo-Murakami, A., Phillips, O. L., Salinas, N., Silveira, M., Talbot, J., Vasquez, R., Mencuccini, M., and Galbraith, D.: Non-structural carbohydrates mediate seasonal water stress across Amazon forests, Nature Communications, 12, 2310, https://doi.org/10.1038/s41467-021-22378-8, number: 1 Publisher: Nature Publishing Group, 2021.

https://doi.org/10.5194/egusphere-2023-3069
Preprint. Discussion started: 29 January 2024

Staver, A. C., Brando, P. M., Barlow, J., Morton, D. C., Paine, C. T., Malhi, Y., Araujo Murakami, A., and Pasquel, J.: Thinner bark increases sensitivity of wetter Amazonian tropical forests to fire, Ecology Letters, 23, 99–106, https://doi.org/10.1111/ele.13409, 2020.

Tan, P. Y., Wong, N. H., Tan, C. L., Jusuf, S. K., Chang, M. F., and Chiam, Z. Q.: A method to partition the relative effects of evaporative cooling and shading on air temperature within vegetation canopy, Journal of Urban Ecology, 4, juy012, https://doi.org/10.1093/jue/juy012, 2018.

te Wierik, S. A., Cammeraat, E. L. H., Gupta, J., and Artzy-Randrup, Y. A.: Reviewing the Impact of Land Use and Land-Use Change on Moisture Recycling and Precipitation Patterns, Water Resources Research, 57, e2020WR029 234, https://doi.org/10.1029/2020WR029234, _eprint: https://onlinelibrary.wiley.com/doi/pdf/10.1029/2020WR029234, 2021.

Tuinenburg, O. A. and Staal, A.: Tracking the global flows of atmospheric moisture and associated uncertainties, Hydrology and Earth System Sciences, 24, 2419–2435, https://doi.org/10.5194/hess-24-2419-2020, 2020.

Turner, B. L., Brenes-Arguedas, T., and Condit, R.: Pervasive phosphorus limitation of tree species but not communities in tropical forests, Nature, 555, 367–370, https://doi.org/10.1038/nature25789, number: 7696 Publisher: Nature Publishing Group, 2018.

Ustin, S. L. and Middleton, E. M.: Current and near-term advances in Earth observation for ecological applications, 10, 1, https://doi.org/10.1186/s13717-020-00255-4, 2021.

Van Bodegom, P. M., Douma, J. C., Witte, J. P. M., Ordoñez, J. C., Bartholomeus, R. P., and Aerts, R.: Going beyond limitations of plant functional types when predicting global ecosystem–atmosphere fluxes: exploring the merits of traits-based approaches, Global Ecology and Biogeography, 21, 625–636, https://doi.org/10.1111/j.1466-8238.2011.00717.x, _eprint: https://onlinelibrary.wiley.com/doi/pdf/10.1111/j.1466-8238.2011.00717.x, 2012.

Van Der Ent, R. J., Savenije, H. H., Schaefli, B., and Steele-Dunne, S. C.: Origin and fate of atmospheric moisture over continents, Water Resources Research, 46, https://doi.org/10.1029/2010WR009127, publisher: John Wiley & Sons, Ltd, 2010.

Van Der Ent, R. J., Wang-Erlandsson, L., Keys, P. W., and Savenije, H. H. G.: Contrasting roles of interception and transpiration in the hydrological cycle-Part 2: Moisture recycling, Earth Syst. Dynam, 5, 471–489, https://doi.org/10.5194/esd-5-471-2014, 2014.

Van Dijk, A. I. and Bruijnzeel, L. A.: Modelling rainfall interception by vegetation of variable density using an adapted analytical model. Part 1. Model description, Journal of Hydrology, 247, 230–238, https://doi.org/10.1016/S0022-1694(01)00392-4, 2001.

Van Heerwaarden, C. C. and Teuling, A. J.: Disentangling the response of forest and grassland energy exchange to heatwaves under idealized land–atmosphere coupling, 11, 6159–6171, https://doi.org/10.5194/bg-11-6159-2014, 2014.

Verma, S. and Verma, M.: Textbook of plant physiology, biochemistry and biotechnology, S Chand, New Delhi, India, 2007.

Vourlitis, G. L., de Souza Nogueira, J., de Almeida Lobo, F., Sendall, K. M., de Paulo, S. R., Antunes Dias, C. A., Pinto Jr., O. B., and de Andrade, N. L. R.: Energy balance and canopy conductance of a tropical semi-deciduous forest of the southern Amazon Basin, 44, https://doi.org/10.1029/2006WR005526, _eprint: https://onlinelibrary.wiley.com/doi/pdf/10.1029/2006WR005526, 2008.

Walker, A. P., Beckerman, A. P., Gu, L., Kattge, J., Cernusak, L. A., Domingues, T. F., Scales, J. C., Wohlfahrt, G., Wullschleger, S. D., and Woodward, F. I.: The relationship of leaf photosynthetic traits – Vcmax and Jmax – to leaf nitrogen, leaf phosphorus, and specific leaf area: a meta-analysis and modeling study, 4, 3218–3235, https://doi.org/10.1002/ece3.1173, _eprint: https://onlinelibrary.wiley.com/doi/pdf/10.1002/ece3.1173, 2014.

Wan, Z., Hook, S., and Hulley, G.: MOD11C3 MODIS/Terra Land Surface Temperature/Emissivity Monthly L3 Global 0.05Deg CMG V006, https://doi.org/10.5067/MODIS/MOD11C3.006, 2015.

Wang, C., He, J., Zhao, T.-H., Cao, Y., Wang, G., Sun, B., Yan, X., Guo, W., and Li, M.-H.: The Smaller the Leaf Is, the Faster the Leaf Water Loses in a Temperate Forest, Frontiers in Plant Science, 10, https://www.frontiersin.org/articles/10.3389/fpls.2019.00058, 2019a.

https://doi.org/10.5194/egusphere-2023-3069
Preprint. Discussion started: 29 January 2024

Wang, C., He, J., Zhao, T.-H., Cao, Y., Wang, G., Sun, B., Yan, X., Guo, W., and Li, M.-H.: The Smaller the Leaf Is, the Faster the Leaf Water Loses in a Temperate Forest, 10, 58, https://doi.org/10.3389/fpls.2019.00058, 2019b.

Wang, L., Caylor, K. K., Villegas, J. C., Barron-Gafford, G. A., Breshears, D. D., and Huxman, T. E.: Partitioning evapotranspiration across gradients of woody plant cover: Assessment of a stable isotope technique, Geophysical Research Letters, 37, https://doi.org/10.1029/2010GL043228, publisher: John Wiley & Sons, Ltd, 2010.

Wang, Y., Zhang, Y., Yu, X., Jia, G., Liu, Z., Sun, L., Zheng, P., and Zhu, X.: Grassland soil moisture fluctuation and its relationship with evapotranspiration, Ecological Indicators, 131, 108 196, https://doi.org/10.1016/j.ecolind.2021.108196, 2021.

Ward, R. C.: Measuring evapotranspiration; a review, Journal of Hydrology, 13, 1–21, https://doi.org/10.1016/0022-1694(71)90197-1, 1971.

Wehr, R., Commane, R., Munger, J. W., McManus, J. B., Nelson, D. D., Zahniser, M. S., Saleska, S. R., and Wofsy, S. C.: Dynamics of canopy stomatal conductance, transpiration, and evaporation in a temperate deciduous forest, validated by carbonyl sulfide uptake, 14, 389–401, https://doi.org/10.5194/bg-14-389-2017, number: 2 Publisher: Copernicus GmbH, 2017.

Wolf, S., Mahecha, M. D., Sabatini, F. M., Wirth, C., Bruelheide, H., Kattge, J., Moreno Martínez, , Mora, K., and Kattenborn, T.: Citizen science plant observations encode global trait patterns, Nature Ecology & Evolution, 6, 1850–1859, https://doi.org/10.1038/s41559-022-01904-x, number: 12 Publisher: Nature Publishing Group, 2022.

Xu, D., Agee, E., Wang, J., and Ivanov, V. Y.: Estimation of Evapotranspiration of Amazon Rainforest Using the Maximum Entropy Production Method, Geophysical Research Letters, 46, https://doi.org/10.1029/2018gl080907, institution: Univ. of Michigan, Ann Arbor, MI (United States) Publisher: American Geophysical Union, 2019.

Yan, P., Fernández-Martínez, M., Van Meerbeek, K., Yu, G., Migliavacca, M., and He, N.: The essential role of biodiversity in the key axes of ecosystem function, 29, 4569–4585, https://doi.org/10.1111/gcb.16666, _eprint: https://onlinelibrary.wiley.com/doi/pdf/10.1111/gcb.16666, 2023.

Yang, L., Wei, W., Chen, L., and Mo, B.: Response of deep soil moisture to land use and afforestation in the semi-arid Loess Plateau, China, Journal of Hydrology, 475, 111–122, https://doi.org/10.1016/j.jhydrol.2012.09.041, 2012.

Yu, W., Zhou, W., Qian, Y., and Yan, J.: A new approach for land cover classification and change analysis: Integrating backdating and an object-based method, Remote Sensing of Environment, 177, 37–47, https://doi.org/10.1016/j.rse.2016.02.030, 2016.

Zemp, D. C., Schleussner, C.-F., Barbosa, H. M. J., van der Ent, R. J., Donges, J. F., Heinke, J., Sampaio, G., and Rammig, A.: On the importance of cascading moisture recycling in South America, Atmospheric Chemistry and Physics, 14, 13 337–13 359, https://doi.org/10.5194/acp-14-13337-2014, publisher: Copernicus GmbH, 2014.

Zemp, D. C., Schleussner, C. F., Barbosa, H. M., and Rammig, A.: Deforestation effects on Amazon forest resilience, Geophysical Research Letters, 44, 6182–6190, https://doi.org/10.1002/2017GL072955, 2017.

Zhang, Q., Wei, W., Chen, L., Yang, L., Luo, Y., and Cai, A.: Plant traits in influencing soil moisture in semiarid grasslands of the Loess Plateau, China, The Science of the Total Environment, 718, 137 355, https://doi.org/10.1016/j.scitotenv.2020.137355, 2020.

Zhao, L., Xia, J., yu Xu, C., Wang, Z., Sobkowiak, L., and Long, C.: Evapotranspiration estimation methods in hydrological models, Journal of Geographical Sciences, 23, 359–369, https://doi.org/10.1007/s11442-013-1015-9, 2013.

Zheng, C. and Jia, L.: Global canopy rainfall interception loss derived from satellite earth observations, Ecohydrology, 13, e2186, https://doi.org/10.1002/eco.2186, _eprint: https://onlinelibrary.wiley.com/doi/pdf/10.1002/eco.2186, 2020.

https://doi.org/10.5194/egusphere-2023-3069
Preprint. Discussion started: 29 January 2024

Appendix A: VIF Results

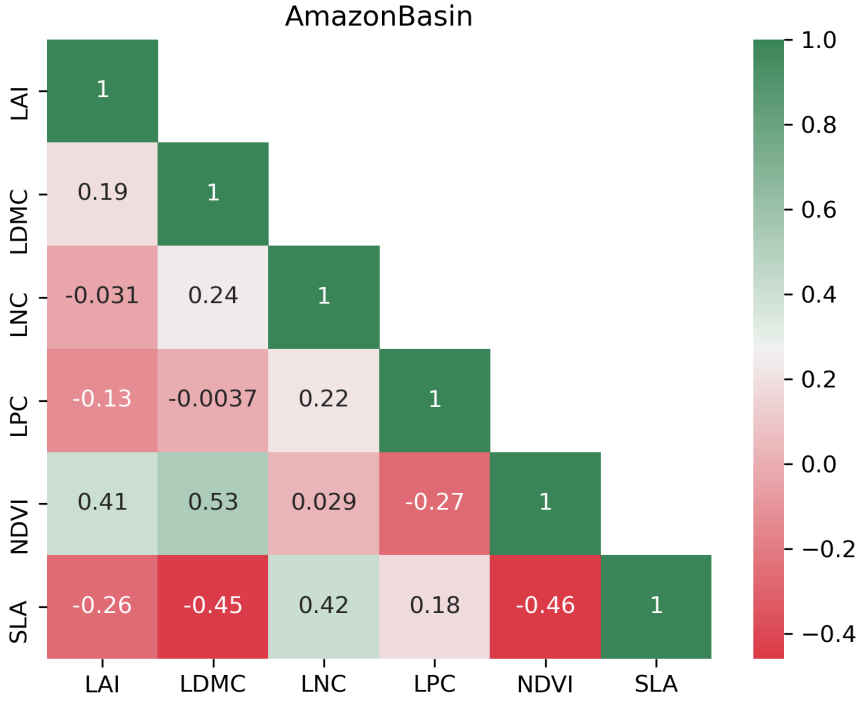

Figure A1. VIF of plant traits in the Amazon Basin

https://doi.org/10.5194/egusphere-2023-3069
Preprint. Discussion started: 29 January 2024

Appendix B: Multivariate Regression and Quantile Regression Results

Table B1. Multivariate regression results for the Amazonas Sub-basin

ENV_PARAM	STAT	LAI	LDMC	LNC	LPC	NDVI	SLA
ET_MEAN	Slope	-0.121	-0.060	0.270	0.025	0.511	-0.403
(R-squared: 0.474)	t-value	-11.358	-3.807	15.191	1.997	43.732	-26.235
	p-value	0.000	0.000	0.000	0.046	0.000	0.000
PET_MEAN	Slope	-0.129	-0.025	0.249	-0.006	0.504	-0.399
(R-squared: 0.484)	t-value	-12.166	-1.597	14.135	-0.450	43.516	-26.207
	p-value	0.000	0.110	0.000	0.653	0.000	0.000
SM_MEAN	Slope	-0.021	0.052	-0.107	-0.140	-0.218	0.203
(R-squared: 0.098)	t-value	-1.500	2.509	-4.619	-8.418	-14.279	10.107
	p-value	0.134	0.012	0.000	0.000	0.000	0.000
VPD_MEAN	Slope	-0.571	0.052	0.039	-0.136	0.158	-0.032
(R-squared: 0.245)	t-value	-44.650	2.713	1.858	-8.976	11.267	-1.764
	p-value	0.000	0.007	0.063	0.000	0.000	0.078
LSTDAY_MEAN	Slope	-0.446	-0.075	-0.060	-0.031	0.002	0.566
(R-squared: 0.598)	t-value	-47.809	-5.399	-3.848	-2.758	0.160	42.176
	p-value	0.000	0.000	0.000	0.006	0.873	0.000
LSTNIGHT_MEAN	Slope	-0.081	0.048	-0.201	-0.025	-0.555	0.371
(R-squared: 0.605)	t-value	-8.722	3.509	-13.081	-2.310	-54.889	27.864
	p-value	0.000	0.000	0.000	0.021	0.000	0.000
ET_STD	Slope	-0.004	0.006	-0.023	-0.081	-0.068	0.271
(R-squared: 0.064)	t-value	-0.256	0.298	-0.992	-4.771	-4.367	13.216
	p-value	0.798	0.766	0.321	0.000	0.000	0.000
PET_STD	Slope	-0.033	0.017	-0.010	-0.071	0.002	0.219
(R-squared: 0.034)	t-value	-2.263	0.777	-0.398	-4.162	0.119	10.546
	p-value	0.024	0.437	0.691	0.000	0.905	0.000
SM_STD	Slope	0.119	-0.056	0.034	0.070	-0.144	-0.103
(R-squared: 0.02)	t-value	8.144	-2.589	1.386	4.064	-9.033	-4.930
	p-value	0.000	0.010	0.166	0.000	0.000	0.000
VPD_STD	Slope	-0.546	-0.121	0.050	0.159	0.189	0.031
(R-squared: 0.329)	t-value	-45.283	-6.753	2.492	11.097	14.291	1.791
	p-value	0.000	0.000	0.013	0.000	0.000	0.073
LSTDAY_STD	Slope	-0.331	-0.050	-0.052	-0.094	-0.126	0.532
(R-squared: 0.487)	t-value	-31.449	-3.178	-2.966	-7.514	-10.898	35.110
	p-value	0.000	0.001	0.003	0.000	0.000	0.000
LSTNIGHT_STD	Slope	0.077	0.089	-0.036	-0.044	-0.314	-0.071
(R-squared: 0.082)	t-value	5.470	4.227	-1.553	-2.641	-20.356	-3.508
	p-value	0.000	0.000	0.120	0.008	0.000	0.000

https://doi.org/10.5194/egusphere-2023-3069
Preprint. Discussion started: 29 January 2024

Table B2. Multivariate regression results for the Madeira Sub-basin

ENV_PARAM	STAT	LAI	LDMC	LNC	LPC	NDVI	SLA
ET_MEAN	Slope	0.261	-0.155	0.060	0.180	0.610	-0.224
(R-squared: 0.627)	t-value	70.169	-38.448	14.928	51.118	145.870	-47.788
	p-value	0.000	0.000	0.000	0.000	0.000	0.000
PET_MEAN	Slope	-0.504	0.067	0.012	-0.281	0.139	0.389
(R-squared: 0.422)	t-value	-108.894	13.418	2.302	-64.141	26.705	66.762
	p-value	0.000	0.000	0.021	0.000	0.000	0.000
SM_MEAN	Slope	-0.040	0.021	0.069	-0.125	0.215	-0.053
(R-squared: 0.098)	t-value	-6.974	3.397	10.945	-22.900	33.015	-7.330
	p-value	0.000	0.001	0.000	0.000	0.000	0.000
VPD_MEAN	Slope	-0.594	0.126	0.022	-0.268	0.027	0.224
(R-squared: 0.437)	t-value	-130.097	25.502	4.430	-61.937	5.233	39.005
	p-value	0.000	0.000	0.000	0.000	0.000	0.000
LSTDAY_MEAN	Slope	-0.306	-0.307	0.307	-0.285	0.232	0.224
(R-squared: 0.373)	t-value	-63.444	-58.823	58.762	-62.444	42.800	36.970
	p-value	0.000	0.000	0.000	0.000	0.000	0.000
LSTNIGHT_MEAN	Slope	-0.246	-0.147	0.226	-0.341	0.587	0.120
(R-squared: 0.439)	t-value	-53.961	-29.795	45.745	-78.981	114.418	20.898
	p-value	0.000	0.000	0.000	0.000	0.000	0.000
ET_STD	Slope	-0.281	0.067	-0.001	-0.214	-0.052	0.238
(R-squared: 0.179)	t-value	-50.857	11.184	-0.231	-40.891	-8.427	34.282
	p-value	0.000	0.000	0.817	0.000	0.000	0.000
PET_STD	Slope	0.104	-0.013	0.012	-0.006	-0.033	-0.083
(R-squared: 0.019)	t-value	17.259	-1.961	1.838	-1.136	-4.826	-10.899
	p-value	0.000	0.050	0.066	0.256	0.000	0.000
SM_STD	Slope	-0.037	-0.112	0.056	-0.078	0.201	0.120
(R-squared: 0.047)	t-value	-6.254	-17.430	8.667	-13.827	30.046	16.011
	p-value	0.000	0.000	0.000	0.000	0.000	0.000
VPD_STD	Slope	-0.258	-0.025	0.099	-0.352	0.087	0.419
(R-squared: 0.315)	t-value	-51.126	-4.545	18.074	-73.827	15.410	66.171
	p-value	0.000	0.000	0.000	0.000	0.000	0.000
LSTDAY_STD	Slope	-0.215	0.064	-0.100	-0.020	-0.589	0.272
(R-squared: 0.736)	t-value	-68.784	19.034	-29.546	-6.740	-167.391	69.082
	p-value	0.000	0.000	0.000	0.000	0.000	0.000
LSTNIGHT_STD	Slope	-0.521	0.192	-0.200	0.050	-0.039	0.161
(R-squared: 0.335)	t-value	-104.903	35.604	-37.246	10.725	-7.062	25.748
	p-value	0.000	0.000	0.000	0.000	0.000	0.000

https://doi.org/10.5194/egusphere-2023-3069
Preprint. Discussion started: 29 January 2024

Table B3. Multivariate regression results for the Negro Sub-basin

ENV_PARAM	STAT	LAI	LDMC	LNC	LPC	NDVI	SLA
ET_MEAN	Slope	-0.031	-0.045	-0.008	-0.050	0.852	0.033
(R-squared: 0.632)	t-value	-6.893	-7.774	-1.509	-11.886	129.957	5.026
	p-value	0.000	0.000	0.131	0.000	0.000	0.000
PET_MEAN	Slope	0.030	-0.299	0.065	0.121	-0.080	0.216
(R-squared: 0.265)	t-value	4.652	-36.580	8.590	20.468	-8.667	23.139
	p-value	0.000	0.000	0.000	0.000	0.000	0.000
SM_MEAN	Slope	-0.218	0.054	0.022	-0.012	-0.038	-0.205
(R-squared: 0.086)	t-value	-30.800	5.955	2.598	-1.778	-3.646	-19.646
	p-value	0.000	0.000	0.009	0.075	0.000	0.000
VPD_MEAN	Slope	-0.150	-0.168	0.016	-0.203	-0.100	0.476
(R-squared: 0.549)	t-value	-30.155	-26.179	2.671	-43.906	-13.754	64.960
	p-value	0.000	0.000	0.008	0.000	0.000	0.000
LSTDAY_MEAN	Slope	-0.377	-0.130	0.051	0.009	-0.534	0.091
(R-squared: 0.775)	t-value	-107.004	-28.678	12.118	2.671	-104.166	17.492
	p-value	0.000	0.000	0.000	0.008	0.000	0.000
LSTNIGHT_MEAN	Slope	-0.509	0.150	-0.090	-0.086	-0.291	0.092
(R-squared: 0.46)	t-value	-93.421	21.390	-13.897	-16.978	-36.722	11.442
	p-value	0.000	0.000	0.000	0.000	0.000	0.000
ET_STD	Slope	0.148	-0.119	-0.051	0.022	-0.223	0.085
(R-squared: 0.126)	t-value	21.354	-13.381	-6.206	3.355	-22.092	8.296
	p-value	0.000	0.000	0.000	0.001	0.000	0.000
PET_STD	Slope	0.162	-0.043	-0.060	-0.002	-0.141	0.028
(R-squared: 0.045)	t-value	22.309	-4.644	-7.010	-0.349	-13.343	2.665
	p-value	0.000	0.000	0.000	0.727	0.000	0.008
SM_STD	Slope	-0.007	0.026	-0.113	0.052	0.062	0.091
(R-squared: 0.01)	t-value	-0.985	2.789	-12.924	7.508	5.740	8.379
	p-value	0.325	0.005	0.000	0.000	0.000	0.000
VPD_STD	Slope	-0.019	-0.189	0.013	-0.189	-0.176	0.389
(R-squared: 0.484)	t-value	-3.612	-27.620	2.118	-38.163	-22.686	49.603
	p-value	0.000	0.000	0.034	0.000	0.000	0.000
LSTDAY_STD	Slope	-0.049	-0.037	-0.080	-0.043	-0.710	0.231
(R-squared: 0.815)	t-value	-15.435	-9.072	-21.111	-14.439	-152.977	49.206
	p-value	0.000	0.000	0.000	0.000	0.000	0.000
LSTNIGHT_STD	Slope	-0.162	0.160	-0.085	-0.030	-0.152	-0.206
(R-squared: 0.119)	t-value	-23.324	17.880	-10.323	-4.690	-15.037	-20.119
	p-value	0.000	0.000	0.000	0.000	0.000	0.000

https://doi.org/10.5194/egusphere-2023-3069
Preprint. Discussion started: 29 January 2024

Table B4. Multivariate regression results for the Solimoes Sub-basin

ENV_PARAM	STAT	LAI	LDMC	LNC	LPC	NDVI	SLA
ET_MEAN	Slope	-0.355	0.055	0.044	-0.010	0.761	-0.043
(R-squared: 0.624)	t-value	-144.123	16.389	12.935	-3.772	230.954	-12.473
	p-value	0.000	0.000	0.000	0.000	0.000	0.000
PET_MEAN	Slope	-0.054	-0.103	0.016	-0.184	0.453	0.182
(R-squared: 0.199)	t-value	-15.076	-21.080	3.177	-47.580	94.234	35.937
	p-value	0.000	0.000	0.001	0.000	0.000	0.000
SM_MEAN	Slope	-0.381	0.122	-0.112	0.200	0.495	-0.095
(R-squared: 0.349)	t-value	-117.622	27.844	-24.952	57.327	114.088	-20.814
	p-value	0.000	0.000	0.000	0.000	0.000	0.000
VPD_MEAN	Slope	-0.164	-0.039	-0.117	-0.010	0.499	0.236
(R-squared: 0.165)	t-value	-44.752	-7.877	-23.195	-2.438	101.629	45.735
	p-value	0.000	0.000	0.000	0.015	0.000	0.000
LSTDAY_MEAN	Slope	-0.615	-0.165	0.082	-0.009	0.850	0.108
(R-squared: 0.695)	t-value	-277.481	-54.838	26.942	-3.619	285.921	34.547
	p-value	0.000	0.000	0.000	0.000	0.000	0.000
LSTNIGHT_MEAN	Slope	-0.406	0.017	-0.022	0.021	0.935	0.020
(R-squared: 0.803)	t-value	-227.608	7.067	-9.031	11.069	391.468	8.093
	p-value	0.000	0.000	0.000	0.000	0.000	0.000
ET_STD	Slope	0.455	-0.013	-0.090	-0.039	0.064	0.111
(R-squared: 0.23)	t-value	129.168	-2.667	-18.566	-10.170	13.574	22.457
	p-value	0.000	0.008	0.000	0.000	0.000	0.000
PET_STD	Slope	0.402	0.049	-0.084	-0.033	0.064	0.058
(R-squared: 0.203)	t-value	112.165	10.094	-16.896	-8.505	13.358	11.496
	p-value	0.000	0.000	0.000	0.000	0.000	0.000
SM_STD	Slope	0.068	-0.012	0.009	-0.235	-0.031	0.130
(R-squared: 0.056)	t-value	17.555	-2.195	1.621	-55.941	-5.881	23.760
	p-value	0.000	0.028	0.105	0.000	0.000	0.000
VPD_STD	Slope	-0.160	0.081	-0.002	-0.540	0.048	0.234
(R-squared: 0.284)	t-value	-46.963	17.624	-0.381	-147.396	10.583	48.973
	p-value	0.000	0.000	0.704	0.000	0.000	0.000
LSTDAY_STD	Slope	0.183	-0.136	0.071	-0.037	-0.831	0.080
(R-squared: 0.821)	t-value	107.491	-59.171	30.356	-20.027	-364.644	33.563
	p-value	0.000	0.000	0.000	0.000	0.000	0.000
LSTNIGHT_STD	Slope	-0.230	0.181	-0.114	-0.271	-0.075	0.078
(R-squared: 0.11)	t-value	-60.673	35.207	-21.862	-66.468	-14.682	14.551
	p-value	0.000	0.000	0.000	0.000	0.000	0.000

https://doi.org/10.5194/egusphere-2023-3069
Preprint. Discussion started: 29 January 2024

Table B5. Multivariate regression results for the Tapajos Sub-basin

ENV_PARAM	STAT	LAI	LDMC	LNC	LPC	NDVI	SLA
ET_MEAN	Slope	0.151	0.016	-0.033	-0.028	0.687	-0.023
(R-squared: 0.702)	t-value	25.885	1.942	-5.983	-3.837	104.962	-2.267
	p-value	0.000	0.052	0.000	0.000	0.000	0.023
PET_MEAN	Slope	-0.442	-0.052	0.070	0.106	-0.383	-0.058
(R-squared: 0.667)	t-value	-71.512	-5.965	12.027	13.688	-55.340	-5.479
	p-value	0.000	0.000	0.000	0.000	0.000	0.000
SM_MEAN	Slope	-0.210	0.102	-0.003	-0.041	-0.342	0.080
(R-squared: 0.225)	t-value	-22.240	7.731	-0.349	-3.498	-32.363	4.996
	p-value	0.000	0.000	0.727	0.000	0.000	0.000
VPD_MEAN	Slope	-0.482	-0.200	0.129	-0.111	0.509	0.194
(R-squared: 0.216)	t-value	-50.807	-14.998	14.422	-9.318	47.967	12.049
	p-value	0.000	0.000	0.000	0.000	0.000	0.000
LSTDAY_MEAN	Slope	-0.255	-0.029	0.018	0.005	-0.602	0.152
(R-squared: 0.838)	t-value	-59.063	-4.838	4.372	0.953	-124.832	20.750
	p-value	0.000	0.000	0.000	0.341	0.000	0.000
LSTNIGHT_MEAN	Slope	0.578	0.017	-0.035	-0.304	0.157	0.263
(R-squared: 0.564)	t-value	81.723	1.676	-5.214	-34.393	19.773	21.861
	p-value	0.000	0.094	0.000	0.000	0.000	0.000
ET_STD	Slope	-0.237	-0.012	0.032	-0.127	-0.253	0.275
(R-squared: 0.323)	t-value	-26.890	-0.939	3.894	-11.541	-25.686	18.355
	p-value	0.000	0.348	0.000	0.000	0.000	0.000
PET_STD	Slope	-0.216	-0.014	-0.022	-0.016	-0.146	0.263
(R-squared: 0.27)	t-value	-23.628	-1.099	-2.510	-1.429	-14.296	16.886
	p-value	0.000	0.272	0.012	0.153	0.000	0.000
SM_STD	Slope	-0.096	0.002	0.010	-0.040	-0.055	-0.011
(R-squared: 0.014)	t-value	-9.030	0.114	1.008	-3.028	-4.647	-0.622
	p-value	0.000	0.910	0.314	0.002	0.000	0.534
VPD_STD	Slope	-0.431	-0.295	0.128	0.212	0.571	-0.142
(R-squared: 0.21)	t-value	-45.271	-22.024	14.291	17.775	53.567	-8.762
	p-value	0.000	0.000	0.000	0.000	0.000	0.000
LSTDAY_STD	Slope	-0.127	0.051	-0.006	-0.042	-0.717	0.162
(R-squared: 0.726)	t-value	-22.563	6.508	-1.165	-5.917	-114.117	17.028
	p-value	0.000	0.000	0.244	0.000	0.000	0.000
LSTNIGHT_STD	Slope	-0.053	0.239	-0.142	-0.138	-0.568	0.191
(R-squared: 0.28)	t-value	-5.815	18.692	-16.567	-12.162	-55.879	12.328
	p-value	0.000	0.000	0.000	0.000	0.000	0.000

https://doi.org/10.5194/egusphere-2023-3069
Preprint. Discussion started: 29 January 2024

Table B6. Multivariate regression results for the Trombetas Sub-basin

ENV_PARAM	STAT	LAI	LDMC	LNC	LPC	NDVI	SLA
ET_MEAN	Slope	0.006	0.036	0.055	-0.159	0.549	0.026
(R-squared: 0.352)	t-value	0.757	4.057	4.915	-20.018	63.572	2.465
	p-value	0.449	0.000	0.000	0.000	0.000	0.014
PET_MEAN	Slope	0.120	0.148	-0.033	-0.358	0.164	0.109
(R-squared: 0.177)	t-value	13.866	14.898	-2.644	-40.053	16.829	9.323
	p-value	0.000	0.000	0.008	0.000	0.000	0.000
SM_MEAN	Slope	-0.037	0.009	-0.032	0.232	-0.238	-0.059
(R-squared: 0.118)	t-value	-4.120	0.877	-2.458	25.012	-23.629	-4.886
	p-value	0.000	0.381	0.014	0.000	0.000	0.000
VPD_MEAN	Slope	-0.019	0.070	0.088	-0.366	-0.132	0.046
(R-squared: 0.13)	t-value	-2.159	6.885	6.791	-39.767	-13.173	3.841
	p-value	0.031	0.000	0.000	0.000	0.000	0.000
LSTDAY_MEAN	Slope	-0.477	0.090	-0.244	-0.195	-0.009	0.516
(R-squared: 0.398)	t-value	-64.310	10.597	-22.747	-25.498	-1.117	51.503
	p-value	0.000	0.000	0.000	0.000	0.264	0.000
LSTNIGHT_MEAN	Slope	-0.229	0.213	-0.246	0.113	-0.551	-0.042
(R-squared: 0.559)	t-value	-36.114	29.222	-26.824	17.281	-77.289	-4.924
	p-value	0.000	0.000	0.000	0.000	0.000	0.000
ET_STD	Slope	0.091	-0.012	-0.096	0.014	-0.218	0.100
(R-squared: 0.077)	t-value	9.876	-1.160	-7.224	1.499	-21.138	8.093
	p-value	0.000	0.246	0.000	0.134	0.000	0.000
PET_STD	Slope	0.116	0.110	-0.156	-0.148	-0.270	0.127
(R-squared: 0.123)	t-value	12.903	10.683	-12.075	-16.070	-26.872	10.509
	p-value	0.000	0.000	0.000	0.000	0.000	0.000
SM_STD	Slope	0.012	0.029	-0.048	0.017	0.161	0.016
(R-squared: 0.025)	t-value	1.281	2.703	-3.493	1.742	15.157	1.226
	p-value	0.200	0.007	0.000	0.082	0.000	0.220
VPD_STD	Slope	0.021	-0.027	0.119	-0.486	-0.174	0.169
(R-squared: 0.282)	t-value	2.554	-2.869	10.152	-58.184	-19.156	15.491
	p-value	0.011	0.004	0.000	0.000	0.000	0.000
LSTDAY_STD	Slope	0.033	-0.095	-0.150	0.054	-0.436	0.409
(R-squared: 0.468)	t-value	4.729	-11.894	-14.839	7.516	-55.751	43.504
	p-value	0.000	0.000	0.000	0.000	0.000	0.000
LSTNIGHT_STD	Slope	-0.113	0.183	-0.127	-0.031	-0.206	-0.021
(R-squared: 0.102)	t-value	-12.474	17.606	-9.716	-3.323	-20.240	-1.740
	p-value	0.000	0.000	0.000	0.001	0.000	0.082

https://doi.org/10.5194/egusphere-2023-3069
Preprint. Discussion started: 29 January 2024

Table B7. Multivariate regression results for the Xingu Sub-basin

ENV_PARAM	STAT	LAI	LDMC	LNC	LPC	NDVI	SLA
ET_MEAN	Slope	0.352	-0.051	0.036	-0.013	0.607	-0.054
(R-squared: 0.741)	t-value	67.583	-7.344	6.481	-1.846	97.664	-5.702
	p-value	0.000	0.000	0.000	0.065	0.000	0.000
PET_MEAN	Slope	-0.853	0.003	0.102	-0.047	-0.098	0.025
(R-squared: 0.799)	t-value	-186.249	0.525	20.878	-7.428	-17.949	2.940
	p-value	0.000	0.600	0.000	0.000	0.000	0.003
SM_MEAN	Slope	0.023	0.092	0.046	-0.165	-0.316	0.046
(R-squared: 0.057)	t-value	2.345	6.897	4.373	-12.067	-26.704	2.553
	p-value	0.019	0.000	0.000	0.000	0.000	0.011
VPD_MEAN	Slope	-0.866	-0.057	0.185	-0.127	0.073	-0.066
(R-squared: 0.614)	t-value	-136.277	-6.707	27.366	-14.499	9.626	-5.683
	p-value	0.000	0.000	0.000	0.000	0.000	0.000
LSTDAY_MEAN	Slope	-0.434	-0.020	0.039	-0.070	-0.539	0.189
(R-squared: 0.862)	t-value	-114.230	-3.973	9.738	-13.312	-119.062	27.274
	p-value	0.000	0.000	0.000	0.000	0.000	0.000
LSTNIGHT_MEAN	Slope	0.732	0.117	-0.118	-0.044	-0.053	0.019
(R-squared: 0.561)	t-value	108.047	12.883	-16.396	-4.700	-6.616	1.562
	p-value	0.000	0.000	0.000	0.000	0.000	0.118
ET_STD	Slope	-0.669	0.076	-0.030	-0.066	-0.151	0.127
(R-squared: 0.565)	t-value	-99.148	8.385	-4.125	-7.045	-18.823	10.293
	p-value	0.000	0.000	0.000	0.000	0.000	0.000
PET_STD	Slope	-0.559	0.007	0.110	-0.070	-0.294	-0.069
(R-squared: 0.477)	t-value	-75.540	0.715	13.896	-6.820	-33.343	-5.087
	p-value	0.000	0.475	0.000	0.000	0.000	0.000
SM_STD	Slope	0.039	0.043	-0.034	-0.041	-0.101	0.058
(R-squared: 0.009)	t-value	3.874	3.115	-3.151	-2.949	-8.290	3.095
	p-value	0.000	0.002	0.002	0.003	0.000	0.002
VPD_STD	Slope	-0.881	-0.114	0.148	0.069	0.244	-0.213
(R-squared: 0.644)	t-value	-144.419	-13.897	22.707	8.247	33.521	-19.103
	p-value	0.000	0.000	0.000	0.000	0.000	0.000
LSTDAY_STD	Slope	-0.090	-0.009	-0.022	-0.103	-0.643	0.297
(R-squared: 0.721)	t-value	-16.737	-1.274	-3.801	-13.799	-99.732	30.026
	p-value	0.000	0.203	0.000	0.000	0.000	0.000
LSTNIGHT_STD	Slope	-0.153	0.155	-0.139	-0.093	-0.606	0.116
(R-squared: 0.434)	t-value	-19.835	14.962	-16.930	-8.772	-66.045	8.213
	p-value	0.000	0.000	0.000	0.000	0.000	0.000

https://doi.org/10.5194/egusphere-2023-3069
Preprint. Discussion started: 29 January 2024

Table B8. Quantile regression results (Q5) for the Amazon Basin

ENV_PARAM	STAT	SLA	LDMC	LNC	LPC	NDVI	LAI
ET_MEAN	R-squared	0.175	0.117	0.002	0.002	0.462	0.141
	Slope	-0.808	0.838	-0.074	-0.101	1.578	0.590
	t-value	-65.432	94.509	-4.668	-11.113	521.361	40.802
	p-value	0.000	0.000	0.000	0.000	0.000	0.000
ET_STD	R-squared	0.003	0.000	0.001	0.025	0.010	0.002
	Slope	0.032	0.005	0.011	-0.066	0.043	0.024
	t-value	32.633	3.331	9.141	-48.902	43.338	21.870
	p-value	0.000	0.001	0.000	0.000	0.000	0.000
PET_MEAN	R-squared	0.001	0.004	0.008	0.059	0.052	0.001
	Slope	0.032	0.052	0.073	-0.240	0.192	-0.026
	t-value	10.733	13.939	21.868	-63.852	92.229	-6.288
	p-value	0.000	0.000	0.000	0.000	0.000	0.000
PET_STD	R-squared	0.000	0.011	0.000	0.051	0.023	0.016
	Slope	-0.005	0.043	0.002	-0.107	0.052	0.063
	t-value	-4.706	33.890	0.861	-73.764	43.442	49.200
	p-value	0.000	0.000	0.389	0.000	0.000	0.000
SM_MEAN	R-squared	0.020	0.045	0.000	0.039	0.090	0.001
	Slope	-0.209	0.265	0.008	-0.208	0.293	0.038
	t-value	-35.196	58.740	0.720	-36.406	74.607	4.570
	p-value	0.000	0.000	0.472	0.000	0.000	0.000
SM_STD	R-squared	0.031	0.007	0.002	0.031	0.004	0.003
	Slope	0.202	-0.068	0.049	-0.154	-0.057	0.063
	t-value	84.185	-14.741	26.626	-50.242	-21.497	30.519
	p-value	0.000	0.000	0.000	0.000	0.000	0.000
VPD_MEAN	R-squared	0.000	0.019	0.006	0.044	0.085	0.046
	Slope	0.010	0.131	0.075	-0.213	0.399	-0.272
	t-value	4.197	47.270	20.805	-63.692	190.741	-53.986
	p-value	0.000	0.000	0.000	0.000	0.000	0.000
VPD_STD	R-squared	0.010	0.000	0.002	0.042	0.003	0.008
	Slope	0.070	-0.003	0.026	-0.106	0.022	-0.045
	t-value	92.698	-2.497	32.507	-94.517	24.351	-42.531
	p-value	0.000	0.013	0.000	0.000	0.000	0.000
LSTDAY_MEAN	R-squared	0.004	0.013	0.065	0.071	0.193	0.081
	Slope	0.219	0.258	0.729	-0.606	1.059	-0.642
	t-value	11.486	11.528	27.972	-30.745	141.636	-23.727
	p-value	0.000	0.000	0.000	0.000	0.000	0.000
LSTDAY_STD	R-squared	0.037	0.013	0.000	0.001	0.092	0.006
	Slope	0.163	-0.070	-0.013	-0.012	-0.302	-0.040
	t-value	180.588	-37.518	-15.786	-11.824	-260.194	-52.134
	p-value	0.000	0.000	0.000	0.000	0.000	0.000
LSTNIGHT_MEAN	R-squared	0.018	0.137	0.009	0.224	0.447	0.007
	Slope	-0.498	0.930	0.354	-1.270	1.255	-0.206
	t-value	-11.195	35.901	7.064	-109.380	159.577	-4.789
	p-value	0.000	0.000	0.000	0.000	0.000	0.000
LSTNIGHT_STD	R-squared	0.003	0.000	0.000	0.001	0.005	0.027
	Slope	0.042	-0.009	-0.002	0.021	-0.041	-0.122
	t-value	27.660	-6.224	-1.638	12.831	-17.700	-74.152
	p-value	0.000	0.000	0.101	0.000	0.000	0.000

https://doi.org/10.5194/egusphere-2023-3069
Preprint. Discussion started: 29 January 2024

Table B9. Quantile regression results (Q5) for the Amazonas Sub-basin

ENV_PARAM	STAT	SLA	LDMC	LNC	LPC	NDVI	LAI
ET_MEAN	R-squared	0.065	0.161	0.118	0.009	0.362	0.107
	Slope	-0.754	1.497	0.797	-0.218	1.505	0.631
	t-value	-7.511	38.855	20.413	-1.583	63.115	9.589
	p-value	0.000	0.000	0.000	0.114	0.000	0.000
ET_STD	R-squared	0.004	0.000	0.001	0.001	0.001	0.005
	Slope	0.062	-0.013	0.070	0.037	0.031	-0.098
	t-value	3.689	-0.547	7.341	2.649	1.731	-6.791
	p-value	0.000	0.585	0.000	0.008	0.084	0.000
PET_MEAN	R-squared	0.047	0.132	0.094	0.008	0.285	0.067
	Slope	-0.447	1.167	0.629	-0.151	1.141	0.398
	t-value	-5.668	33.345	22.768	-1.597	56.445	7.378
	p-value	0.000	0.000	0.000	0.110	0.000	0.000
PET_STD	R-squared	0.000	0.000	0.001	0.000	0.000	0.019
	Slope	0.032	0.014	0.052	-0.016	-0.004	-0.173
	t-value	2.157	1.240	5.548	-0.871	-0.247	-12.214
	p-value	0.031	0.215	0.000	0.384	0.805	0.000
SM_MEAN	R-squared	0.014	0.006	0.001	0.000	0.001	0.000
	Slope	0.110	-0.079	0.063	-0.009	0.035	0.008
	t-value	7.348	-2.640	6.880	-0.635	1.733	0.517
	p-value	0.000	0.008	0.000	0.525	0.083	0.605
SM_STD	R-squared	0.003	0.002	0.000	0.000	0.002	0.002
	Slope	-0.050	0.084	0.036	-0.013	0.090	0.047
	t-value	-2.868	7.413	3.053	-0.898	7.041	2.418
	p-value	0.004	0.000	0.002	0.369	0.000	0.016
VPD_MEAN	R-squared	0.001	0.001	0.003	0.014	0.000	0.049
	Slope	-0.032	0.041	0.122	-0.165	0.015	-0.387
	t-value	-1.931	2.998	9.553	-5.264	0.837	-23.325
	p-value	0.053	0.003	0.000	0.000	0.403	0.000
VPD_STD	R-squared	0.009	0.010	0.015	0.005	0.031	0.001
	Slope	-0.109	0.143	0.222	-0.084	0.155	-0.059
	t-value	-8.529	14.281	25.458	-5.107	17.555	-4.152
	p-value	0.000	0.000	0.000	0.000	0.000	0.000
LSTDAY_MEAN	R-squared	0.069	0.013	0.019	0.048	0.022	0.079
	Slope	0.319	-0.086	0.225	0.229	-0.132	-0.389
	t-value	37.188	-4.042	55.027	30.859	-12.529	-68.879
	p-value	0.000	0.000	0.000	0.000	0.000	0.000
LSTDAY_STD	R-squared	0.012	0.001	0.002	0.001	0.003	0.018
	Slope	0.101	-0.028	0.062	0.026	-0.030	-0.105
	t-value	14.558	-2.528	15.847	4.857	-3.302	-15.725
	p-value	0.000	0.012	0.000	0.000	0.001	0.000
LSTNIGHT_MEAN	R-squared	0.055	0.024	0.004	0.018	0.106	0.040
	Slope	0.281	-0.166	0.085	0.130	-0.537	-0.210
	t-value	40.577	-11.052	26.992	28.954	-57.824	-42.271
	p-value	0.000	0.000	0.000	0.000	0.000	0.000
LSTNIGHT_STD	R-squared	0.000	0.000	0.000	0.003	0.000	0.001
	Slope	-0.015	0.001	0.000	-0.038	0.002	0.022
	t-value	-0.873	0.022	0.015	-1.543	0.156	1.412
	p-value	0.383	0.983	0.988	0.123	0.876	0.158

https://doi.org/10.5194/egusphere-2023-3069
Preprint. Discussion started: 29 January 2024

Table B10. Quantile regression results (Q5) for the Madeira Sub-basin

ENV_PARAM	STAT	SLA	LDMC	LNC	LPC	NDVI	LAI
ET_MEAN	R-squared	0.067	0.051	0.001	0.004	0.446	0.220
	Slope	-0.440	0.563	-0.028	-0.079	1.401	0.634
	t-value	-35.560	88.908	-2.366	-10.082	408.629	37.261
	p-value	0.000	0.000	0.018	0.000	0.000	0.000
ET_STD	R-squared	0.006	0.001	0.010	0.003	0.001	0.007
	Slope	0.049	-0.010	0.072	-0.024	0.015	-0.051
	t-value	15.875	-2.623	34.510	-6.775	4.712	-16.295
	p-value	0.000	0.009	0.000	0.000	0.000	0.000
PET_MEAN	R-squared	0.045	0.000	0.036	0.058	0.042	0.028
	Slope	0.292	-0.010	0.243	-0.199	0.186	-0.208
	t-value	40.134	-0.728	38.751	-23.197	24.932	-26.918
	p-value	0.000	0.467	0.000	0.000	0.000	0.000
PET_STD	R-squared	0.019	0.020	0.000	0.021	0.055	0.043
	Slope	-0.106	0.116	-0.003	-0.101	0.153	0.149
	t-value	-21.557	28.523	-0.416	-15.276	48.549	25.816
	p-value	0.000	0.000	0.677	0.000	0.000	0.000
SM_MEAN	R-squared	0.044	0.052	0.002	0.056	0.149	0.079
	Slope	-0.363	0.405	0.050	-0.303	0.485	0.359
	t-value	-21.750	30.356	1.769	-13.815	44.610	18.508
	p-value	0.000	0.000	0.077	0.000	0.000	0.000
SM_STD	R-squared	0.006	0.001	0.007	0.008	0.009	0.000
	Slope	0.099	-0.032	0.119	-0.085	0.085	0.005
	t-value	12.206	-2.946	18.063	-9.339	12.208	0.513
	p-value	0.000	0.003	0.000	0.000	0.000	0.608
VPD_MEAN	R-squared	0.010	0.000	0.075	0.012	0.046	0.146
	Slope	0.079	-0.016	0.377	-0.098	0.257	-0.465
	t-value	12.011	-1.870	76.390	-8.455	35.194	-87.561
	p-value	0.000	0.061	0.000	0.000	0.000	0.000
VPD_STD	R-squared	0.084	0.009	0.023	0.056	0.002	0.075
	Slope	0.445	-0.100	0.190	-0.179	0.060	-0.290
	t-value	80.450	-8.630	35.768	-20.471	6.435	-62.451
	p-value	0.000	0.000	0.000	0.000	0.000	0.000
LSTDAY_MEAN	R-squared	0.078	0.011	0.196	0.058	0.090	0.105
	Slope	0.724	-0.147	1.016	-0.447	0.694	-0.649
	t-value	25.730	-2.044	46.608	-7.573	22.727	-17.400
	p-value	0.000	0.041	0.000	0.000	0.000	0.000
LSTDAY_STD	R-squared	0.147	0.034	0.002	0.007	0.179	0.109
	Slope	0.344	-0.152	0.065	0.066	-0.567	-0.380
	t-value	98.267	-19.609	41.444	20.594	-154.993	-177.047
	p-value	0.000	0.000	0.000	0.000	0.000	0.000
LSTNIGHT_MEAN	R-squared	0.002	0.011	0.098	0.185	0.307	0.006
	Slope	0.129	0.282	1.028	-1.121	1.053	-0.155
	t-value	3.423	5.970	20.116	-20.539	45.703	-2.615
	p-value	0.001	0.000	0.000	0.000	0.000	0.009
LSTNIGHT_STD	R-squared	0.010	0.001	0.003	0.002	0.014	0.093
	Slope	0.064	-0.023	0.071	0.034	-0.078	-0.289
	t-value	16.209	-5.731	39.879	10.034	-15.998	-92.143
	p-value	0.000	0.000	0.000	0.000	0.000	0.000

https://doi.org/10.5194/egusphere-2023-3069
Preprint. Discussion started: 29 January 2024

Table B11. Quantile regression results (Q5) for the Negro Sub-basin

ENV_PARAM	STAT	SLA	LDMC	LNC	LPC	NDVI	LAI
ET_MEAN	R-squared	0.303	0.301	0.004	0.006	0.681	0.115
	Slope	-1.068	0.950	-0.101	-0.214	1.291	0.486
	t-value	-21.614	15.851	-1.070	-3.375	174.169	5.067
	p-value	0.000	0.000	0.285	0.001	0.000	0.000
ET_STD	R-squared	0.002	0.005	0.004	0.000	0.002	0.006
	Slope	0.025	-0.038	0.033	-0.006	0.023	0.041
	t-value	6.869	-5.811	9.515	-1.449	7.533	9.697
	p-value	0.000	0.000	0.000	0.147	0.000	0.000
PET_MEAN	R-squared	0.010	0.018	0.061	0.002	0.092	0.040
	Slope	0.146	-0.160	0.284	0.065	0.535	0.236
	t-value	12.581	-6.071	27.318	5.255	105.329	19.056
	p-value	0.000	0.000	0.000	0.000	0.000	0.000
PET_STD	R-squared	0.003	0.003	0.000	0.008	0.003	0.003
	Slope	0.027	-0.023	0.004	-0.037	-0.025	0.026
	t-value	8.002	-4.313	1.322	-9.239	-7.462	8.005
	p-value	0.000	0.000	0.186	0.000	0.000	0.000
SM_MEAN	R-squared	0.002	0.001	0.004	0.012	0.002	0.002
	Slope	0.061	-0.054	0.103	-0.151	-0.047	-0.036
	t-value	4.089	-4.612	8.562	-8.731	-2.917	-1.883
	p-value	0.000	0.000	0.000	0.000	0.004	0.060
SM_STD	R-squared	0.009	0.003	0.000	0.001	0.006	0.002
	Slope	0.063	-0.036	0.011	-0.015	-0.049	0.046
	t-value	14.538	-6.000	3.507	-3.484	-12.165	16.324
	p-value	0.000	0.000	0.000	0.000	0.000	0.000
VPD_MEAN	R-squared	0.086	0.002	0.045	0.023	0.025	0.011
	Slope	0.350	-0.036	0.129	0.088	-0.232	-0.117
	t-value	132.094	-8.633	48.082	21.385	-67.470	-30.809
	p-value	0.000	0.000	0.000	0.000	0.000	0.000
VPD_STD	R-squared	0.041	0.019	0.000	0.059	0.077	0.005
	Slope	0.275	-0.141	0.007	-0.134	-0.364	-0.049
	t-value	164.138	-31.229	4.045	-51.983	-166.666	-17.685
	p-value	0.000	0.000	0.000	0.000	0.000	0.000
LSTDAY_MEAN	R-squared	0.001	0.007	0.001	0.051	0.062	0.287
	Slope	-0.048	0.174	0.102	-0.289	-0.482	-0.421
	t-value	-3.662	17.510	9.258	-15.165	-31.884	-33.200
	p-value	0.000	0.000	0.000	0.000	0.000	0.000
LSTDAY_STD	R-squared	0.002	0.013	0.009	0.038	0.176	0.025
	Slope	0.040	-0.076	-0.054	-0.091	-0.457	-0.075
	t-value	23.528	-15.450	-13.252	-27.816	-145.868	-33.116
	p-value	0.000	0.000	0.000	0.000	0.000	0.000
LSTNIGHT_MEAN	R-squared	0.000	0.016	0.006	0.085	0.003	0.266
	Slope	-0.052	0.662	0.272	-0.569	-0.109	-0.741
	t-value	-2.823	39.116	18.689	-26.405	-4.052	-25.859
	p-value	0.005	0.000	0.000	0.000	0.000	0.000
LSTNIGHT_STD	R-squared	0.029	0.029	0.016	0.014	0.002	0.057
	Slope	-0.204	0.331	-0.128	0.133	-0.038	-0.160
	t-value	-19.501	67.896	-6.452	14.328	-3.141	-12.767
	p-value	0.000	0.000	0.000	0.000	0.002	0.000

https://doi.org/10.5194/egusphere-2023-3069
Preprint. Discussion started: 29 January 2024

Table B12. Quantile regression results (Q5) for the Solimoes Sub-basin

ENV_PARAM	STAT	SLA	LDMC	LNC	LPC	NDVI	LAI
ET_MEAN	R-squared	0.087	0.177	0.000	0.107	0.365	0.001
	Slope	-0.480	0.703	-0.009	-0.815	1.021	0.046
	t-value	-13.457	30.799	-0.250	-25.967	124.746	1.020
	p-value	0.000	0.000	0.803	0.000	0.000	0.308
ET_STD	R-squared	0.010	0.016	0.000	0.033	0.057	0.004
	Slope	-0.037	0.059	-0.005	-0.075	0.084	0.027
	t-value	-13.056	41.512	-1.454	-31.051	65.357	11.222
	p-value	0.000	0.000	0.146	0.000	0.000	0.000
PET_MEAN	R-squared	0.012	0.032	0.002	0.067	0.124	0.018
	Slope	-0.102	0.188	0.041	-0.363	0.456	-0.142
	t-value	-9.297	29.387	3.305	-47.555	143.374	-8.382
	p-value	0.000	0.000	0.001	0.000	0.000	0.000
PET_STD	R-squared	0.038	0.064	0.002	0.076	0.095	0.036
	Slope	-0.067	0.084	-0.016	-0.124	0.085	0.073
	t-value	-24.776	57.334	-3.447	-52.924	57.686	27.695
	p-value	0.000	0.000	0.001	0.000	0.000	0.000
SM_MEAN	R-squared	0.041	0.067	0.000	0.049	0.119	0.001
	Slope	-0.201	0.286	-0.017	-0.263	0.344	0.025
	t-value	-15.279	36.006	-1.027	-27.065	56.346	1.804
	p-value	0.000	0.000	0.304	0.000	0.000	0.071
SM_STD	R-squared	0.008	0.004	0.000	0.010	0.008	0.009
	Slope	0.093	-0.051	0.018	-0.087	-0.091	0.075
	t-value	32.782	-8.956	6.710	-23.874	-29.894	23.411
	p-value	0.000	0.000	0.000	0.000	0.000	0.000
VPD_MEAN	R-squared	0.009	0.043	0.016	0.090	0.254	0.076
	Slope	-0.174	0.522	0.255	-0.531	0.796	-0.296
	t-value	-4.809	21.521	10.912	-42.037	166.239	-11.147
	p-value	0.000	0.000	0.000	0.000	0.000	0.000
VPD_STD	R-squared	0.001	0.006	0.007	0.019	0.039	0.066
	Slope	-0.031	0.066	0.097	-0.151	0.247	-0.214
	t-value	-6.000	14.462	23.230	-26.083	87.405	-31.460
	p-value	0.000	0.000	0.000	0.000	0.000	0.000
LSTDAY_MEAN	R-squared	0.001	0.001	0.055	0.018	0.264	0.126
	Slope	0.078	0.065	0.494	-0.352	1.656	-0.528
	t-value	3.162	2.154	20.298	-10.654	228.578	-19.144
	p-value	0.002	0.031	0.000	0.000	0.000	0.000
LSTDAY_STD	R-squared	0.037	0.016	0.001	0.003	0.074	0.017
	Slope	0.123	-0.076	0.022	-0.023	-0.269	0.068
	t-value	94.064	-25.212	29.061	-18.361	-229.847	46.810
	p-value	0.000	0.000	0.000	0.000	0.000	0.000
LSTNIGHT_MEAN	R-squared	0.080	0.145	0.000	0.157	0.483	0.011
	Slope	-0.375	0.452	-0.014	-0.788	1.257	0.112
	t-value	-16.443	26.220	-0.560	-41.466	230.313	4.692
	p-value	0.000	0.000	0.575	0.000	0.000	0.000
LSTNIGHT_STD	R-squared	0.000	0.000	0.006	0.001	0.000	0.026
	Slope	0.012	0.004	0.049	0.014	0.003	-0.079
	t-value	6.835	2.873	30.481	7.249	1.448	-40.225
	p-value	0.000	0.004	0.000	0.000	0.148	0.000

https://doi.org/10.5194/egusphere-2023-3069
Preprint. Discussion started: 29 January 2024

Table B13. Quantile regression results (Q5) for the Tapajos Sub-basin

ENV_PARAM	STAT	SLA	LDMC	LNC	LPC	NDVI	LAI
ET_MEAN	R-squared	0.108	0.174	0.004	0.157	0.542	0.368
	Slope	-0.752	0.842	-0.071	-0.744	1.162	0.841
	t-value	-51.136	58.497	-2.987	-31.736	176.250	50.322
	p-value	0.000	0.000	0.003	0.000	0.000	0.000
ET_STD	R-squared	0.040	0.032	0.000	0.037	0.025	0.039
	Slope	0.176	-0.161	0.006	0.147	-0.147	-0.142
	t-value	28.832	-13.878	0.802	26.934	-20.123	-25.683
	p-value	0.000	0.000	0.422	0.000	0.000	0.000
PET_MEAN	R-squared	0.061	0.027	0.000	0.026	0.072	0.263
	Slope	0.403	-0.328	0.002	0.241	-0.602	-0.766
	t-value	40.456	-12.934	0.100	23.497	-36.156	-131.882
	p-value	0.000	0.000	0.920	0.000	0.000	0.000
PET_STD	R-squared	0.005	0.002	0.001	0.000	0.008	0.001
	Slope	0.110	-0.039	0.030	-0.011	0.103	0.019
	t-value	12.426	-2.577	3.538	-1.123	12.152	1.562
	p-value	0.000	0.010	0.000	0.262	0.000	0.118
SM_MEAN	R-squared	0.010	0.006	0.000	0.010	0.022	0.035
	Slope	0.144	-0.079	-0.015	0.127	-0.213	-0.264
	t-value	11.441	-3.638	-0.994	10.165	-14.543	-21.313
	p-value	0.000	0.000	0.320	0.000	0.000	0.000
SM_STD	R-squared	0.013	0.008	0.002	0.007	0.018	0.032
	Slope	0.142	-0.085	0.057	0.107	-0.157	-0.206
	t-value	10.290	-3.268	3.568	7.806	-10.939	-16.953
	p-value	0.000	0.001	0.000	0.000	0.000	0.000
VPD_MEAN	R-squared	0.037	0.014	0.001	0.001	0.021	0.090
	Slope	0.254	-0.185	-0.038	0.046	-0.165	-0.250
	t-value	26.769	-8.887	-1.640	6.875	-14.288	-23.717
	p-value	0.000	0.000	0.101	0.000	0.000	0.000
VPD_STD	R-squared	0.034	0.020	0.001	0.006	0.039	0.177
	Slope	0.166	-0.172	-0.018	0.110	-0.156	-0.179
	t-value	27.789	-11.818	-1.058	27.445	-20.953	-39.579
	p-value	0.000	0.000	0.290	0.000	0.000	0.000
LSTDAY_MEAN	R-squared	0.107	0.061	0.003	0.067	0.101	0.115
	Slope	0.300	-0.259	0.027	0.251	-0.632	-0.307
	t-value	73.182	-33.092	7.808	81.297	-92.507	-92.108
	p-value	0.000	0.000	0.000	0.000	0.000	0.000
LSTDAY_STD	R-squared	0.106	0.085	0.000	0.098	0.218	0.068
	Slope	0.263	-0.233	-0.002	0.230	-0.499	-0.212
	t-value	66.013	-33.234	-0.397	77.713	-94.244	-87.393
	p-value	0.000	0.000	0.692	0.000	0.000	0.000
LSTNIGHT_MEAN	R-squared	0.016	0.031	0.001	0.099	0.173	0.278
	Slope	-0.201	0.313	-0.043	-0.481	0.583	0.808
	t-value	-18.865	30.954	-2.908	-29.750	55.495	55.051
	p-value	0.000	0.000	0.004	0.000	0.000	0.000
LSTNIGHT_STD	R-squared	0.017	0.011	0.001	0.007	0.103	0.016
	Slope	0.138	-0.111	-0.020	0.096	-0.434	-0.177
	t-value	15.109	-7.867	-1.369	11.631	-51.650	-27.002
	p-value	0.000	0.000	0.171	0.000	0.000	0.000

https://doi.org/10.5194/egusphere-2023-3069
Preprint. Discussion started: 29 January 2024

Table B14. Quantile regression results (Q5) for the Trombetas Sub-basin

ENV_PARAM	STAT	SLA	LDMC	LNC	LPC	NDVI	LAI
ET_MEAN	R-squared	0.017	0.027	0.094	0.008	0.441	0.054
	Slope	-0.215	0.277	0.820	-0.209	1.379	0.426
	t-value	-1.394	2.067	23.355	-1.574	158.889	4.776
	p-value	0.163	0.039	0.000	0.116	0.000	0.000
ET_STD	R-squared	0.002	0.004	0.000	0.002	0.002	0.009
	Slope	0.065	-0.077	0.030	-0.039	-0.054	0.086
	t-value	5.305	-3.628	2.635	-2.837	-4.198	5.341
	p-value	0.000	0.000	0.008	0.005	0.000	0.000
PET_MEAN	R-squared	0.001	0.000	0.010	0.032	0.028	0.058
	Slope	-0.022	0.005	0.170	-0.207	0.151	0.206
	t-value	-1.526	0.336	18.237	-12.823	11.558	12.584
	p-value	0.127	0.737	0.000	0.000	0.000	0.000
PET_STD	R-squared	0.000	0.002	0.000	0.012	0.016	0.014
	Slope	-0.005	-0.043	-0.021	-0.106	-0.125	0.075
	t-value	-0.694	-3.475	-1.964	-13.457	-15.649	7.198
	p-value	0.488	0.001	0.050	0.000	0.000	0.000
SM_MEAN	R-squared	0.002	0.000	0.001	0.017	0.011	0.011
	Slope	0.052	0.014	-0.034	0.137	-0.149	-0.136
	t-value	3.693	1.031	-1.958	11.177	-9.618	-8.177
	p-value	0.000	0.303	0.050	0.000	0.000	0.000
SM_STD	R-squared	0.000	0.000	0.006	0.007	0.025	0.006
	Slope	0.004	0.007	0.076	-0.083	0.097	0.054
	t-value	0.384	0.526	11.651	-7.649	13.570	5.855
	p-value	0.701	0.599	0.000	0.000	0.000	0.000
VPD_MEAN	R-squared	0.000	0.001	0.000	0.066	0.006	0.006
	Slope	0.032	-0.055	0.020	-0.275	-0.136	0.104
	t-value	1.651	-1.895	0.822	-8.562	-5.621	3.940
	p-value	0.099	0.058	0.411	0.000	0.000	0.000
VPD_STD	R-squared	0.002	0.015	0.003	0.223	0.005	0.113
	Slope	0.129	-0.133	0.092	-0.626	-0.116	0.397
	t-value	9.700	-2.388	5.366	-32.900	-6.882	16.588
	p-value	0.000	0.017	0.000	0.000	0.000	0.000
LSTDAY_MEAN	R-squared	0.022	0.051	0.002	0.067	0.016	0.272
	Slope	0.308	0.560	-0.078	0.461	-0.158	-0.605
	t-value	20.908	42.331	-3.299	36.731	-7.669	-33.106
	p-value	0.000	0.000	0.001	0.000	0.000	0.000
LSTDAY_STD	R-squared	0.012	0.015	0.001	0.026	0.047	0.000
	Slope	0.132	-0.086	-0.031	0.095	-0.233	0.005
	t-value	29.088	-6.106	-4.985	14.940	-27.027	1.062
	p-value	0.000	0.000	0.000	0.000	0.000	0.288
LSTNIGHT_MEAN	R-squared	0.010	0.126	0.018	0.068	0.003	0.224
	Slope	-0.133	0.915	-0.191	0.427	-0.070	-0.474
	t-value	-8.228	81.473	-4.803	42.191	-4.327	-36.086
	p-value	0.000	0.000	0.000	0.000	0.000	0.000
LSTNIGHT_STD	R-squared	0.002	0.005	0.007	0.010	0.011	0.015
	Slope	-0.067	0.183	-0.078	0.145	-0.123	-0.107
	t-value	-5.615	23.676	-2.986	14.385	-6.990	-5.875
	p-value	0.000	0.000	0.003	0.000	0.000	0.000

https://doi.org/10.5194/egusphere-2023-3069
Preprint. Discussion started: 29 January 2024

Table B15. Quantile regression results (Q5) for the Xingu Sub-basin

ENV_PARAM	STAT	SLA	LDMC	LNC	LPC	NDVI	LAI
ET_MEAN	R-squared	0.179	0.197	0.004	0.148	0.523	0.395
	Slope	-0.748	0.941	-0.101	-0.646	1.030	0.949
	t-value	-29.780	46.573	-4.657	-17.893	156.534	70.829
	p-value	0.000	0.000	0.000	0.000	0.000	0.000
ET_STD	R-squared	0.003	0.000	0.003	0.029	0.004	0.208
	Slope	0.043	0.004	0.050	0.152	-0.075	-0.498
	t-value	10.511	0.531	12.828	32.610	-12.110	-115.692
	p-value	0.000	0.595	0.000	0.000	0.000	0.000
PET_MEAN	R-squared	0.031	0.048	0.012	0.001	0.013	0.500
	Slope	-0.323	0.468	0.186	0.024	0.171	-0.989
	t-value	-30.229	63.124	14.592	1.454	20.082	-133.347
	p-value	0.000	0.000	0.000	0.146	0.000	0.000
PET_STD	R-squared	0.001	0.004	0.003	0.005	0.001	0.089
	Slope	-0.022	0.050	0.048	0.053	-0.016	-0.242
	t-value	-4.611	12.918	12.792	10.980	-2.439	-43.633
	p-value	0.000	0.000	0.000	0.000	0.015	0.000
SM_MEAN	R-squared	0.000	0.001	0.001	0.000	0.005	0.006
	Slope	-0.005	0.027	0.031	-0.021	-0.128	-0.108
	t-value	-0.379	2.054	2.990	-1.313	-10.278	-10.132
	p-value	0.705	0.040	0.003	0.189	0.000	0.000
SM_STD	R-squared	0.007	0.002	0.002	0.009	0.012	0.028
	Slope	0.096	-0.043	0.054	0.092	-0.124	-0.168
	t-value	9.906	-2.615	6.743	9.536	-11.121	-16.408
	p-value	0.000	0.009	0.000	0.000	0.000	0.000
VPD_MEAN	R-squared	0.002	0.000	0.002	0.022	0.024	0.232
	Slope	0.041	-0.007	0.053	0.110	-0.173	-0.534
	t-value	15.442	-1.084	26.551	33.376	-39.073	-167.150
	p-value	0.000	0.278	0.000	0.000	0.000	0.000
VPD_STD	R-squared	0.005	0.008	0.007	0.001	0.000	0.212
	Slope	-0.058	0.075	0.090	0.022	-0.025	-0.708
	t-value	-12.917	19.999	21.852	3.523	-4.075	-106.129
	p-value	0.000	0.000	0.000	0.000	0.000	0.000
LSTDAY_MEAN	R-squared	0.008	0.001	0.022	0.082	0.015	0.234
	Slope	0.092	0.018	0.129	0.297	-0.210	-0.409
	t-value	23.402	3.735	51.558	83.990	-31.924	-119.091
	p-value	0.000	0.000	0.000	0.000	0.000	0.000
LSTDAY_STD	R-squared	0.060	0.027	0.002	0.008	0.135	0.001
	Slope	0.213	-0.105	-0.020	0.088	-0.482	-0.018
	t-value	63.854	-12.685	-3.763	47.836	-102.871	-6.510
	p-value	0.000	0.000	0.000	0.000	0.000	0.000
LSTNIGHT_MEAN	R-squared	0.052	0.067	0.001	0.072	0.197	0.309
	Slope	-0.359	0.430	0.084	-0.387	0.619	0.853
	t-value	-23.841	29.100	3.985	-13.342	62.089	43.180
	p-value	0.000	0.000	0.000	0.000	0.000	0.000
LSTNIGHT_STD	R-squared	0.009	0.004	0.000	0.027	0.111	0.174
	Slope	0.110	-0.070	0.003	0.152	-0.506	-0.462
	t-value	14.281	-5.082	0.197	18.364	-60.281	-105.290
	p-value	0.000	0.000	0.844	0.000	0.000	0.000

https://doi.org/10.5194/egusphere-2023-3069
Preprint. Discussion started: 29 January 2024

Table B16. Quantile regression results (Q50) for the Amazon Basin

ENV_PARAM	STAT	SLA	LDMC	LNC	LPC	NDVI	LAI
ET_MEAN	R-squared	0.066	0.052	0.003	0.003	0.238	0.049
	Slope	-0.331	0.349	0.055	-0.045	0.614	0.209
	t-value	-321.375	342.584	54.249	-44.201	667.473	211.382
	p-value	0.000	0.000	0.000	0.000	0.000	0.000
ET_STD	R-squared	0.048	0.007	0.002	0.021	0.001	0.007
	Slope	0.274	-0.124	0.051	-0.149	-0.041	-0.089
	t-value	156.400	-66.321	26.734	-79.343	-21.603	-46.512
	p-value	0.000	0.000	0.000	0.000	0.000	0.000
PET_MEAN	R-squared	0.095	0.020	0.012	0.075	0.000	0.025
	Slope	0.478	-0.346	0.218	-0.384	-0.015	-0.253
	t-value	175.585	-104.742	63.448	-143.917	-4.041	-68.796
	p-value	0.000	0.000	0.000	0.000	0.000	0.000
PET_STD	R-squared	0.004	0.000	0.000	0.057	0.010	0.001
	Slope	0.081	0.030	0.024	-0.280	0.132	-0.041
	t-value	27.662	10.143	8.044	-125.249	46.774	-14.268
	p-value	0.000	0.000	0.000	0.000	0.000	0.000
SM_MEAN	R-squared	0.017	0.024	0.001	0.015	0.016	0.017
	Slope	-0.173	0.268	-0.064	0.206	0.206	-0.176
	t-value	-58.476	94.327	-21.062	69.800	68.353	-59.929
	p-value	0.000	0.000	0.000	0.000	0.000	0.000
SM_STD	R-squared	0.022	0.007	0.003	0.041	0.001	0.000
	Slope	0.181	-0.136	0.077	-0.267	0.030	0.002
	t-value	68.222	-49.132	26.803	-104.884	10.579	0.666
	p-value	0.000	0.000	0.000	0.000	0.000	0.505
VPD_MEAN	R-squared	0.055	0.008	0.001	0.054	0.014	0.071
	Slope	0.370	-0.204	0.054	-0.345	-0.234	-0.371
	t-value	104.734	-46.443	12.730	-122.196	-57.489	-108.527
	p-value	0.000	0.000	0.000	0.000	0.000	0.000
VPD_STD	R-squared	0.121	0.043	0.006	0.122	0.013	0.008
	Slope	0.497	-0.426	0.144	-0.434	-0.181	-0.146
	t-value	189.782	-140.419	39.422	-230.688	-51.037	-37.860
	p-value	0.000	0.000	0.000	0.000	0.000	0.000
LSTDAY_MEAN	R-squared	0.045	0.009	0.001	0.000	0.024	0.102
	Slope	0.224	-0.124	0.021	-0.000	-0.300	-0.278
	t-value	252.106	-176.427	32.576	-0.076	-468.321	-411.350
	p-value	0.000	0.000	0.000	0.939	0.000	0.000
LSTDAY_STD	R-squared	0.166	0.142	0.000	0.000	0.386	0.034
	Slope	0.451	-0.582	0.005	-0.007	-0.864	-0.182
	t-value	397.440	-498.066	3.670	-5.709	-831.983	-136.116
	p-value	0.000	0.000	0.000	0.000	0.000	0.000
LSTNIGHT_MEAN	R-squared	0.031	0.038	0.005	0.000	0.044	0.000
	Slope	-0.083	0.150	-0.047	-0.005	0.184	-0.008
	t-value	-161.390	280.706	-84.502	-7.852	323.170	-12.704
	p-value	0.000	0.000	0.000	0.000	0.000	0.000
LSTNIGHT_STD	R-squared	0.018	0.007	0.000	0.003	0.030	0.012
	Slope	0.149	-0.096	-0.020	0.049	-0.204	-0.132
	t-value	84.119	-54.122	-10.949	27.755	-124.070	-76.932
	p-value	0.000	0.000	0.000	0.000	0.000	0.000

https://doi.org/10.5194/egusphere-2023-3069
Preprint. Discussion started: 29 January 2024

Table B17. Quantile regression results (Q50) for the Amazonas Sub-basin

ENV_PARAM	STAT	SLA	LDMC	LNC	LPC	NDVI	LAI
ET_MEAN	R-squared	0.121	0.149	0.011	0.016	0.190	0.000
	Slope	-0.407	0.693	0.194	-0.204	0.709	0.016
	t-value	-49.899	86.330	17.455	-21.093	80.633	1.422
	p-value	0.000	0.000	0.000	0.000	0.000	0.155
ET_STD	R-squared	0.021	0.006	0.000	0.002	0.006	0.002
	Slope	0.189	-0.134	0.004	0.047	-0.109	-0.064
	t-value	14.639	-10.103	0.310	3.472	-8.167	-4.746
	p-value	0.000	0.000	0.756	0.001	0.000	0.000
PET_MEAN	R-squared	0.121	0.161	0.011	0.029	0.188	0.002
	Slope	-0.466	0.858	0.176	-0.289	0.701	0.083
	t-value	-47.944	91.650	13.569	-27.982	66.517	6.547
	p-value	0.000	0.000	0.000	0.000	0.000	0.000
PET_STD	R-squared	0.015	0.003	0.000	0.004	0.001	0.007
	Slope	0.159	-0.068	0.030	0.086	-0.048	-0.113
	t-value	11.436	-4.868	2.143	6.207	-3.439	-8.118
	p-value	0.000	0.000	0.032	0.000	0.001	0.000
SM_MEAN	R-squared	0.010	0.017	0.011	0.001	0.043	0.005
	Slope	0.131	-0.229	-0.180	-0.032	-0.362	-0.097
	t-value	9.498	-16.539	-13.080	-2.320	-26.767	-7.233
	p-value	0.000	0.000	0.000	0.020	0.000	0.000
SM_STD	R-squared	0.001	0.000	0.000	0.000	0.000	0.006
	Slope	-0.058	0.015	0.015	0.008	0.041	0.093
	t-value	-4.240	1.113	1.077	0.581	2.998	6.978
	p-value	0.000	0.266	0.282	0.561	0.003	0.000
VPD_MEAN	R-squared	0.005	0.001	0.001	0.003	0.005	0.155
	Slope	-0.105	0.062	-0.037	0.095	-0.129	-0.485
	t-value	-7.013	4.058	-2.412	6.238	-8.198	-43.002
	p-value	0.000	0.000	0.016	0.000	0.000	0.000
VPD_STD	R-squared	0.019	0.003	0.013	0.071	0.019	0.144
	Slope	0.191	-0.071	0.301	0.419	-0.212	-0.549
	t-value	13.383	-5.093	23.107	30.776	-16.152	-41.916
	p-value	0.000	0.000	0.000	0.000	0.000	0.000
LSTDAY_MEAN	R-squared	0.243	0.078	0.000	0.102	0.069	0.126
	Slope	0.690	-0.650	-0.008	0.515	-0.431	-0.574
	t-value	71.863	-43.725	-0.469	44.435	-25.650	-45.505
	p-value	0.000	0.000	0.639	0.000	0.000	0.000
LSTDAY_STD	R-squared	0.127	0.035	0.001	0.039	0.086	0.073
	Slope	0.463	-0.373	0.058	0.206	-0.451	-0.298
	t-value	58.140	-41.975	6.674	26.073	-54.044	-38.277
	p-value	0.000	0.000	0.000	0.000	0.000	0.000
LSTNIGHT_MEAN	R-squared	0.187	0.151	0.005	0.063	0.253	0.046
	Slope	0.533	-0.745	-0.160	0.397	-0.800	-0.349
	t-value	51.792	-58.603	-8.275	27.240	-52.400	-15.401
	p-value	0.000	0.000	0.000	0.000	0.000	0.000
LSTNIGHT_STD	R-squared	0.008	0.000	0.016	0.009	0.023	0.000
	Slope	-0.112	0.022	-0.279	-0.133	-0.279	0.002
	t-value	-8.062	1.539	-20.458	-9.723	-19.586	0.163
	p-value	0.000	0.124	0.000	0.000	0.000	0.870

https://doi.org/10.5194/egusphere-2023-3069
Preprint. Discussion started: 29 January 2024

Table B18. Quantile regression results (Q50) for the Madeira Sub-basin

ENV_PARAM	STAT	SLA	LDMC	LNC	LPC	NDVI	LAI
ET_MEAN	R-squared	0.141	0.062	0.001	0.023	0.298	0.168
	Slope	-0.562	0.406	0.034	-0.224	0.766	0.589
	t-value	-201.277	131.827	9.595	-57.495	220.769	143.723
	p-value	0.000	0.000	0.000	0.000	0.000	0.000
ET_STD	R-squared	0.064	0.019	0.009	0.001	0.029	0.086
	Slope	0.343	-0.237	0.170	-0.046	-0.317	-0.387
	t-value	70.010	-41.535	28.216	-7.320	-56.996	-75.792
	p-value	0.000	0.000	0.000	0.000	0.000	0.000
PET_MEAN	R-squared	0.084	0.014	0.015	0.000	0.042	0.178
	Slope	0.452	-0.219	0.228	-0.033	-0.460	-0.584
	t-value	81.643	-38.639	43.598	-6.404	-89.228	-127.367
	p-value	0.000	0.000	0.000	0.000	0.000	0.000
PET_STD	R-squared	0.006	0.000	0.000	0.002	0.017	0.020
	Slope	-0.095	0.028	-0.031	-0.058	0.168	0.162
	t-value	-21.726	6.495	-7.313	-13.370	39.208	38.726
	p-value	0.000	0.000	0.000	0.000	0.000	0.000
SM_MEAN	R-squared	0.008	0.008	0.001	0.022	0.019	0.000
	Slope	-0.118	0.148	0.032	-0.223	0.221	0.005
	t-value	-20.405	25.576	5.489	-39.189	37.232	0.853
	p-value	0.000	0.000	0.000	0.000	0.000	0.393
SM_STD	R-squared	0.006	0.002	0.005	0.003	0.011	0.000
	Slope	0.098	-0.070	0.114	-0.071	0.138	0.030
	t-value	19.655	-13.726	22.128	-14.044	26.116	5.675
	p-value	0.000	0.000	0.000	0.000	0.000	0.000
VPD_MEAN	R-squared	0.076	0.008	0.003	0.002	0.060	0.205
	Slope	0.415	-0.149	0.087	-0.065	-0.324	-0.578
	t-value	97.010	-28.240	15.110	-11.813	-68.011	-133.672
	p-value	0.000	0.000	0.000	0.000	0.000	0.000
VPD_STD	R-squared	0.093	0.025	0.036	0.000	0.012	0.075
	Slope	0.444	-0.371	0.447	-0.024	-0.250	-0.462
	t-value	62.829	-44.003	62.848	-2.724	-28.232	-62.515
	p-value	0.000	0.000	0.000	0.006	0.000	0.000
LSTDAY_MEAN	R-squared	0.104	0.074	0.009	0.000	0.098	0.049
	Slope	0.305	-0.368	0.126	0.008	-0.392	-0.213
	t-value	129.214	-153.791	58.974	4.184	-233.125	-90.604
	p-value	0.000	0.000	0.000	0.000	0.000	0.000
LSTDAY_STD	R-squared	0.235	0.138	0.000	0.072	0.419	0.269
	Slope	0.652	-0.645	0.015	0.374	-0.829	-0.672
	t-value	187.101	-148.365	2.345	86.887	-299.236	-176.028
	p-value	0.000	0.000	0.019	0.000	0.000	0.000
LSTNIGHT_MEAN	R-squared	0.016	0.008	0.000	0.043	0.021	0.019
	Slope	-0.074	0.083	-0.005	-0.162	0.123	0.091
	t-value	-42.842	45.490	-2.753	-97.785	73.975	59.848
	p-value	0.000	0.000	0.006	0.000	0.000	0.000
LSTNIGHT_STD	R-squared	0.069	0.012	0.001	0.009	0.112	0.232
	Slope	0.383	-0.191	-0.038	0.129	-0.531	-0.627
	t-value	84.109	-35.139	-6.372	22.657	-130.894	-160.701
	p-value	0.000	0.000	0.000	0.000	0.000	0.000

https://doi.org/10.5194/egusphere-2023-3069
Preprint. Discussion started: 29 January 2024

Table B19. Quantile regression results (Q50) for the Negro Sub-basin

ENV_PARAM	STAT	SLA	LDMC	LNC	LPC	NDVI	LAI
ET_MEAN	R-squared	0.010	0.023	0.008	0.000	0.291	0.016
	Slope	-0.132	0.237	0.081	0.002	0.782	0.104
	t-value	-34.745	63.096	23.623	0.607	258.540	30.937
	p-value	0.000	0.000	0.000	0.544	0.000	0.000
ET_STD	R-squared	0.027	0.048	0.001	0.000	0.041	0.003
	Slope	0.138	-0.205	0.025	-0.007	-0.190	0.039
	t-value	44.802	-67.761	8.182	-2.158	-62.084	13.079
	p-value	0.000	0.000	0.000	0.031	0.000	0.000
PET_MEAN	R-squared	0.040	0.066	0.012	0.001	0.020	0.017
	Slope	0.280	-0.450	0.130	0.035	-0.273	0.148
	t-value	47.363	-73.856	23.794	5.477	-40.889	25.527
	p-value	0.000	0.000	0.000	0.000	0.000	0.000
PET_STD	R-squared	0.004	0.006	-0.000	0.000	0.005	0.004
	Slope	0.036	-0.054	-0.000	-0.005	-0.049	0.034
	t-value	13.124	-20.012	-0.010	-1.901	-18.496	12.569
	p-value	0.000	0.000	0.992	0.057	0.000	0.000
SM_MEAN	R-squared	0.032	0.014	0.010	0.001	0.003	0.039
	Slope	-0.249	0.185	-0.159	0.038	0.069	-0.291
	t-value	-29.224	20.918	-18.552	4.174	7.782	-33.633
	p-value	0.000	0.000	0.000	0.000	0.000	0.000
SM_STD	R-squared	0.002	0.000	0.000	0.000	0.000	0.004
	Slope	0.053	-0.024	-0.009	0.000	0.004	0.068
	t-value	8.204	-3.576	-1.402	0.026	0.657	10.343
	p-value	0.000	0.000	0.161	0.979	0.511	0.000
VPD_MEAN	R-squared	0.223	0.143	0.016	0.080	0.127	0.021
	Slope	0.752	-0.761	0.192	-0.446	-0.626	-0.185
	t-value	111.805	-107.803	25.697	-80.869	-98.259	-26.314
	p-value	0.000	0.000	0.000	0.000	0.000	0.000
VPD_STD	R-squared	0.229	0.190	0.030	0.045	0.138	0.002
	Slope	0.738	-0.783	0.300	-0.368	-0.597	-0.069
	t-value	100.753	-85.300	30.734	-33.522	-60.242	-6.430
	p-value	0.000	0.000	0.000	0.000	0.000	0.000
LSTDAY_MEAN	R-squared	0.013	0.064	0.003	0.000	0.341	0.160
	Slope	0.130	-0.363	-0.037	0.001	-0.823	-0.393
	t-value	57.149	-166.067	-20.451	0.356	-463.790	-171.920
	p-value	0.000	0.000	0.000	0.722	0.000	0.000
LSTDAY_STD	R-squared	0.052	0.098	0.003	0.017	0.417	0.027
	Slope	0.269	-0.532	-0.041	-0.083	-0.886	-0.109
	t-value	83.279	-161.036	-14.199	-29.066	-351.578	-36.326
	p-value	0.000	0.000	0.000	0.000	0.000	0.000
LSTNIGHT_MEAN	R-squared	0.021	0.008	0.000	0.000	0.144	0.171
	Slope	0.188	-0.131	-0.008	0.017	-0.450	-0.555
	t-value	54.450	-36.133	-2.296	4.865	-122.052	-130.499
	p-value	0.000	0.000	0.022	0.000	0.000	0.000
LSTNIGHT_STD	R-squared	0.027	0.012	0.022	0.000	0.000	0.015
	Slope	-0.209	0.166	-0.227	0.024	0.013	-0.192
	t-value	-30.274	24.131	-32.270	3.483	1.832	-26.820
	p-value	0.000	0.000	0.000	0.000	0.067	0.000

https://doi.org/10.5194/egusphere-2023-3069
Preprint. Discussion started: 29 January 2024

Table B20. Quantile regression results (Q50) for the Solimoes Sub-basin

ENV_PARAM	STAT	SLA	LDMC	LNC	LPC	NDVI	LAI
ET_MEAN	R-squared	0.017	0.092	0.011	0.005	0.265	0.014
	Slope	-0.149	0.607	0.112	-0.049	0.680	-0.138
	t-value	-103.872	400.161	74.347	-34.630	464.094	-90.500
	p-value	0.000	0.000	0.000	0.000	0.000	0.000
ET_STD	R-squared	0.004	0.008	0.001	0.014	0.037	0.046
	Slope	-0.060	0.079	-0.044	-0.102	0.139	0.241
	t-value	-25.266	32.846	-18.917	-43.213	59.939	106.057
	p-value	0.000	0.000	0.000	0.000	0.000	0.000
PET_MEAN	R-squared	0.000	0.007	0.000	0.075	0.072	0.038
	Slope	-0.030	0.116	0.012	-0.296	0.310	0.322
	t-value	-8.135	29.823	3.120	-116.914	81.299	96.757
	p-value	0.000	0.000	0.002	0.000	0.000	0.000
PET_STD	R-squared	0.021	0.036	0.002	0.064	0.091	0.026
	Slope	-0.163	0.223	-0.060	-0.235	0.233	0.233
	t-value	-44.564	64.726	-15.630	-86.667	80.756	60.090
	p-value	0.000	0.000	0.000	0.000	0.000	0.000
SM_MEAN	R-squared	0.052	0.072	0.000	0.006	0.095	0.057
	Slope	-0.414	0.509	-0.032	0.125	0.449	-0.352
	t-value	-82.584	102.238	-5.859	23.737	88.125	-76.311
	p-value	0.000	0.000	0.000	0.000	0.000	0.000
SM_STD	R-squared	0.004	0.001	0.000	0.027	0.000	0.003
	Slope	0.076	-0.040	0.011	-0.220	0.009	0.062
	t-value	16.253	-8.747	2.310	-47.373	1.985	13.912
	p-value	0.000	0.000	0.021	0.000	0.047	0.000
VPD_MEAN	R-squared	0.000	0.007	0.000	0.001	0.032	0.002
	Slope	0.010	0.119	-0.008	-0.023	0.203	-0.057
	t-value	4.624	54.056	-3.901	-10.813	90.899	-27.875
	p-value	0.000	0.000	0.000	0.000	0.000	0.000
VPD_STD	R-squared	0.000	0.001	0.000	0.153	0.015	0.000
	Slope	-0.025	0.060	-0.023	-0.524	0.165	-0.020
	t-value	-5.628	13.602	-5.014	-141.476	36.931	-4.593
	p-value	0.000	0.000	0.000	0.000	0.000	0.000
LSTDAY_MEAN	R-squared	0.011	0.050	0.003	0.000	0.132	0.047
	Slope	-0.086	0.283	0.039	-0.011	0.418	-0.228
	t-value	-129.728	455.407	50.041	-13.491	609.985	-261.083
	p-value	0.000	0.000	0.000	0.000	0.000	0.000
LSTDAY_STD	R-squared	0.075	0.151	0.000	0.000	0.365	0.008
	Slope	0.249	-0.683	-0.003	0.003	-0.843	0.071
	t-value	202.793	-533.405	-2.363	2.251	-629.096	55.718
	p-value	0.000	0.000	0.018	0.024	0.000	0.000
LSTNIGHT_MEAN	R-squared	0.016	0.076	0.000	0.004	0.290	0.038
	Slope	-0.078	0.421	0.013	0.025	0.826	-0.155
	t-value	-127.109	694.045	24.182	50.835	927.563	-236.683
	p-value	0.000	0.000	0.000	0.000	0.000	0.000
LSTNIGHT_STD	R-squared	0.001	0.000	0.002	0.012	0.000	0.009
	Slope	-0.025	0.011	-0.054	-0.123	0.009	-0.102
	t-value	-8.501	3.646	-18.553	-44.440	2.945	-34.801
	p-value	0.000	0.000	0.000	0.000	0.003	0.000

https://doi.org/10.5194/egusphere-2023-3069
Preprint. Discussion started: 29 January 2024

Table B21. Quantile regression results (Q50) for the Tapajos Sub-basin

ENV_PARAM	STAT	SLA	LDMC	LNC	LPC	NDVI	LAI
ET_MEAN	R-squared	0.146	0.122	0.001	0.115	0.427	0.148
	Slope	-0.523	0.437	-0.027	-0.295	0.882	0.304
	t-value	-126.988	101.352	-6.384	-84.081	277.263	85.114
	p-value	0.000	0.000	0.000	0.000	0.000	0.000
ET_STD	R-squared	0.078	0.069	0.002	0.055	0.110	0.093
	Slope	0.386	-0.349	0.057	0.266	-0.450	-0.328
	t-value	54.408	-48.543	8.817	39.946	-67.134	-52.437
	p-value	0.000	0.000	0.000	0.000	0.000	0.000
PET_MEAN	R-squared	0.131	0.133	0.001	0.174	0.360	0.300
	Slope	0.505	-0.529	0.040	0.530	-0.771	-0.610
	t-value	70.643	-76.558	5.245	77.279	-139.302	-107.977
	p-value	0.000	0.000	0.000	0.000	0.000	0.000
PET_STD	R-squared	0.086	0.083	0.001	0.097	0.100	0.124
	Slope	0.372	-0.371	0.034	0.355	-0.439	-0.368
	t-value	45.270	-47.553	4.189	53.285	-57.879	-64.204
	p-value	0.000	0.000	0.000	0.000	0.000	0.000
SM_MEAN	R-squared	0.028	0.024	0.000	0.031	0.093	0.074
	Slope	0.206	-0.202	0.005	0.213	-0.441	-0.351
	t-value	26.292	-26.437	0.612	26.797	-56.348	-44.267
	p-value	0.000	0.000	0.540	0.000	0.000	0.000
SM_STD	R-squared	0.001	0.001	0.000	0.000	0.001	0.005
	Slope	0.044	-0.040	0.015	0.026	-0.044	-0.089
	t-value	4.700	-4.365	1.695	2.765	-4.678	-9.291
	p-value	0.000	0.000	0.090	0.006	0.000	0.000
VPD_MEAN	R-squared	0.017	0.015	0.009	0.006	0.000	0.029
	Slope	0.127	-0.142	0.124	0.084	0.026	-0.196
	t-value	19.959	-22.931	18.547	13.616	3.613	-31.924
	p-value	0.000	0.000	0.000	0.000	0.000	0.000
VPD_STD	R-squared	0.002	0.005	0.002	0.006	0.012	0.004
	Slope	0.050	-0.088	0.057	0.083	0.102	-0.081
	t-value	8.054	-13.935	9.249	13.452	16.844	-12.116
	p-value	0.000	0.000	0.000	0.000	0.000	0.000
LSTDAY_MEAN	R-squared	0.296	0.297	0.001	0.255	0.608	0.321
	Slope	0.701	-0.715	0.070	0.595	-0.965	-0.682
	t-value	123.734	-129.944	5.952	91.282	-261.929	-109.098
	p-value	0.000	0.000	0.000	0.000	0.000	0.000
LSTDAY_STD	R-squared	0.231	0.239	0.000	0.217	0.511	0.219
	Slope	0.532	-0.556	0.025	0.479	-0.874	-0.513
	t-value	103.721	-115.513	2.767	87.242	-255.452	-77.315
	p-value	0.000	0.000	0.006	0.000	0.000	0.000
LSTNIGHT_MEAN	R-squared	0.084	0.093	0.000	0.169	0.278	0.373
	Slope	-0.331	0.392	0.001	-0.475	0.654	0.639
	t-value	-37.829	44.250	0.083	-75.356	107.150	137.137
	p-value	0.000	0.000	0.933	0.000	0.000	0.000
LSTNIGHT_STD	R-squared	0.028	0.023	0.006	0.026	0.153	0.086
	Slope	0.240	-0.229	-0.128	0.220	-0.513	-0.406
	t-value	24.797	-23.057	-12.810	22.417	-63.186	-47.058
	p-value	0.000	0.000	0.000	0.000	0.000	0.000

https://doi.org/10.5194/egusphere-2023-3069
Preprint. Discussion started: 29 January 2024

Table B22. Quantile regression results (Q50) for the Trombetas Sub-basin

ENV_PARAM	STAT	SLA	LDMC	LNC	LPC	NDVI	LAI
ET_MEAN	R-squared	0.003	0.003	0.013	0.033	0.081	0.005
	Slope	-0.066	0.088	0.160	-0.174	0.462	0.077
	t-value	-9.940	13.051	24.047	-28.013	69.398	11.652
	p-value	0.000	0.000	0.000	0.000	0.000	0.000
ET_STD	R-squared	0.006	0.004	0.004	0.002	0.019	0.000
	Slope	0.107	-0.111	-0.099	0.054	-0.221	0.021
	t-value	10.852	-11.404	-9.989	5.591	-22.775	2.118
	p-value	0.000	0.000	0.000	0.000	0.000	0.034
PET_MEAN	R-squared	0.000	0.002	0.005	0.086	0.020	0.014
	Slope	-0.022	0.066	0.095	-0.409	0.218	0.174
	t-value	-1.775	5.148	7.623	-47.289	18.801	15.284
	p-value	0.076	0.000	0.000	0.000	0.000	0.000
PET_STD	R-squared	0.005	0.001	0.010	0.007	0.039	0.000
	Slope	0.124	-0.056	-0.184	-0.114	-0.331	-0.026
	t-value	8.793	-3.805	-12.864	-7.863	-24.613	-1.810
	p-value	0.000	0.000	0.000	0.000	0.000	0.070
SM_MEAN	R-squared	0.001	0.000	0.004	0.033	0.035	0.005
	Slope	0.036	0.000	-0.096	0.285	-0.276	-0.102
	t-value	3.175	0.015	-8.554	25.608	-25.072	-8.495
	p-value	0.002	0.988	0.000	0.000	0.000	0.000
SM_STD	R-squared	0.002	0.001	0.001	0.004	0.017	0.003
	Slope	-0.057	0.044	0.046	-0.079	0.150	0.064
	t-value	-6.208	4.697	4.949	-8.340	16.574	6.920
	p-value	0.000	0.000	0.000	0.000	0.000	0.000
VPD_MEAN	R-squared	0.002	0.000	0.000	0.037	0.003	0.001
	Slope	-0.069	0.010	0.018	-0.346	-0.065	-0.046
	t-value	-5.188	0.779	1.360	-24.006	-4.771	-3.502
	p-value	0.000	0.436	0.174	0.000	0.000	0.000
VPD_STD	R-squared	0.028	0.019	0.005	0.053	0.022	0.001
	Slope	0.215	-0.289	0.143	-0.385	-0.166	0.055
	t-value	22.651	-31.526	14.442	-37.493	-16.550	5.807
	p-value	0.000	0.000	0.000	0.000	0.000	0.000
LSTDAY_MEAN	R-squared	0.014	0.001	0.000	0.012	0.011	0.060
	Slope	0.181	0.046	0.001	-0.118	-0.146	-0.319
	t-value	25.927	6.846	0.212	-18.257	-21.342	-36.505
	p-value	0.000	0.000	0.832	0.000	0.000	0.000
LSTDAY_STD	R-squared	0.043	0.022	0.006	0.008	0.142	0.000
	Slope	0.338	-0.253	-0.085	0.085	-0.527	-0.016
	t-value	52.518	-42.144	-14.106	13.589	-92.701	-2.532
	p-value	0.000	0.000	0.000	0.000	0.000	0.011
LSTNIGHT_MEAN	R-squared	0.000	0.010	0.030	0.012	0.191	0.038
	Slope	0.026	0.287	-0.276	0.084	-0.670	-0.307
	t-value	4.913	55.228	-49.716	15.921	-132.246	-47.060
	p-value	0.000	0.000	0.000	0.000	0.000	0.000
LSTNIGHT_STD	R-squared	0.004	0.007	0.012	0.004	0.024	0.017
	Slope	-0.090	0.192	-0.198	-0.081	-0.251	-0.193
	t-value	-8.654	18.605	-19.483	-8.083	-24.477	-19.137
	p-value	0.000	0.000	0.000	0.000	0.000	0.000

https://doi.org/10.5194/egusphere-2023-3069
Preprint. Discussion started: 29 January 2024

Table B23. Quantile regression results (Q50) for the Xingu Sub-basin

ENV_PARAM	STAT	SLA	LDMC	LNC	LPC	NDVI	LAI
ET_MEAN	R-squared	0.069	0.053	0.018	0.145	0.372	0.268
	Slope	-0.355	0.336	0.211	-0.411	0.868	0.482
	t-value	-49.090	48.650	32.122	-90.873	187.441	126.064
	p-value	0.000	0.000	0.000	0.000	0.000	0.000
ET_STD	R-squared	0.033	0.018	0.002	0.102	0.152	0.363
	Slope	0.262	-0.234	-0.097	0.442	-0.574	-0.655
	t-value	25.923	-23.916	-9.911	53.418	-66.572	-116.251
	p-value	0.000	0.000	0.000	0.000	0.000	0.000
PET_MEAN	R-squared	0.031	0.017	0.003	0.121	0.185	0.536
	Slope	0.202	-0.160	-0.088	0.444	-0.506	-0.787
	t-value	33.115	-30.265	-16.721	70.501	-80.791	-217.102
	p-value	0.000	0.000	0.000	0.000	0.000	0.000
PET_STD	R-squared	0.008	0.001	0.002	0.060	0.107	0.302
	Slope	0.148	-0.044	0.048	0.345	-0.493	-0.599
	t-value	13.362	-4.137	4.631	37.849	-47.732	-108.984
	p-value	0.000	0.000	0.000	0.000	0.000	0.000
SM_MEAN	R-squared	0.002	0.001	0.000	0.000	0.019	0.001
	Slope	0.059	-0.037	-0.008	0.010	-0.194	-0.053
	t-value	6.162	-3.801	-0.857	0.972	-20.721	-5.429
	p-value	0.000	0.000	0.391	0.331	0.000	0.000
SM_STD	R-squared	0.001	0.000	0.000	0.000	0.002	0.002
	Slope	0.028	-0.021	0.005	0.019	-0.043	-0.050
	t-value	3.619	-2.702	0.643	2.521	-5.608	-6.522
	p-value	0.000	0.007	0.520	0.012	0.000	0.000
VPD_MEAN	R-squared	0.014	0.001	0.003	0.055	0.071	0.430
	Slope	0.219	-0.074	0.066	0.375	-0.370	-0.765
	t-value	15.241	-4.600	3.906	29.171	-31.333	-157.603
	p-value	0.000	0.000	0.000	0.000	0.000	0.000
VPD_STD	R-squared	0.008	0.001	0.001	0.071	0.035	0.413
	Slope	0.129	-0.070	0.050	0.354	-0.218	-0.707
	t-value	11.643	-4.994	3.428	33.908	-19.905	-137.094
	p-value	0.000	0.000	0.001	0.000	0.000	0.000
LSTDAY_MEAN	R-squared	0.183	0.139	0.004	0.195	0.519	0.294
	Slope	0.622	-0.597	-0.098	0.546	-0.938	-0.494
	t-value	96.851	-102.904	-15.508	87.040	-225.331	-106.724
	p-value	0.000	0.000	0.000	0.000	0.000	0.000
LSTDAY_STD	R-squared	0.281	0.242	0.002	0.133	0.486	0.048
	Slope	0.700	-0.724	-0.055	0.508	-0.904	-0.272
	t-value	146.312	-146.758	-8.500	70.167	-258.413	-37.540
	p-value	0.000	0.000	0.000	0.000	0.000	0.000
LSTNIGHT_MEAN	R-squared	0.044	0.028	0.000	0.154	0.139	0.434
	Slope	-0.312	0.307	0.001	-0.500	0.496	0.702
	t-value	-26.804	26.006	0.087	-69.838	50.702	172.384
	p-value	0.000	0.000	0.931	0.000	0.000	0.000
LSTNIGHT_STD	R-squared	0.065	0.051	0.020	0.050	0.246	0.131
	Slope	0.390	-0.385	-0.285	0.343	-0.662	-0.528
	t-value	43.064	-41.084	-30.218	35.606	-99.816	-62.424
	p-value	0.000	0.000	0.000	0.000	0.000	0.000

https://doi.org/10.5194/egusphere-2023-3069
Preprint. Discussion started: 29 January 2024

Table B24. Quantile regression results (Q95) for the Amazon Basin

ENV_PARAM	STAT	SLA	LDMC	LNC	LPC	NDVI	LAI
ET_MEAN	R-squared	0.003	0.000	0.003	0.010	0.062	0.042
	Slope	-0.038	0.013	0.027	-0.049	0.225	0.098
	t-value	-40.949	10.585	15.438	-48.376	202.324	119.658
	p-value	0.000	0.000	0.000	0.000	0.000	0.000
ET_STD	R-squared	0.050	0.029	0.002	0.004	0.077	0.007
	Slope	0.406	-0.534	-0.146	-0.210	-0.689	-0.207
	t-value	42.654	-86.136	-17.898	-25.055	-131.843	-13.206
	p-value	0.000	0.000	0.000	0.000	0.000	0.000
PET_MEAN	R-squared	0.182	0.121	0.005	0.028	0.229	0.209
	Slope	0.492	-0.704	0.103	-0.378	-0.620	-0.538
	t-value	117.982	-261.845	8.059	-113.454	-324.129	-102.942
	p-value	0.000	0.000	0.000	0.000	0.000	0.000
PET_STD	R-squared	0.020	0.013	0.003	0.000	0.054	0.001
	Slope	0.193	-0.225	-0.144	0.033	-0.482	-0.082
	t-value	41.410	-64.183	-35.195	7.514	-161.481	-12.045
	p-value	0.000	0.000	0.000	0.000	0.000	0.000
SM_MEAN	R-squared	0.042	0.012	0.013	0.062	0.012	0.030
	Slope	-0.277	0.129	-0.174	0.293	0.166	-0.331
	t-value	-70.070	19.004	-74.903	69.865	52.243	-128.684
	p-value	0.000	0.000	0.000	0.000	0.000	0.000
SM_STD	R-squared	0.000	0.000	0.005	0.000	0.000	0.000
	Slope	-0.010	0.001	-0.173	-0.004	0.014	0.020
	t-value	-1.285	0.071	-26.915	-0.600	2.151	2.440
	p-value	0.199	0.943	0.000	0.549	0.031	0.015
VPD_MEAN	R-squared	0.133	0.076	0.006	0.011	0.103	0.114
	Slope	0.467	-0.474	0.094	-0.276	-0.612	-0.465
	t-value	86.256	-118.690	6.566	-44.230	-217.457	-57.882
	p-value	0.000	0.000	0.000	0.000	0.000	0.000
VPD_STD	R-squared	0.027	0.017	0.007	0.034	0.000	0.048
	Slope	0.317	-0.367	0.109	-0.555	0.011	-0.430
	t-value	30.121	-90.892	11.066	-144.323	3.279	-78.303
	p-value	0.000	0.000	0.000	0.000	0.001	0.000
LSTDAY_MEAN	R-squared	0.264	0.279	0.004	0.017	0.509	0.228
	Slope	0.533	-0.706	0.067	0.228	-0.860	-0.497
	t-value	112.075	-171.753	5.638	34.107	-946.873	-77.788
	p-value	0.000	0.000	0.000	0.000	0.000	0.000
LSTDAY_STD	R-squared	0.179	0.263	0.002	0.121	0.603	0.088
	Slope	1.002	-0.969	0.068	0.749	-1.189	-0.492
	t-value	67.346	-83.839	2.395	56.191	-319.170	-21.599
	p-value	0.000	0.000	0.017	0.000	0.000	0.000
LSTNIGHT_MEAN	R-squared	0.006	0.003	0.041	0.008	0.116	0.030
	Slope	-0.051	-0.033	-0.120	0.052	-0.179	-0.080
	t-value	-28.519	-14.237	-95.261	31.135	-337.535	-52.565
	p-value	0.000	0.000	0.000	0.000	0.000	0.000
LSTNIGHT_STD	R-squared	0.044	0.048	0.000	0.001	0.030	0.009
	Slope	0.390	-0.580	0.014	0.074	-0.446	0.150
	t-value	31.228	-74.178	1.285	9.178	-53.747	10.964
	p-value	0.000	0.000	0.199	0.000	0.000	0.000

https://doi.org/10.5194/egusphere-2023-3069
Preprint. Discussion started: 29 January 2024

Table B25. Quantile regression results (Q95) for the Amazonas Sub-basin

ENV_PARAM	STAT	SLA	LDMC	LNC	LPC	NDVI	LAI
ET_MEAN	R-squared	0.007	0.010	0.002	0.000	0.046	0.009
	Slope	-0.066	0.050	0.045	0.002	0.255	-0.060
	t-value	-10.071	3.379	4.911	0.294	30.858	-10.012
	p-value	0.000	0.001	0.000	0.769	0.000	0.000
ET_STD	R-squared	0.059	0.031	0.001	0.007	0.041	0.000
	Slope	0.407	-0.544	0.031	0.122	-0.563	0.004
	t-value	6.675	-15.592	0.502	1.741	-18.317	0.078
	p-value	0.000	0.000	0.615	0.082	0.000	0.938
PET_MEAN	R-squared	0.000	0.009	0.006	0.000	0.042	0.014
	Slope	-0.007	0.087	0.085	0.012	0.334	-0.075
	t-value	-0.907	5.810	6.030	1.281	34.872	-10.489
	p-value	0.364	0.000	0.000	0.200	0.000	0.000
PET_STD	R-squared	0.014	0.000	0.002	0.000	0.000	0.015
	Slope	0.206	-0.013	0.030	-0.016	0.031	0.173
	t-value	3.414	-0.415	0.330	-0.454	0.885	3.847
	p-value	0.001	0.678	0.741	0.650	0.376	0.000
SM_MEAN	R-squared	0.001	0.020	0.031	0.001	0.077	0.036
	Slope	0.031	-0.298	-0.366	-0.033	-0.380	-0.238
	t-value	0.604	-9.878	-14.440	-0.580	-17.258	-7.873
	p-value	0.546	0.000	0.000	0.562	0.000	0.000
SM_STD	R-squared	0.004	0.019	0.019	0.002	0.061	0.017
	Slope	0.152	-0.409	-0.359	0.103	-0.493	-0.346
	t-value	3.119	-16.210	-10.385	1.350	-12.644	-9.326
	p-value	0.002	0.000	0.000	0.177	0.000	0.000
VPD_MEAN	R-squared	0.008	0.003	0.000	0.008	0.001	0.018
	Slope	-0.088	0.037	0.014	-0.088	0.026	-0.164
	t-value	-4.391	0.809	0.521	-4.285	1.124	-9.899
	p-value	0.000	0.418	0.602	0.000	0.261	0.000
VPD_STD	R-squared	0.081	0.051	0.003	0.028	0.072	0.295
	Slope	0.255	-0.345	0.026	0.253	-0.508	-0.514
	t-value	10.832	-24.352	0.400	3.278	-71.745	-27.910
	p-value	0.000	0.000	0.689	0.001	0.000	0.000
LSTDAY_MEAN	R-squared	0.235	0.175	0.006	0.082	0.321	0.267
	Slope	0.674	-1.033	0.069	0.564	-2.227	-0.656
	t-value	12.110	-32.373	0.566	5.975	-299.151	-22.476
	p-value	0.000	0.000	0.571	0.000	0.000	0.000
LSTDAY_STD	R-squared	0.281	0.261	0.000	0.065	0.445	0.228
	Slope	1.057	-1.580	-0.004	0.742	-2.869	-0.895
	t-value	15.472	-40.205	-0.030	4.238	-336.538	-16.467
	p-value	0.000	0.000	0.976	0.000	0.000	0.000
LSTNIGHT_MEAN	R-squared	0.006	0.137	0.183	0.000	0.497	0.218
	Slope	0.221	-1.135	-0.844	-0.040	-0.999	-0.674
	t-value	1.994	-30.365	-28.776	-0.275	-132.049	-10.878
	p-value	0.046	0.000	0.000	0.783	0.000	0.000
LSTNIGHT_STD	R-squared	0.000	0.004	0.022	0.002	0.063	0.018
	Slope	0.005	-0.146	-0.368	0.050	-0.409	-0.262
	t-value	0.119	-4.876	-13.507	0.742	-15.112	-9.378
	p-value	0.905	0.000	0.000	0.458	0.000	0.000

https://doi.org/10.5194/egusphere-2023-3069
Preprint. Discussion started: 29 January 2024

Table B26. Quantile regression results (Q95) for the Madeira Sub-basin

ENV_PARAM	STAT	SLA	LDMC	LNC	LPC	NDVI	LAI
ET_MEAN	R-squared	0.011	0.004	0.000	0.010	0.069	0.020
	Slope	-0.040	0.024	0.010	-0.033	0.223	0.084
	t-value	-28.803	13.526	8.097	-23.984	195.333	83.108
	p-value	0.000	0.000	0.000	0.000	0.000	0.000
ET_STD	R-squared	0.029	0.012	0.000	0.001	0.067	0.094
	Slope	0.339	-0.390	-0.004	-0.059	-0.563	-0.552
	t-value	25.916	-53.200	-0.409	-6.591	-66.036	-37.339
	p-value	0.000	0.000	0.682	0.000	0.000	0.000
PET_MEAN	R-squared	0.070	0.040	0.002	0.003	0.208	0.271
	Slope	0.389	-0.447	0.033	-0.102	-0.786	-0.567
	t-value	48.819	-137.236	3.528	-29.001	-283.131	-87.414
	p-value	0.000	0.000	0.000	0.000	0.000	0.000
PET_STD	R-squared	0.000	0.002	0.004	0.004	0.085	0.038
	Slope	0.043	-0.121	-0.176	0.146	-0.544	-0.346
	t-value	3.136	-9.620	-13.138	8.852	-72.799	-23.762
	p-value	0.002	0.000	0.000	0.000	0.000	0.000
SM_MEAN	R-squared	0.039	0.013	0.000	0.003	0.024	0.014
	Slope	-0.238	0.114	0.014	-0.070	0.211	0.153
	t-value	-38.421	8.481	3.110	-11.490	36.935	31.109
	p-value	0.000	0.000	0.002	0.000	0.000	0.000
SM_STD	R-squared	0.000	0.001	0.000	0.001	0.000	0.006
	Slope	0.005	-0.075	-0.053	-0.064	-0.032	-0.155
	t-value	0.378	-5.136	-3.444	-5.131	-2.992	-10.987
	p-value	0.705	0.000	0.001	0.000	0.003	0.000
VPD_MEAN	R-squared	0.124	0.053	0.004	0.027	0.197	0.257
	Slope	0.667	-0.787	0.075	-0.352	-0.918	-0.721
	t-value	42.056	-76.507	2.359	-24.305	-171.589	-46.255
	p-value	0.000	0.000	0.018	0.000	0.000	0.000
VPD_STD	R-squared	0.080	0.016	0.012	0.032	0.050	0.087
	Slope	0.267	-0.225	0.083	-0.199	-0.218	-0.224
	t-value	79.607	-95.770	6.135	-62.423	-88.632	-51.769
	p-value	0.000	0.000	0.000	0.000	0.000	0.000
LSTDAY_MEAN	R-squared	0.118	0.141	0.002	0.045	0.351	0.068
	Slope	0.321	-0.513	0.029	0.218	-0.853	-0.301
	t-value	36.860	-94.583	2.333	24.157	-682.082	-56.152
	p-value	0.000	0.000	0.020	0.000	0.000	0.000
LSTDAY_STD	R-squared	0.168	0.161	0.000	0.144	0.488	0.206
	Slope	0.817	-0.824	-0.006	0.581	-1.019	-0.656
	t-value	51.850	-77.167	-0.249	31.274	-202.864	-27.271
	p-value	0.000	0.000	0.804	0.000	0.000	0.000
LSTNIGHT_MEAN	R-squared	0.032	0.004	0.011	0.003	0.005	0.000
	Slope	-0.079	0.023	-0.058	0.023	-0.039	0.003
	t-value	-40.146	5.112	-32.311	10.558	-22.449	1.467
	p-value	0.000	0.000	0.000	0.000	0.000	0.142
LSTNIGHT_STD	R-squared	0.035	0.016	0.000	0.023	0.060	0.091
	Slope	0.319	-0.310	-0.025	0.251	-0.531	-0.451
	t-value	22.585	-29.629	-1.991	14.667	-49.935	-20.501
	p-value	0.000	0.000	0.047	0.000	0.000	0.000

https://doi.org/10.5194/egusphere-2023-3069
Preprint. Discussion started: 29 January 2024

Table B27. Quantile regression results (Q95) for the Negro Sub-basin

ENV_PARAM	STAT	SLA	LDMC	LNC	LPC	NDVI	LAI
ET_MEAN	R-squared	0.041	0.015	0.021	0.002	0.019	0.007
	Slope	0.175	-0.170	0.107	-0.037	0.216	-0.055
	t-value	23.277	-34.701	8.355	-5.241	32.595	-7.079
	p-value	0.000	0.000	0.000	0.000	0.000	0.000
ET_STD	R-squared	0.168	0.214	0.000	0.000	0.237	0.018
	Slope	0.498	-0.595	0.001	-0.023	-0.611	-0.143
	t-value	27.266	-34.023	0.033	-1.042	-68.878	-3.652
	p-value	0.000	0.000	0.974	0.297	0.000	0.000
PET_MEAN	R-squared	0.300	0.339	0.006	0.007	0.305	0.087
	Slope	0.878	-1.039	0.153	-0.390	-0.754	-0.350
	t-value	31.068	-55.476	1.448	-9.444	-50.557	-4.381
	p-value	0.000	0.000	0.148	0.000	0.000	0.000
PET_STD	R-squared	0.022	0.030	0.002	0.000	0.042	0.001
	Slope	0.144	-0.210	-0.044	0.031	-0.238	0.021
	t-value	11.364	-18.434	-4.394	3.554	-31.838	1.737
	p-value	0.000	0.000	0.000	0.000	0.000	0.082
SM_MEAN	R-squared	0.032	0.009	0.008	0.005	0.010	0.008
	Slope	-0.161	0.071	-0.075	0.055	0.107	-0.128
	t-value	-27.560	7.326	-18.744	8.138	22.166	-44.120
	p-value	0.000	0.000	0.000	0.000	0.000	0.000
SM_STD	R-squared	0.025	0.011	0.025	0.010	0.010	0.013
	Slope	-0.332	0.168	-0.419	0.182	0.258	-0.175
	t-value	-10.757	3.032	-17.740	4.931	10.080	-4.752
	p-value	0.000	0.002	0.000	0.000	0.000	0.000
VPD_MEAN	R-squared	0.328	0.370	0.018	0.002	0.276	0.102
	Slope	0.690	-0.667	0.181	-0.121	-0.506	-0.436
	t-value	38.374	-68.398	3.570	-5.592	-83.551	-23.944
	p-value	0.000	0.000	0.000	0.000	0.000	0.000
VPD_STD	R-squared	0.244	0.293	0.018	0.004	0.217	0.064
	Slope	0.458	-0.522	0.166	-0.221	-0.361	-0.356
	t-value	28.645	-66.247	4.350	-16.500	-47.899	-20.921
	p-value	0.000	0.000	0.000	0.000	0.000	0.000
LSTDAY_MEAN	R-squared	0.460	0.492	0.010	0.005	0.776	0.252
	Slope	0.986	-0.967	0.203	0.224	-1.016	-0.875
	t-value	49.369	-30.535	0.941	2.841	-207.821	-10.239
	p-value	0.000	0.000	0.347	0.005	0.000	0.000
LSTDAY_STD	R-squared	0.433	0.413	0.005	0.001	0.747	0.148
	Slope	1.075	-1.018	0.135	0.128	-1.305	-0.617
	t-value	33.656	-20.660	0.666	1.695	-235.346	-6.736
	p-value	0.000	0.000	0.505	0.090	0.000	0.000
LSTNIGHT_MEAN	R-squared	0.093	0.091	0.012	0.003	0.396	0.272
	Slope	0.296	-0.261	-0.147	0.092	-0.906	-0.687
	t-value	9.521	-9.518	-4.145	3.822	-235.693	-41.660
	p-value	0.000	0.000	0.000	0.000	0.000	0.000
LSTNIGHT_STD	R-squared	0.026	0.004	0.020	0.007	0.000	0.012
	Slope	-0.290	0.080	-0.253	-0.151	-0.034	-0.244
	t-value	-14.903	2.539	-15.423	-8.649	-2.174	-12.716
	p-value	0.000	0.011	0.000	0.000	0.030	0.000

https://doi.org/10.5194/egusphere-2023-3069
Preprint. Discussion started: 29 January 2024

Table B28. Quantile regression results (Q95) for the Solimoes Sub-basin

ENV_PARAM	STAT	SLA	LDMC	LNC	LPC	NDVI	LAI
ET_MEAN	R-squared	0.003	0.001	0.005	0.003	0.085	0.000
	Slope	0.034	0.017	0.035	0.022	0.332	0.007
	t-value	17.639	7.642	10.724	10.958	216.546	4.734
	p-value	0.000	0.000	0.000	0.000	0.000	0.000
ET_STD	R-squared	0.000	0.000	0.065	0.005	0.001	0.310
	Slope	-0.055	0.022	-0.913	-0.229	0.243	1.016
	t-value	-2.501	0.969	-56.346	-14.935	19.774	66.712
	p-value	0.012	0.333	0.000	0.000	0.000	0.000
PET_MEAN	R-squared	0.000	0.000	0.007	0.002	0.045	0.017
	Slope	-0.023	0.011	-0.115	-0.053	0.382	0.145
	t-value	-5.265	2.258	-36.687	-14.496	82.293	29.958
	p-value	0.000	0.024	0.000	0.000	0.000	0.000
PET_STD	R-squared	0.000	0.001	0.029	0.006	0.000	0.305
	Slope	-0.030	0.070	-0.653	0.127	-0.125	1.082
	t-value	-5.939	11.040	-98.066	34.197	-51.314	102.556
	p-value	0.000	0.000	0.000	0.000	0.000	0.000
SM_MEAN	R-squared	0.008	0.004	0.005	0.020	0.009	0.051
	Slope	-0.115	0.076	-0.095	0.163	0.215	-0.339
	t-value	-33.717	14.217	-41.750	43.778	88.373	-115.473
	p-value	0.000	0.000	0.000	0.000	0.000	0.000
SM_STD	R-squared	0.001	0.000	0.004	0.003	0.001	0.001
	Slope	-0.040	0.029	-0.159	-0.109	0.070	0.045
	t-value	-3.386	2.273	-17.091	-8.566	6.213	3.269
	p-value	0.001	0.023	0.000	0.000	0.000	0.001
VPD_MEAN	R-squared	0.012	0.002	0.000	0.006	0.016	0.009
	Slope	0.178	-0.119	-0.004	-0.145	0.290	0.150
	t-value	14.815	-21.658	-0.373	-18.165	26.796	13.891
	p-value	0.000	0.000	0.709	0.000	0.000	0.000
VPD_STD	R-squared	0.012	0.002	0.000	0.101	0.000	0.008
	Slope	0.130	-0.114	0.026	-0.498	0.005	-0.119
	t-value	12.740	-22.199	2.645	-50.704	0.598	-16.718
	p-value	0.000	0.000	0.008	0.000	0.550	0.000
LSTDAY_MEAN	R-squared	0.105	0.099	0.000	0.001	0.049	0.094
	Slope	0.150	-0.318	0.010	-0.015	-0.378	-0.279
	t-value	38.661	-267.302	1.782	-4.574	-366.731	-166.066
	p-value	0.000	0.000	0.075	0.000	0.000	0.000
LSTDAY_STD	R-squared	0.215	0.374	0.004	0.255	0.713	0.061
	Slope	0.923	-1.073	0.116	1.099	-1.224	-0.376
	t-value	19.987	-34.480	1.804	62.727	-276.380	-7.856
	p-value	0.000	0.000	0.071	0.000	0.000	0.000
LSTNIGHT_MEAN	R-squared	0.008	0.000	0.016	0.016	0.026	0.095
	Slope	-0.040	0.002	-0.047	0.050	-0.094	-0.126
	t-value	-36.764	1.471	-56.421	41.327	-219.291	-225.393
	p-value	0.000	0.141	0.000	0.000	0.000	0.000
LSTNIGHT_STD	R-squared	0.007	0.004	0.022	0.091	0.006	0.032
	Slope	-0.207	0.128	-0.549	-0.710	0.259	-0.359
	t-value	-10.007	4.174	-46.675	-36.289	17.223	-16.740
	p-value	0.000	0.000	0.000	0.000	0.000	0.000

https://doi.org/10.5194/egusphere-2023-3069
Preprint. Discussion started: 29 January 2024

Table B29. Quantile regression results (Q95) for the Tapajos Sub-basin

ENV_PARAM	STAT	SLA	LDMC	LNC	LPC	NDVI	LAI
ET_MEAN	R-squared	0.036	0.029	0.001	0.015	0.055	0.070
	Slope	-0.114	0.101	0.008	-0.055	0.176	0.129
	t-value	-53.091	23.332	1.826	-28.947	62.181	80.340
	p-value	0.000	0.000	0.068	0.000	0.000	0.000
ET_STD	R-squared	0.138	0.132	0.006	0.078	0.285	0.219
	Slope	0.812	-0.921	0.108	0.709	-1.178	-0.843
	t-value	28.741	-36.224	1.925	18.923	-87.853	-30.218
	p-value	0.000	0.000	0.054	0.000	0.000	0.000
PET_MEAN	R-squared	0.125	0.183	0.002	0.149	0.471	0.402
	Slope	0.664	-0.831	0.080	0.702	-0.925	-0.823
	t-value	49.660	-72.198	4.069	32.419	-134.510	-56.897
	p-value	0.000	0.000	0.000	0.000	0.000	0.000
PET_STD	R-squared	0.166	0.155	0.003	0.111	0.318	0.233
	Slope	0.855	-0.899	0.081	0.874	-1.168	-0.862
	t-value	31.169	-33.279	1.481	25.944	-93.479	-36.869
	p-value	0.000	0.000	0.139	0.000	0.000	0.000
SM_MEAN	R-squared	0.082	0.066	0.005	0.051	0.221	0.150
	Slope	0.487	-0.502	0.084	0.416	-0.691	-0.584
	t-value	27.042	-26.851	2.198	14.884	-52.154	-21.924
	p-value	0.000	0.000	0.028	0.000	0.000	0.000
SM_STD	R-squared	0.003	0.002	0.007	0.001	0.004	0.000
	Slope	-0.094	0.085	-0.160	-0.060	-0.117	-0.003
	t-value	-4.033	3.380	-8.094	-2.711	-4.644	-0.111
	p-value	0.000	0.001	0.000	0.007	0.000	0.912
VPD_MEAN	R-squared	0.081	0.087	0.014	0.080	0.024	0.103
	Slope	0.374	-0.418	0.148	0.448	-0.323	-0.838
	t-value	21.987	-27.227	2.688	18.160	-24.690	-95.759
	p-value	0.000	0.000	0.007	0.000	0.000	0.000
VPD_STD	R-squared	0.046	0.046	0.015	0.052	0.008	0.074
	Slope	0.285	-0.296	0.134	0.336	-0.183	-0.709
	t-value	18.871	-19.890	2.868	17.874	-14.799	-81.455
	p-value	0.000	0.000	0.004	0.000	0.000	0.000
LSTDAY_MEAN	R-squared	0.132	0.162	0.003	0.111	0.655	0.374
	Slope	0.640	-0.796	0.065	0.656	-1.168	-0.841
	t-value	48.208	-63.994	3.512	29.639	-295.003	-59.543
	p-value	0.000	0.000	0.000	0.000	0.000	0.000
LSTDAY_STD	R-squared	0.176	0.166	0.005	0.114	0.634	0.303
	Slope	1.029	-1.083	0.101	1.031	-1.280	-0.905
	t-value	42.143	-44.327	1.175	29.273	-161.923	-31.202
	p-value	0.000	0.000	0.240	0.000	0.000	0.000
LSTNIGHT_MEAN	R-squared	0.071	0.039	0.006	0.026	0.024	0.160
	Slope	-0.408	0.369	-0.089	-0.296	0.450	0.735
	t-value	-44.703	17.110	-6.546	-30.582	47.657	91.246
	p-value	0.000	0.000	0.000	0.000	0.000	0.000
LSTNIGHT_STD	R-squared	0.009	0.012	0.006	0.003	0.085	0.038
	Slope	0.150	-0.184	-0.121	0.095	-0.469	-0.321
	t-value	6.542	-9.159	-5.622	3.405	-19.916	-12.329
	p-value	0.000	0.000	0.000	0.001	0.000	0.000

https://doi.org/10.5194/egusphere-2023-3069
Preprint. Discussion started: 29 January 2024

Table B30. Quantile regression results (Q95) for the Trombetas Sub-basin

ENV_PARAM	STAT	SLA	LDMC	LNC	LPC	NDVI	LAI
ET_MEAN	R-squared	0.000	0.002	0.006	0.000	0.014	0.004
	Slope	-0.002	0.034	0.045	-0.011	0.137	-0.036
	t-value	-0.500	3.601	4.279	-1.478	23.481	-5.481
	p-value	0.617	0.000	0.000	0.139	0.000	0.000
ET_STD	R-squared	0.008	0.021	0.019	0.004	0.113	0.000
	Slope	0.117	-0.272	-0.325	-0.144	-0.706	-0.039
	t-value	2.394	-8.910	-13.498	-4.901	-36.451	-1.259
	p-value	0.017	0.000	0.000	0.000	0.000	0.208
PET_MEAN	R-squared	0.000	0.004	0.010	0.023	0.027	0.044
	Slope	-0.002	0.080	-0.278	-0.250	0.299	0.296
	t-value	-0.250	4.118	-54.319	-30.003	22.889	38.241
	p-value	0.803	0.000	0.000	0.000	0.000	0.000
PET_STD	R-squared	0.002	0.010	0.032	0.013	0.112	0.001
	Slope	0.054	-0.113	-0.312	-0.183	-0.506	-0.037
	t-value	2.196	-6.079	-25.052	-14.146	-51.235	-2.315
	p-value	0.028	0.000	0.000	0.000	0.000	0.021
SM_MEAN	R-squared	0.000	0.000	0.013	0.013	0.048	0.021
	Slope	-0.008	0.016	-0.134	0.149	-0.265	-0.159
	t-value	-0.404	0.514	-9.794	8.004	-32.027	-12.052
	p-value	0.686	0.607	0.000	0.000	0.000	0.000
SM_STD	R-squared	0.003	0.005	0.005	0.054	0.009	0.007
	Slope	-0.186	0.103	-0.233	0.394	0.249	-0.178
	t-value	-4.221	0.998	-6.019	9.593	4.268	-4.290
	p-value	0.000	0.318	0.000	0.000	0.000	0.000
VPD_MEAN	R-squared	0.044	0.024	0.005	0.100	0.043	0.000
	Slope	0.197	-0.313	0.082	-0.428	-0.319	0.023
	t-value	6.813	-22.412	3.041	-38.699	-24.898	1.790
	p-value	0.000	0.000	0.002	0.000	0.000	0.073
VPD_STD	R-squared	0.000	0.001	0.001	0.135	0.001	0.006
	Slope	0.012	-0.043	-0.047	-0.399	-0.021	-0.124
	t-value	0.662	-4.423	-4.491	-19.921	-1.045	-9.977
	p-value	0.508	0.000	0.000	0.000	0.296	0.000
LSTDAY_MEAN	R-squared	0.187	0.060	0.000	0.003	0.335	0.074
	Slope	0.508	-0.345	0.017	0.071	-1.141	-0.363
	t-value	14.012	-9.902	0.275	2.423	-168.569	-12.883
	p-value	0.000	0.000	0.783	0.015	0.000	0.000
LSTDAY_STD	R-squared	0.145	0.061	0.004	0.000	0.436	0.017
	Slope	0.705	-0.463	-0.088	0.037	-1.689	-0.259
	t-value	6.987	-8.571	-1.656	0.853	-132.031	-6.274
	p-value	0.000	0.000	0.098	0.394	0.000	0.000
LSTNIGHT_MEAN	R-squared	0.003	0.003	0.194	0.006	0.563	0.186
	Slope	-0.094	-0.061	-0.792	0.228	-1.560	-0.742
	t-value	-0.938	-0.426	-22.410	2.020	-376.758	-26.188
	p-value	0.348	0.670	0.000	0.043	0.000	0.000
LSTNIGHT_STD	R-squared	0.000	0.004	0.020	0.022	0.040	0.039
	Slope	-0.005	0.067	-0.270	0.204	-0.332	-0.351
	t-value	-0.137	1.135	-11.428	6.116	-17.199	-15.277
	p-value	0.891	0.256	0.000	0.000	0.000	0.000

https://doi.org/10.5194/egusphere-2023-3069
Preprint. Discussion started: 29 January 2024

Table B31. Quantile regression results (Q95) for the Xingu Sub-basin

ENV_PARAM	STAT	SLA	LDMC	LNC	LPC	NDVI	LAI
ET_MEAN	R-squared	0.004	0.001	0.000	0.025	0.070	0.129
	Slope	-0.042	0.013	0.005	-0.087	0.251	0.272
	t-value	-16.540	2.895	1.209	-28.550	68.071	135.713
	p-value	0.000	0.004	0.227	0.000	0.000	0.000
ET_STD	R-squared	0.088	0.077	0.001	0.066	0.198	0.333
	Slope	0.438	-0.466	-0.058	0.432	-0.708	-0.982
	t-value	26.295	-25.713	-3.112	11.499	-59.132	-54.463
	p-value	0.000	0.000	0.002	0.000	0.000	0.000
PET_MEAN	R-squared	0.153	0.149	0.001	0.113	0.408	0.584
	Slope	0.483	-0.557	0.032	0.391	-0.608	-0.995
	t-value	33.312	-52.221	4.051	13.514	-137.695	-178.739
	p-value	0.000	0.000	0.000	0.000	0.000	0.000
PET_STD	R-squared	0.121	0.111	0.001	0.103	0.305	0.336
	Slope	0.566	-0.614	0.084	0.595	-0.943	-0.984
	t-value	22.918	-33.159	3.285	13.011	-94.328	-51.497
	p-value	0.000	0.000	0.001	0.000	0.000	0.000
SM_MEAN	R-squared	0.005	0.004	0.000	0.000	0.018	0.000
	Slope	0.110	-0.110	0.012	0.010	-0.162	0.002
	t-value	6.049	-6.674	0.688	0.485	-6.596	0.115
	p-value	0.000	0.000	0.491	0.627	0.000	0.908
SM_STD	R-squared	0.001	0.003	0.004	0.000	0.003	0.024
	Slope	0.096	-0.115	-0.170	-0.025	-0.123	0.357
	t-value	3.394	-4.042	-5.074	-0.887	-4.433	13.661
	p-value	0.001	0.000	0.000	0.375	0.000	0.000
VPD_MEAN	R-squared	0.001	0.002	0.019	0.019	0.001	0.155
	Slope	0.044	-0.048	0.118	0.183	0.049	-0.911
	t-value	4.175	-4.796	4.737	24.501	6.416	-156.446
	p-value	0.000	0.000	0.000	0.000	0.000	0.000
VPD_STD	R-squared	0.000	0.002	0.015	0.017	0.003	0.200
	Slope	0.019	-0.050	0.119	0.195	0.121	-1.021
	t-value	1.718	-5.218	5.653	25.217	13.158	-100.094
	p-value	0.086	0.000	0.000	0.000	0.000	0.000
LSTDAY_MEAN	R-squared	0.231	0.237	0.004	0.164	0.668	0.393
	Slope	0.687	-0.869	0.099	0.658	-1.112	-0.975
	t-value	34.359	-53.812	4.180	17.227	-324.787	-51.972
	p-value	0.000	0.000	0.000	0.000	0.000	0.000
LSTDAY_STD	R-squared	0.203	0.197	0.000	0.108	0.544	0.213
	Slope	0.761	-0.925	0.023	0.597	-1.312	-0.706
	t-value	34.129	-39.511	1.653	14.799	-171.340	-29.191
	p-value	0.000	0.000	0.098	0.000	0.000	0.000
LSTNIGHT_MEAN	R-squared	0.005	0.004	0.080	0.034	0.045	0.153
	Slope	-0.116	-0.088	-0.476	-0.295	-0.579	0.664
	t-value	-8.637	-4.627	-44.511	-19.152	-59.453	35.990
	p-value	0.000	0.000	0.000	0.000	0.000	0.000
LSTNIGHT_STD	R-squared	0.053	0.059	0.007	0.030	0.211	0.024
	Slope	0.334	-0.427	-0.146	0.265	-0.696	-0.236
	t-value	18.254	-27.499	-6.449	8.409	-50.547	-7.795
	p-value	0.000	0.000	0.000	0.000	0.000	0.000